Flexible Criteria for Assessing EV Hosting Capacity in Stochastic Load-Flow Simulations

Euan McGill

A thesis presented for the degree of
Doctor of Philosophy
in
Electrical and Computer Engineering
at the
University of Canterbury,
Christchurch, New Zealand.

31 January 2021

ABSTRACT

Low-voltage (LV) distribution networks are bound by operational limits for voltage, conductor loading and transformer loading. Networks are described as being constrained when these limits are violated. In the future, LV distribution networks may become constrained because of the additional load due to electric vehicle (EV) charging. The EV hosting capacity is the maximum EV penetration level a network can accommodate before becoming constrained. Distribution network operators (DNOs) need to understand EV hosting capacity in order to allocate planning and investment.

EV hosting capacity can be assessed using load-flow modelling. When modelling LV distribution networks, individual customer loads are explicitly modelled. At the level of individual customers, loads are highly uncertain, and therefore, a stochastic approach is appropriate. Unlike deterministic load-flow simulations which produce a single EV hosting capacity, stochastic load-flow simulations produce a distribution of EV hosting capacities. A high EV hosting capacity is preferable because it allows network reinforcement to be deferred; reducing the costs which are ultimately passed on to customers. On the other hand, a compromise is necessary between deferring network reinforcement and the possibility of violating operational limits.

In the literature, constraints are assessed using hard criteria. When using hard criteria, all voltages must be within the statutory limits. Similarly, all conductor and transformer loadings must be within the continuous rating. Using hard criteria can restrict the EV hosting capacity, when, in reality, customer equipment can handle a small number of minor voltage violations; this is typically referred to as device immunity. Similarly, conductors and transformers can handle a small number of minor overloads; in practice, DNOs consider emergency and cyclic ratings. Together, the magnitude and duration of violations provide a clear indication of severity. When using hard criteria, the severity of violations is not considered, which makes understanding the necessary compromise difficult.

The contribution of this thesis is a novel framework for assessing EV hosting capacity using flexible constraint criteria. When using flexible criteria, a small number of violations are permitted. The number of permitted violations depends on the violation magnitude.

Using flexible criteria allows the EV hosting capacity to be increased, while still ensuring that severe violations are not permitted. Severe violations are explicitly defined in terms of magnitude and duration; the definition can be adjusted as deemed appropriate by DNOs. The proposed framework allows EVs to be integrated in a safe and cost-effective manner.

CONTENTS

ACKNOWLEDGEMENTS

Firstly, I would like to express a great thanks to my supervisors Prof. Alan Wood and Dr Bill Heffernan, for their continued support during my PhD. Their guidance throughout has helped me overcome many challenges; without them, I doubt I could have got my thesis to the point of submission.

I would also like to thank the wider electrical department for making me feel at home during my time here in New Zealand. In particular, I am grateful to Ken, Edsel and all others associated with Wednesday soccer.

I am also incredibly grateful for my research funding. I would, therefore, like to thank both the Ministry of Business, Innovation and Employment and the University of Canterbury.

Last but not least, I would like to thank my many friends, whom without, I would not have had such a great time over the last four years.

ABBREVIATIONS

Table 1 List of Abbreviated Terms

Abbreviation	Description
AC	Alternating Current
BES	Battery Energy Systems
BEV	Battery Electric Vehicle
BM	By-Morning
CDF	Cumulative Distribution Function
CH_4	Methane
CO_2	Carbon Dioxide
DC	Direct Current
DER	Distributed Energy Resources
DG	Distributed Generation
DNO	Distribution Network Operator
DNT	Day-Night Tariff
EV	Electric Vehicle
EVI	Electric Vehicle Initiative
GHG	Greenhouse Gas
HEV	Hybrid Electric Vehicle
ICCB	In-Cable Control Box
KS	Kolmogorov-Smirnov
LULUCF	Land-Use, Land-Use Change and Forestry
LV	Low-Voltage
PHEV	Plug-in Hybrid Electric Vehicle
MV	Medium-Voltage
MC	Monte Carlo
NZ	New Zealand
N_2O	Nitrous Oxide
OA	On-Arrival
PV	Photovoltaics
QSS	Quasi-Steady-State
RCD	Residual Current Device
SM	Smart Meter
SOC	State Of Charge
SS	Steady-State
TFC	Total Final Consumption
TPES	Total Primary Energy Supply
UNNFC	United Nations Framework Convention on Climate Change

NOMENCLATURE

Bold notation is used for matrix variables. Elements within these matrices are referenced using the appropriate indices. As an example, the variable $\mathbf{\Omega}$ is the EV load data. The element $\Omega_{j,t}$ is the EV load for the j^{th} customer during the t^{th} time interval. Table 2 provides a list of the various indices used in this thesis. The work presented in this thesis can be broken down into two main parts: the stochastic EV load model and the stochastic load-flow simulation. Table 3 provides a list of the variables in the stochastic EV load model. Table 4 provides a list of the variables in the stochastic load-flow simulation.

Table 2 List of Variable Indices

Index	Description	Range
d	Day	$d \in \mathbb{Z} : d \in [1, 7]$
t	Time	$t \in \mathbb{Z} : t \in [1, 336]$
j	Customer	$j \in \mathbb{Z} : j \in [1, 71]$
l	Conductor	$l \in \mathbb{Z} : l \in [1, 7]$
k	Smart Meter	$k \in \mathbb{Z} : k \in [1, 400]$
m	Monte Carlo Repetition	$m \in \mathbb{Z} : m \in [1, \infty]$

Table 3 List of Variables: Stochastic EV Load Model

Variable	Description	Units
$\boldsymbol{\delta}$, δ_d	Departure time	time index
$\boldsymbol{\alpha}$, α_d	Arrival time	time index
$\underline{\boldsymbol{\lambda}}$, $\underline{\lambda}_d$	Charging start time	time index
$\overline{\boldsymbol{\lambda}}$, $\overline{\lambda}_d$	Charging end time	time index
$\boldsymbol{\zeta}$, ζ_d	Night tariff start time	time index
$\ddot{\boldsymbol{S}}$, $\ddot{S}_d$	Departure SOC	kWh
$\dot{\boldsymbol{S}}$, $\dot{S}_d$	Arrival SOC	kWh
$\tilde{\boldsymbol{S}}$, $\tilde{S}_d$	Threshold SOC	kWh

$\hat{\boldsymbol{S}}$, $\hat{S}_d$	Target SOC	kWh
$\overline{\ddot{\boldsymbol{S}}}$, $\overline{\ddot{S}}_d$	Maximum departure SOC	kWh
$\underline{S}$	Minimum permissible SOC	kWh
$\overline{S}$	Maximum permissible SOC	kWh
$\boldsymbol{\beta}$, β_d	Driving energy requirement	kWh
$\boldsymbol{\gamma}$, γ_d	Charging energy requirement	kWh
C	Battery capacity	kWh
R	Charger rating	kW
F	Range anxiety factor	p.u.
$\boldsymbol{\phi}$, ϕ_d	Daily distance traveled	km
$\boldsymbol{\eta}$, η_d	Incomplete charge event	0/1
$\boldsymbol{\theta}$, θ_d	Curtailed journey event	0/1
$\boldsymbol{\mu}$, μ_d	Availability window	time indices
$\boldsymbol{\Omega}, \Omega_{j,t}$	EV load	kW

Table 4 List of Variables: Stochastic Load-Flow Simulation

Variable	Description	Units
$\hat{\Psi}$	EV penetration level	%
Ψ	EV penetration level	count
$\boldsymbol{\Phi}$	EV locations	customer index
$\boldsymbol{\Upsilon}, \Upsilon_j$	Smart Meter assignment	Smart Meter index
$\boldsymbol{\Omega}, \Omega_{j,t}$	EV load	kW
$\boldsymbol{\Theta}, \Theta_{k,t}$	Smart Meter load	kW
$\boldsymbol{P}, P_{j,t}$	Customer load	kW
$\boldsymbol{V}, V_{j,t}$	Customer voltage	p.u.
$\boldsymbol{I}, I_{l,t}$	Conductor loading	p.u.
$\boldsymbol{S}, S_t$	Transformer loading	p.u.
$\mathcal{V}$	Voltage magnitude threshold	p.u.
$\mathcal{I}$	Conductor loading magnitude threshold	p.u.
$\mathcal{S}$	Transformer loading magnitude threshold	p.u.
$\Gamma_{\mathcal{V}}$	Voltage duration threshold	hours
$\Gamma_{\mathcal{I}}$	Conductor loading duration threshold	hours
$\Gamma_{\mathcal{S}}$	Transformer loading duration threshold	hours
$\boldsymbol{H}, H_m$	EV hosting capacity	%
Λ	Kolmogorov-Smirnov statistic	p.u.

Chapter 1

INTRODUCTION

Reducing greenhouse gas (GHG) emissions will be one of the critical challenges for the 21st century. As part of this, distributed energy resources (DERs) will play an important role. DERs refer to a variety of technologies that either generate or store electricity near where it will be used (Andren et al. [2014]). In low-voltage (LV) distribution networks, DERs have the potential to provide clean and reliable power while reducing upstream losses in the transmission and distribution networks. Common DERs include photovoltaics (PV), battery energy systems (BES), and electric vehicles (EVs).

This thesis was completed as part of the GREEN Grid project, which was funded by the Ministry of Business Innovation and Employment (MBIE). The project was aimed at modelling future trends in renewable electricity generation and household demand to ensure that New Zealanders have access to reliable, safe, and affordable renewable energy (Stephenson et al. [2018]). Enabling DERs in distribution networks was a critical topic within the project.

In New Zealand (NZ), EVs will play a crucial role in reducing GHG emissions. NZ has a high rate of private vehicle ownership and currently suffers from limited public transport infrastructure (Ministry of Transport [2017]). On the other hand, NZ generates a significant percentage of its electricity from renewable sources, making it well suited to the electrification of transport (Ministry of Business, Innovation & Employment [2019]).

Public charging infrastructure is becoming increasingly common (New Zealand Transport Agency [2020]). Despite this, it is anticipated that the majority of EV charging will take place in residential settings, which are connected to LV distribution networks (Energy Efficiency and Conservation Authority [2019]). LV distributions networks are bound by operational limits for voltage, conductor loading and transformer loading, and are described as being constrained when these limits are violated.

In the future, LV distribution networks may become constrained because of the additional load due to EV charging. The EV hosting capacity is defined as the maximum EV

penetration level a network can accommodate before becoming constrained. The EV hosting capacity can be assessed using load-flow modelling, which allows planning and investment to be allocated ahead of time.

Distribution network operators (DNOs) typically maintain load-flow models for their medium voltage (MV) networks; however, this is less often the case for LV networks (Watson et al. [2015]). When modelling MV networks, downstream LV networks are modelled as aggregated, or lumped, loads. The aggregate load is relatively predictable because each LV network typically contains a significant number of customers. When modelling LV networks, individual customer loads are explicitly modelled. At the level of individual customers, loads are highly uncertain, and therefore, a stochastic approach is suitable.

This thesis presents a stochastic load-flow simulation for assessing EV hosting capacity. In stochastic load-flow simulations, loads are analysed statistically and therefore when repeated, some samples produce more extreme results than others. A Monte Carlo (MC) method allows the range of possible outcomes to be quantified. Unlike deterministic load-flow simulations which produce a single EV hosting capacity, stochastic load-flow simulations produce a distribution of EV hosting capacities.

When modelling LV distribution networks, the residential and EV load components are typically treated separately. The residential load component is modelled using a Smart Meter (SM) dataset. SMs provide historical data, and are, therefore, unlikely to contain EV charging load. The EV load component is modelled using a mathematical model. The EV load model incorporates seven stochastic variables:

- Arrival time
- Departure time
- Daily distance travelled
- Battery capacity
- Charger rating
- Range Anxiety
- Charging strategy

Load-flow simulations can be classified as either steady-state (SS) or quasi-steady-state (QSS). In SS simulations, the network is examined for a single snapshot in time; on the other hand, QSS simulations consider a time series. In this thesis, a week-long QSS simulation is performed.

Voltage, conductor loading and transformer loading vary during the week. Furthermore, at a given time, voltage and conductor loading vary throughout the network. In the

literature, constraints are typically assessed using hard criteria. When using hard criteria, all voltages must be within the steady-state voltage limits. Similarly, all conductor and transformer loadings must be within the continuous rating. In reality, customer equipment can handle a small number of minor voltage violations. This is something which is recognized in the various power quality guidelines and standards which outline assessment criteria for steady-state voltage. Similarly, conductors and transformers can handle a small number of minor overloads. DNOs often consider various rating adjustments including emergency, cyclic and seasonal (Fernandez and Patrick [2019], SP Energy Networks [2015]). It is proposed that using hard criteria can restrict EV hosting capacity. A higher EV hosting capacity is desirable because it allows network reinforcement to be deferred; reducing the costs which are ultimately passed on to customers.

In New Zealand, the steady-state voltage limits are defined in the Electricity Safety Regulations (SR 2010/36 [2010]). This legislation states that the calculated or measured voltage at the point of supply must:

- Be at standard low voltage (230V)
- Except for momentary fluctuations, be kept within 6% of that voltage.

In 2016, the Electricity Engineers Association (EEA) of New Zealand published their Power Quality Guidelines which were a first step towards a national requirement for power quality implemented through the connection codes used by DNOs (Watson [2016]). The EEA guidelines build on the Electricity Safety Regulations by outlining the assessment criteria for steady-state voltage. It is stated that steady-state voltage shall be assessed using 99^{th} and 1^{st} percentiles of 10-minute averaged r.m.s. voltages over a period of one week. Using a percentile assessment allows for a small number of voltage violations; this is because the highest and lowest 1% of 10-minute averaged r.m.s. voltages are ignored. Specifying the averaging period also removes any ambiguity regarding the definition of momentary fluctuations.

The EEA guidelines can be compared with international power quality standards. Standard EN 50160 is an attempt to standardize quality of supply regulation within the European Union (EU). The standard was drafted based on domestic legislation in various EU countries. It is a consensus-driven standard where each country is given equal representation and reflects the lowest agreed-upon limits for each power quality index. The standard has been amended various times following reviews by the Council of European Energy Regulators and Committee of Electro Technical Standardization. The most recent revision was published in 2010 and provided a clarification on assessment criteria for steady-state voltage (Masetti [2010]). The standard states that during each period of one week:

- 95% of the 10 minute averaged r.m.s. voltages shall be within ±10% of the nominal voltage
- 100% of the 10 minute averaged r.m.s. voltages shall be within $+10/-15\%$ of the nominal voltage.

As with the EEA guidelines, standard EN 50160 uses a percentile assessment. Unlike the EEA guidelines which ignore the 1% highest and 1% lowest voltages entirely, EN 50160 compares the 5% lowest voltages against an extended voltage threshold.

Although percentile assessment is often stated in power quality standards, in the literature, constraints are still assessed using hard criteria and as such no allowance is provided for a small number of minor violations. Furthermore, even though power quality standards go someway in clarifying the assessment criteria for steady-state voltage, these standards are intended for manual voltage assessment, as opposed to computational assessment using load-flow simulations. When voltages are assessed using stochastic-load flow simulations, there remains some ambiguity. While manual assessment is typically limited to a single network location, load-flow simulations allow voltages to be assessed at all network locations. Furthermore, while manual assessment provides the voltage profile which did occur, stochastic load-flow simulations produce a significant number of the voltage profiles which could have occurred. When using stochastic load-flow, it is highly probable that a violation may be found if one chooses to observe the:

- Minimum voltage location
- Minimum voltage time interval
- Minimum voltage MC repetition

In some ways, the enhanced observability that stochastic load-flow simulations provide presents a problem for DNOs. If the results from stochastic load-flow simulations indicate that there is even a small chance of a violation, it is unclear whether DNOs should be allowed to knowingly ignore these. Where the decision is that these cannot be ignored, it is likely that a significant number of distribution networks will need to be reinforced; the cost of which is ultimately passed on to customers.

The primary contribution of this thesis is a novel framework for assessing EV hosting capacity using flexible constraint criteria. Unlike hard criteria, flexible criteria allow for a small number of minor violations. The severity of violations is described the magnitude and duration. The probability of violations is obtained by performing a significant number of MC repetitions. The proposed framework does not represent a relaxing of the steady-state voltage limits outlined in legislation, or of the asset ratings provided by the equipment manufacturers. Instead it represents a due diligence framework for assessing EV hosing capacity where both the probability and severity of potential violations are

fully understood. When assessing EV hosting capacity, there is a necessary compromise between deferring network reinforcement and the possibility of violating operational limits. The proposed framework allows this compromise to be fully understood; DNOs can then make informed decisions regarding network reinforcements.

1.1 RESEARCH QUESTIONS

The primary research question is as follows:

"How can we interpret stochastic load-flow results in order to make meaningful conclusions regarding EV hosting capacity?"

The secondary research questions in Table 1.1 allow this broader question to be broken down; also provided are the corresponding chapters where each question is addressed.

Table 1.1 List of Secondary Research Questions

Research Question	Description	Chapter
1	"What are the stochastic variables required to model EV load?"	3, 4
2	"How to determine the uncertainty in EV hosting capacity?"	6
3	"How many MC repetitions are required?"	3, 6
4	"What are the limitations of using hard constraint criteria?"	6
5	"To what extent can these limitations be overcome by using flexible constraint criteria?"	6
6	"To what extent can the EV hosting capacity be increased by alternative charging practices?"	6

1.2 METHODOLOGY

A flow chart of the stochastic load-flow simulation can be seen in Figure 1.1. A typical residential network is modelled in OpenDSS. OpenDSS is an open-source software package developed by the Electric Power Research Institute and was chosen because it can be automated using MATLAB (Roger C. Dugan [2020]). The inputs to OpenDSS are the weekly load profiles for each customer in the network. OpenDSS performs a QSS load-flow simulation and exports a series of network monitors which record voltage, conductor loading and transformer loading during the simulation.

The inputs to OpenDSS are generated in MATLAB. For each customer, the residential load component is sampled from a SM dataset. The EV load component is simulated using the stochastic EV load model. Customer load profiles are then constructed by superimposing the residential and EV load components. The penetration loop allows multiple EV penetration levels to be assessed. At each penetration level, EV locations are randomly assigned during the penetration level adjustment stage.

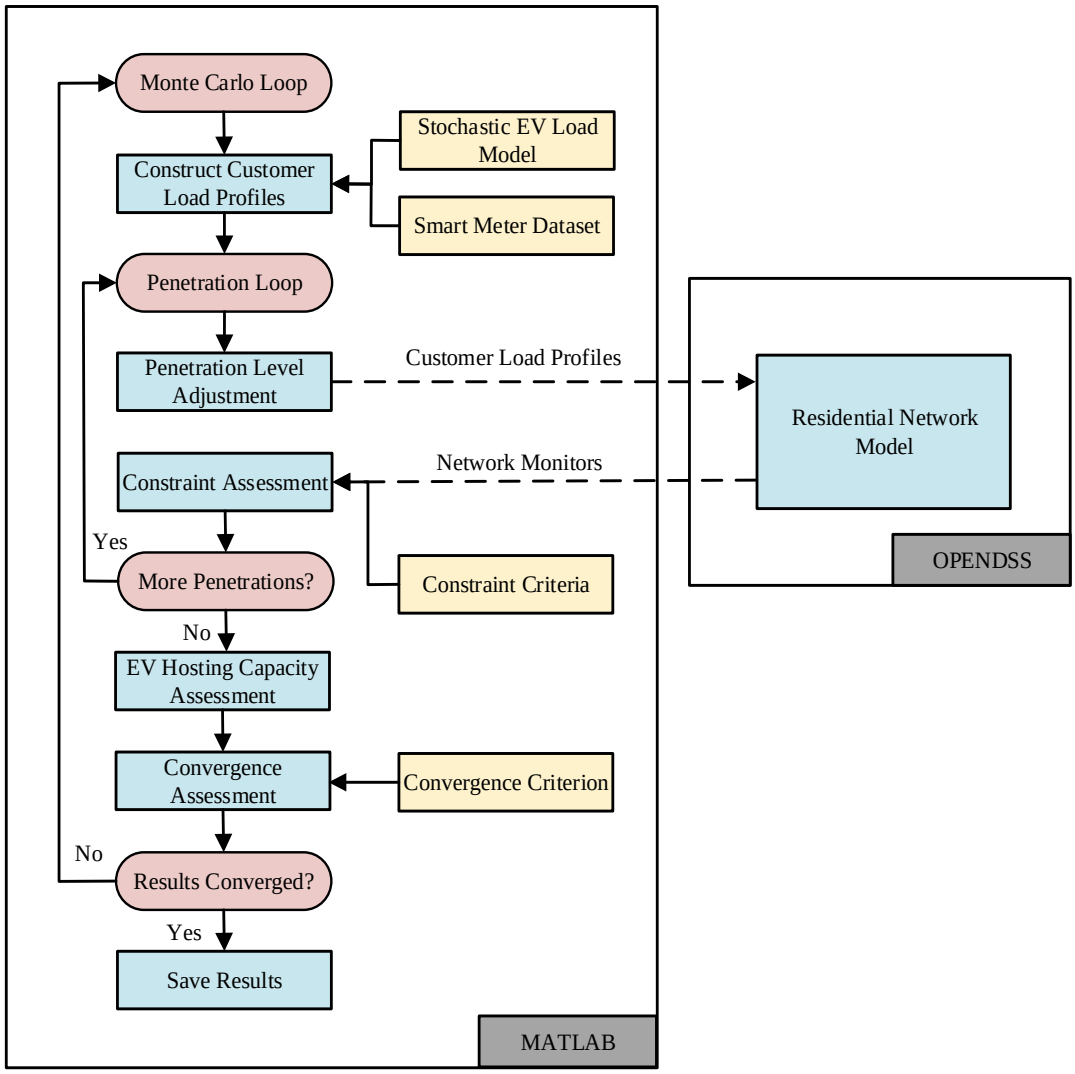

Figure 1.1 Flowchart of Stochastic Load-Flow Simulation

The outputs from OpenDSS are also processed in MATLAB. Constraints are assessed using the exported network monitors, and the constraint criteria provided as input; either hard or flexible criteria. The EV hosting capacity is then assessed using the constraint assessments at each penetration level.

The entire process is repeated within the Monte Carlo loop. For each repetition, the residential loads are re-sampled from the SM dataset. Similarly, the EV loads are re-generated using the stochastic EV load model. The distribution of EV hosting capacities is described by a cumulative distribution function (CDF).

The Monte Carlo loop could continue ad infinitum, and therefore, it is necessary to show that for a finite number of repetitions, the CDF has stabilised. At the convergence assessment stage, the stability of the CDF is assessed using the Kolmogorov-Smirnov (KS) statistic. The Monte Carlo loop is terminated when the KS statistic converges within the specified tolerance; at this point, the significant results are saved.

1.3 THESIS STRUCTURE

Chapter 2
The motivation for this research is established in Chapter 2. The chapter begins by examining NZ's GHG emissions, including the contribution of various sectors. NZ's GHG emissions are also considered alongside the reduction targets established by the government.

The NZ energy landscape is then presented, including both overall energy and electricity. Based on this analysis, the electrification of transport is identified as an effective means of reducing GHG emissions in NZ. EV technologies are then discussed, including uptake forecasts, charging options and user preferences.

It is anticipated that the majority of EV charging will take place in residential settings which are connected at LV. LV distribution networks are also discussed, including the impact of EV charging.

Chapter 3
Chapter 3 provides a review of the relevant literature. The review is broken down into three sections: residential load modelling, EV load modelling, and stochastic load-flow simulations. The chapter concludes by discussing gaps and limitations in the existing body of knowledge.

Chapter 4
The stochastic EV load model is described in Chapter 4. The model simulates weekly EV load profiles with half-hour temporal resolution. Time indexing is first discussed, followed the relationships through which the numerous variables are related.

The charging strategy describes how EV load is scheduled, subject to the relevant constraints. Three charging strategies are considered in this thesis: on-arrival (OA), day-night tariff (DNT) and by-morning (BM). These strategies are also described.

The stochastic EV load model incorporates seven stochastic variables; these allow a diverse range of charging practices to be captured. Each of the stochastic variables is sampled from a statistical distribution. The distributions for the baseline charging scenario describe the charging practices which EV owners are expected to adopt naturally. These distributions are also described.

Chapter 5
The stochastic load-flow simulation is described in Chapter 5. The typical residential network is described first; this includes both the topology and the Multiple Earthed Neutral (MEN) system used in NZ. The process of constructing customer load profiles is then described; this includes the superposition of the residential and EV load components, and the penetration level adjustment.

In science and engineering, black-box systems are described by their inputs and outputs, without any knowledge of the system internal workings. In this thesis, OpenDSS may be considered a 'black box'. Although not essential, a basic understanding of the OpenDSS is useful, and therefore, a brief overview is provided.

The inputs to OpenDSS are the customer load profiles. Using these, OpenDSS performs a week-long QSS load-flow simulation and outputs the various network monitors; each of these is also described. The network monitors are then assessed for constraints; this process is described for when using both hard and flexible criteria.

The stochastic load-flow simulation produces a distribution of EV hosting capacities. The simulation convergence criterion ensures that for a finite number of MC repetitions, the EV hosting capacity CDF has stabilized. The simulation convergence criterion is also described.

When the convergence criterion is satisfied, the MC simulation is terminated. At this point the significant results are saved; these results are also described.

Chapter 6
Chapter 6 presents the results produced by the stochastic load-flow simulation. The results demonstrate the process of assessing EV hosting capacity when using both hard and flexible criteria. The differences between the two are then discussed, highlighting the limitations of using hard criteria and the extent to which these can be overcome by using flexible criteria.

In the literature, the number of MC repetitions is typically defined a priori. Here, the simulation is terminated when the convergence criterion is satisfied. Demonstration of the convergence criterion is, therefore, also provided.

The EV hosting capacity will depend on the charging practices adopted by EV owners. Examples of more favourable charging practices include:

- Using lower-rated chargers
- Reducing range anxiety
- Using an even mix of charging strategies

Various scenarios can be examined by altering the statistical distributions from which the stochastic variables are sampled. The baseline charging scenario is compared with an alternative charging scenario which describes more favourable charging practices, from an LV network perspective.

Chapter 7
Chapter 7 provides a summary of the key findings. Firstly, each of the secondary research questions is revisited. Limitations and avenues for future work are then discussed.

Chapter 2

BACKGROUND

Reducing GHG emissions will be one of the critical challenges for the 21st century. Although NZ's gross emissions are low, the per capita emissions are relatively high (World Resources Institute [2020]). NZ's GHG emissions are discussed in Section 2.1, including the contribution of various sectors and reduction targets.

There are four primary methods for reducing GHG emissions (Intergovernmental Panel on Climate Change [2014]):

- Transitioning towards low-carbon energy sources
- Improving energy efficiency
- Carbon sequestration
- Climate engineering

The most effective method for a particular country depends on the energy landscape. The NZ energy landscape is discussed in Section 2.2.

In NZ, transport contributes significantly to Total Final Consumption (TFC). Relative to other developed nations, NZ has a high rate of private vehicle ownership and limited public transport infrastructure (Ministry of Transport [2017]). On the other hand, more than 80% of NZ's electricity is generated from renewable sources; and therefore the electrification of transport provides an effective means of transitioning towards low-carbon energy sources (Ministry of Business, Innovation & Employment [2019]).

EV uptake is increasing, both globally and in NZ. The primary drivers behind EV uptake are economic, environmental, and social benefits. Section 2.3 provides an overview of the EV landscape in NZ, including uptake projections and charging options.

Although EVs can offer a wide range of benefits, EV charging will present challenges for existing energy markets and power system infrastructure. Section 2.4 provides an overview of the power system architecture in NZ: including generation, transmission, and distribution. The impact of EV charging in LV distribution networks is then discussed in detail.

2.1 GREENHOUSE GAS EMISSIONS

GHGs trap heat from the sun, resulting in a warming of the Earth's atmosphere. Since the start of the industrial revolution, GHG emissions have caused global temperatures to rise by around $0.9°C$ (NASA [2020]). The primary GHGs are carbon dioxide (CO_2), methane (CH_4), nitrous oxide (N_2O), and fluorinated gases. Depending on the specific gas, these can remain in the atmosphere for up to tens of thousands of years (Archer et al. [2009]).

CO_2 emissions come primarily from the burning of fossil fuels, solid waste, and other biological materials. Chemical reactions, including cement production, also contribute. CO_2 can remain in the atmosphere for thousands of years; however, trees and other biomass can absorb CO_2 from the atmosphere, in a process known as CO_2 sequestration.

CH_4 emissions come primarily from the production and transport of fossil fuels, livestock and agriculture, and decay in solid waste landfills. CH_4 is around 25 times more effective at trapping heat than CO_2; however, it only remains in the atmosphere for around 12 years.

N_2O emissions come primarily from agriculture. N_2O is around 298 times more effective at trapping heat than CO_2 and remains in the atmosphere for around 114 years. Fluorinated gasses are emitted by a range of industrial processes and while typically emitted in smaller quantities, they can remain in the atmosphere for up to 50,000 years.

Climate change will have a significant impact on ecology, health, weather, sea-level and agriculture, which will lead to severe geopolitical stresses (Intergovernmental Panel on Climate Change [2014]). As a result, combatting climate change is one of the most significant challenges facing the global community in the 21st century.

2.1.1 International Perspective

Although future generations will be negatively impacted if GHG emissions are not reduced, historically, GHG emissions are correlated with significant improvements in living standards. A measured approach is required to ensure a sustainable future, for both the developed and developing world.

The largest GHGs emitters have changed significantly over the last decade (Intergovernmental Panel on Climate Change [2014]). The UK was the largest global emitter until 1888 when it was overtaken by the US. Today, many of the world's largest emitters are in Asia. The gross GHG emissions of the top 20 global emitters can be seen in Figure 2.1. Gross emissions are the total emissions from agriculture, energy, industrial processes and waste; not including removals due to CO_2 sequestration.

In 2014, NZ's gross GHG emissions were 75.74 $MtCO_2e$, ranking 61st globally (World Resources Institute [2020]). The per capita gross GHG emissions for the top 20 global emitters can be seen in Figure 2.2. In 2014, NZ's per capita gross GHG emissions were 16.8 tCO_2e, ranking 20^{th} globally.

Per capita emissions are correlated with income and living standards and, therefore, vary significantly across the globe. The largest per capita emitters are oil-producing countries including Kuwait, Brunei and Qatar, which all have small populations. Therefore, their gross GHG emissions are relatively low. On the other hand, Australia, Canada and the US combine large populations and high per capita emissions.

Although per capita emissions are correlated with income and living standards; government policies, electricity generation mix, and culture also play a role. As a result, there are examples of countries with similar living standards and vastly different in per capita emissions. The per capita emissions in many European countries are lower than in the US (World Resources Institute [2020]).

2.1.2 New Zealand Emissions by Sector

Figure 2.3a provides a breakdown of NZ's GHG emissions by gas. CO_2 contributes the largest share, followed by CH_4 and N_2O. GHG emissions can also be broken down by sector; these are:

- Energy
- Industrial processes
- Agriculture
- Waste
- Land-Use, Land-Use Change and Forestry (LULUCF)

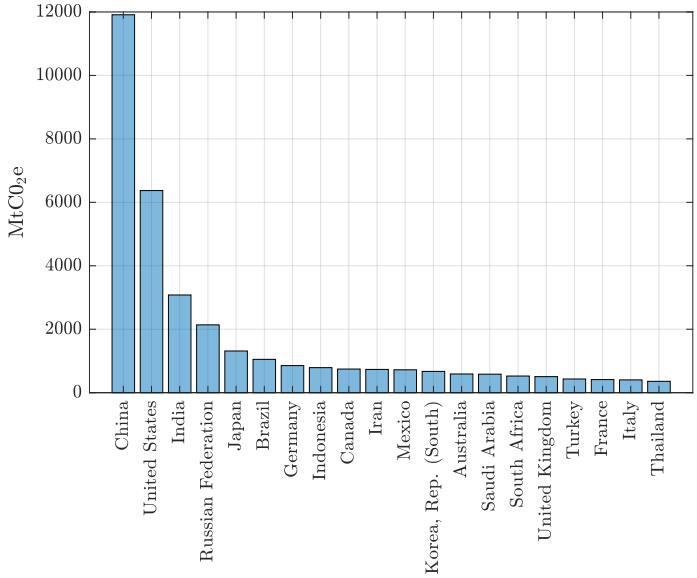

Figure 2.1 Gross GHG Emissions of the Top 20 Global Emitters, 2014
Source: World Resources Institute

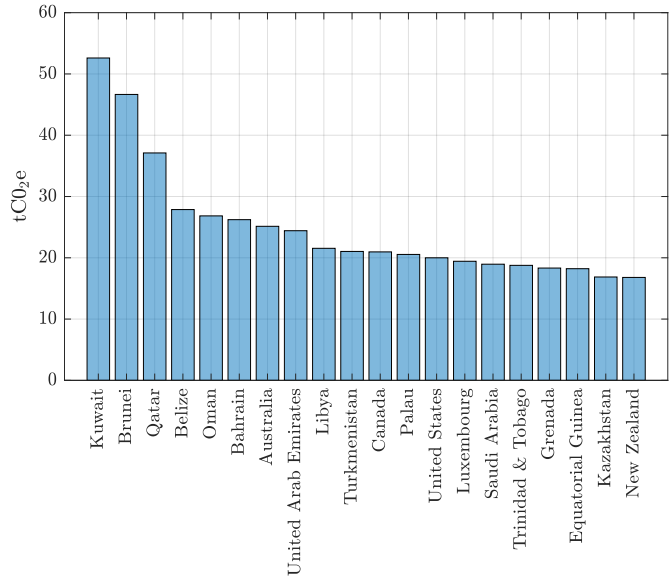

Figure 2.2 Per Capita Gross GHG Emissions of the Top 20 Global Emitters (Per Capita), 2014
Source: World Resources Institute

The energy sector includes transport, manufacturing, construction and electrical generation. Industrial processes include the production of metals, chemicals and refrigerants. The agriculture sector includes livestock, farming and manure, while waste accounts for methane production from landfills. LULUCF keeps track of GHGs absorbed in CO_2 sequestration.

Figure 2.3b provides a breakdown of NZ's GHG emissions by sector. These are the gross emissions, and therefore, LULUCF is not represented. The majority of overall GHG emissions come from the energy and agriculture sectors. The energy sector contributes the majority of CO_2 emissions; around 87.5% in 2016 (The Ministry for the Environment [2018]). The agriculture sector contributes the majority of CH_4 and N_2O emissions. In 2016, around 82.5% of CH_4 emissions came from livestock digestion while around 94.2% of N_2O emissions came from animal waste in agricultural soil (The Ministry for the Environment [2018]).

The energy sector can be further broken down into five subsectors; these are:

- Electricity & heating
- Manufacturing & construction
- Transport
- Other fuel combustion
- Fugitive emissions

Figure 2.4 provides a breakdown of energy sector GHG emissions by subsector. Transport is the single most significant contributor, followed by electricity and heating and then manufacturing and construction.

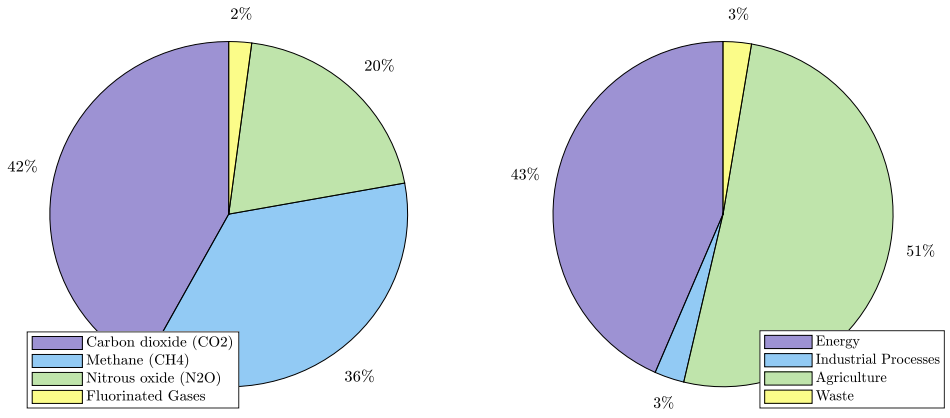

(a) Emissions by Gas

(b) Emissions by Sector

Figure 2.3 Gross GHG Emissions, New Zealand 2014
Source: World Resources Institute

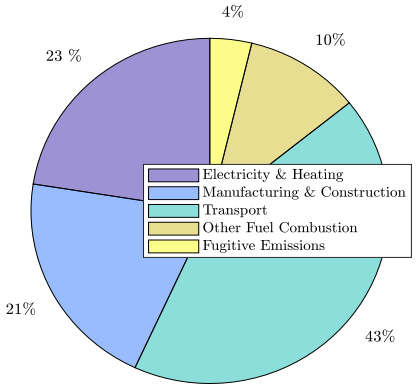

Figure 2.4 Energy Sector Gross GHG Emissions by Sub-sector, New Zealand 2014
Source: World Resources Institute

2.1.3 New Zealand Emissions Reduction Targets

In 2015, the Paris Agreement established a target of limiting average global warming to 2°C above pre-industrial temperatures (United Nations [2015]). The NZ government has established a series of domestic and international targets, which cover both the short and medium-term future.

Domestic Targets

The Climate Change Response (Zero-Carbon) Amendment Act was signed in 2019, establishing a domestic target for the year 2050. The target is for net-zero GHG emissions by 2050; other than CH_4. CH_4 emissions are to be reduced by 10% by 2030, and by between 24% and 47% by 2050; both of which are relative to 2017 levels.

This amendment replaced a former domestic target, bringing NZ in line with the ambition set out in the Paris Agreement (The Ministry for the Environment [2018]). The previous target aimed to reduce GHG emissions to 50% of 1990 levels by 2050.

International Targets

In 2013, the NZ government established its 2020 target under the United Nations Framework Convention on Climate Change (UNFCCC). The 2020 target includes both an unconditional and a conditional target. The unconditional target was to reduce gross GHG emissions to 5% below 1990 levels, between 2013 and 2020. The conditional target was to reduce gross GHG emissions to between 10% and 20% below 1990 levels, during the same period (The Ministry for the Environment [2018]). The more ambitious target was conditional on a comprehensive global agreement.

The NZ government established its 2030 target under the Paris Agreement. The 2030 target is to reduce gross GHG emissions to 30% below 2005 levels - or 11% below 1990 levels - between 2021 and 2030. Emission levels from both 1990 and 2005 were chosen to provide consistency with previously established targets.

2.2 NEW ZEALAND ENERGY LANDSCAPE

The most effective method for reducing GHG emissions depends on the energy landscape. In NZ, CH_4 and N_2O contribute more significantly to overall GHG emissions than in other developed nations; this is due primarily to agriculture and farming, as well as the significant proportion of electricity which is generated from renewable sources (Ministry of Business, Innovation & Employment [2019]). The majority of CO_2 emissions, on the other hand, come from the energy sector. At present, mitigation methods for CH_4 are in their relative infancy, and therefore, the energy sector presents the most opportunity for emissions reduction.

2.2.1 Total Primary Energy Supply

Figure 2.5a provides a breakdown of NZ's Total Primary Energy Supply (TPES) by source. In 2015, non-renewable sources contributed 60% of the TPES. Although NZ has an abundant coal resource; oil and natural gas reserves are limited (The Ministry for the Environment [2018]). Nuclear is not considered a viable option due to the size of the country, and concerns surrounding safety and the environment.

Renewable sources contributed the remaining 40% of the TPES. In NZ, hydropower is used extensively to generate electricity. Geothermal energy is used for both generating electricity and for domestic hot water. At present, geothermal energy dominates the non-hydro renewable sector; however, there is significant potential for expanding wind, solar, wave, and tidal energy in the future.

2.2.2 Electricity Supply

Figure 2.5b provides a breakdown of NZ's electricity supply by source. Renewable sources contribute more significantly to the electricity supply than to TPES. Hydropower contributes the single largest share and has played a crucial role in NZ's electricity system for over 100 years (Ministry of Business, Innovation & Employment [2019]). NZ has over 5,000 MW of installed hydro capacity; the majority of which is located in the South Island.

Geothermal contributes the second-largest share and has played a crucial role in NZ's electricity system for around 55 years; since the opening of the Wairakei power station

in 1958. The majority of geothermal generation is located in the North Island, in the Taupo Volcanic Zone.

Wind generation is one of the fastest-growing renewable sectors in NZ. The majority of NZ's installed wind capacity is in the North Island, primarily at the Tararua and Makara wind farms. Although renewable sources dominate the generation mix, fossil fuels still play a crucial role, providing baseload, backup, and supply during peak loads (Ministry of Business, Innovation & Employment [2019]).

2.2.3 Total Final Consumption

Figure 2.6a provides a breakdown of NZ's Total Final Consumption (TFC) by sector. Transport contributes the single largest share and is fuelled predominantly by oil. The industrial sector contributes the second-largest share but is fuelled by a broader range of sources. In NZ, renewables contribute more significantly to the industrial sector than in other developed nations (International Energy Agency [2020]). Major industries include forestry and metal production.

The residential sector contributes the third-largest share. In NZ, significant efficiency improvements are possible in the residential sector; specifically, improvements in home insulation. The remaining shares are from commerce, agriculture, fishing, and non-energy use, among other small contributors. Non-energy use covers petroleum products that are not used for energy, including white spirit, paraffin waxes, lubricants and bitumen (International Energy Agency [2020]).

2.2.4 Electricity Consumption

Figure 2.6b provides a breakdown of NZ's electricity consumption by sector. The contribution of the transport sector is negligible, and instead, electricity consumption is dominated by the industrial, residential, and commercial sectors.

In NZ, the electrification of transport provides an effective means of transitioning towards low-carbon energy sources because renewable sources dominate the electricity supply. Furthermore, the transport sector contributes significantly to TFC, but very little to electricity consumption. Improving energy efficiency, carbon sequestration, and climate engineering remain possible options and should still be explored. However, given the energy landscape in NZ, the electrification of transport represents the most significant potential for reducing GHG emissions.

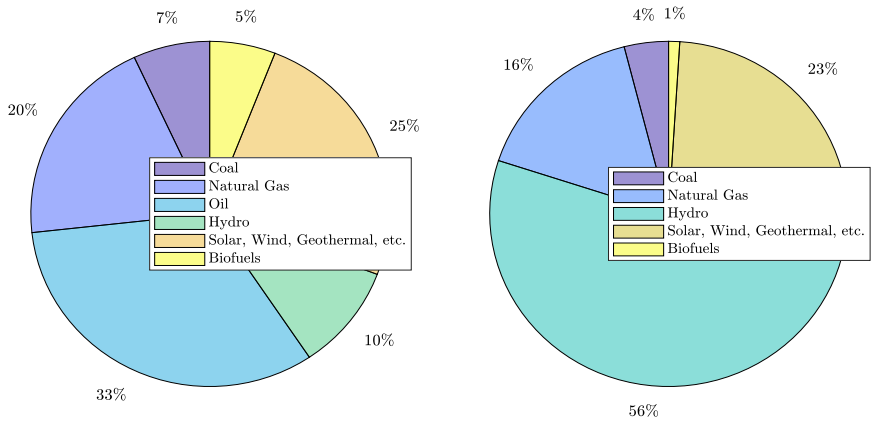

(a) Energy (b) Electricity

Figure 2.5 Total Primary Energy and Electricity Supply by Source, New Zealand 2015
Source: International Energy Agency

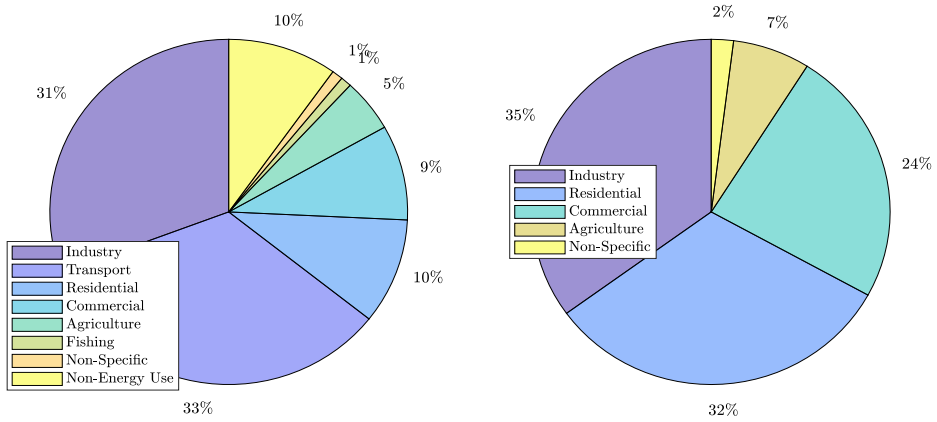

(a) Energy (b) Electricity

Figure 2.6 Total Final Consumption and Electricity Consumption by Sector, New Zealand 2015
Source: International Energy Agency

2.3 ELECTRIC VEHICLES

EVs can be broadly classified as:

- Hybrid electric vehicles (HEVs)
- Plug-in hybrid electric vehicles (PHEVs)
- Battery electric vehicles (BEVs)

HEVs have both an internal combustion engine and a small electric engine. The internal combustion engine provides the majority of the power, while the electric engine contributes

toward improved fuel economy. The internal combustion engine also recharges the battery.

PHEVs have both an internal combustion engine and an electric engine; however, the electric engine and battery are typically larger, and therefore, the vehicle can run on either engine independently. Either the internal combustion engine or an external charger can be used to recharge the battery.

BEVs have an electric engine only and are charged using an external charger. Throughout this thesis, EV refers to both PHEVs and BEVs. HEVs have no impact on the electrical power system.

2.3.1 Electric Vehicle Uptake

EV uptake is increasing, both globally and in NZ. The primary drivers behind EV uptake are economic, social and environmental benefits. In 2018, the global EV fleet exceeded 5.1 million, increasing by over 2 million since 2017 (International Energy Agency [2020]). Figure 2.7 shows the growth of the global EV fleet between 2014 and 2018. The contribution of PHEVs and BEVs are indicated separately.

China contributes the single largest share of the global EV fleet, followed by Europe and the US. Norway is the global leader in terms of EV market share, where, in 2019, EVs accounted for 46% of new car sales. This is partly due to extensive EV subsidies provided by the Norwegian government.

The primary drivers behind EV uptake in NZ have been lower operating costs and sustainability considerations. In addition to fuel savings, EVs are currently exempt from road user charges. In 2019, EVs accounted for 2% of all light passenger vehicle sales, rising from 0.13% in 2014 (Ministry of Transport [2020]).

Figure 2.8 shows the growth of the NZ EV fleet between 2014 and 2018. Again the contribution of PHEVs and BEVs are indicated separately. At present, the NZ fleet is dominated by secondhand Japanese imports. Future uptake will depend on government policies, technology advances, private-sector innovations and public engagement (Energy Efficiency and Conservation Authority [2019]).

The Electric Vehicles Initiative (EVI) is a multi-government forum of the world's top EV markets. In 2017, the EVI launched the EV30@30 campaign, setting a target of 30% EV market share by 2030 (Electric Vehicles Initiative [2019]). The campaign was endorsed by 11 countries:

- Canada
- China
- Finland
- France
- India
- Japan
- Mexico
- Netherlands
- Sweden
- United Kingdom

Figure 2.9 shows the projected growth of the global EV fleet for the EV30@30 scenario. The EV30@30 scenario is an ambitious target and will require significant technological and private sector innovations, as well as global engagement in EV policy support (Electric Vehicles Initiative [2019]). Although NZ has not officially joined the EV30@30 campaign, it is a member of the EVI, and therefore, NZ may experience a similar trend over the next decade.

2.3.2 Electric Vehicle Charging

EV chargers are the link between EVs and the electrical power system. During charging, a conversion stage is required because batteries are direct current (DC) and distribution networks are alternating current (AC). Depending on where and how this conversion takes place, EV chargers can be broadly classified by technology: AC, DC, or Wireless (Energy Efficiency and Conservation Authority [2019]).

AC charging is the most common technology in residential settings; here, conversion takes place inside the car, using the EV's inbuilt inverter. The inverter rating determines the maximum rate of charge. DC charging is more common in public settings; here, conversion takes place outside the car and the charger is connected directly to the EV battery. With DC charging, the maximum rate of charge is no longer determined by the inverter rating.

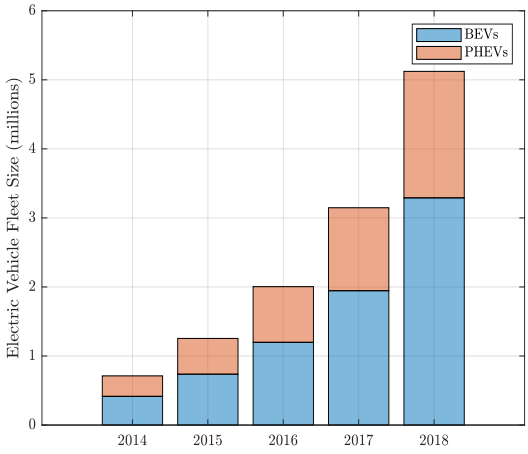

Figure 2.7 Growth of Global EV Fleet, 2014-2018
Source: International Energy Agency

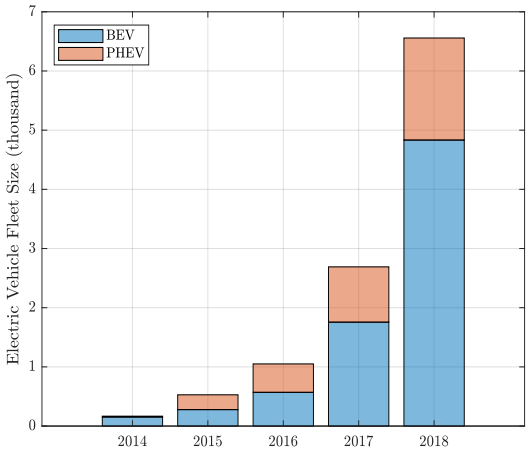

Figure 2.8 Growth of New Zealand EV Fleet, 2014-2018
Source: Ministry of Transport

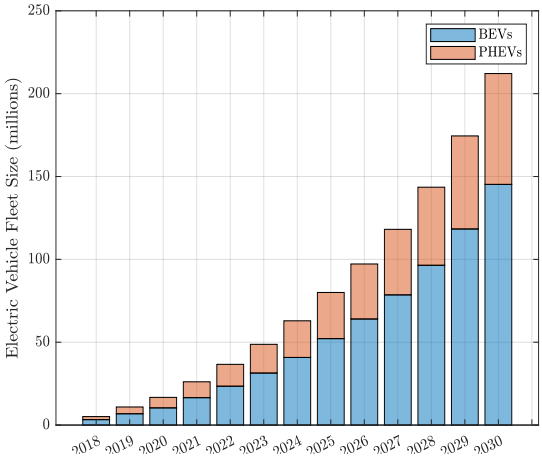

Figure 2.9 Projected Growth of Global EV Fleet, EV30@30 Scenario
Source: International Energy Agency

With wireless charging, EVs are located above a charging pad; the battery is then charged using electromagnetic waves, transmitted between the pad and a plate on the underside of the vehicle. Wireless charging is uncommon for light passenger vehicles and is better suited for public transport applications (Energy Efficiency and Conservation Authority [2019]).

EV chargers can also be classified by mode. Four modes are defined in EN IEC 61851-1. For Modes 1 and 2, charging is carried out using a non-dedicated charging circuit and standard socket outlet. In Mode 1, the charging circuit has no communication or protection capabilities, and the maximum rate of charge is limited to 2.3 kW. In Mode 2, the charging circuit has an in-cable control box (ICCB), and a residual current device (RCD), and the maximum rate of charge is limited to 7.4kW.

For Modes 3 and 4, charging is carried out using a fixed and dedicated supply; that is to say, the EV charger is hard-wired into the building. Communication between the charger and the vehicle determines the appropriate rate of charge. Mode 3 refers to AC charging, while Mode 4 refers to DC charging. In Mode 3, the maximum rate of charge is 22kW, while in Mode 4 the maximum rate of charge can be as high as 175 kW. Mode 4 charging is typically found in public settings such as service stations.

EV chargers can also be classified by connector type, which varies depending on the country, EV model, and charging technology (Energy Efficiency and Conservation Authority [2019]). Some EV models have two connectors; one for AC charging and another for DC charging. Other EV models have a single connector for both AC charging and DC charging. The various connector types are summarized in Table 2.1.

Finally, EV chargers can also be classified by speed. The EV charger speed is a measure of time taken to recharge the battery. The labels slow, medium, and fast are typically used to describe different charger ratings; however, the exact rating brackets vary in the literature. Alternative labels such as rapid charging are also used interchangeably.

In NZ, the majority of EV charging takes place in residential settings using a non-dedicated charging circuit. The reason for this is because dedicated supplies are significantly more expensive. Charging cables are required to operate in Mode 2 and can be rated between 1.8kW and 7.4kW. A smaller number of EVs are charged using dedicated supplies, which are required to operate in Mode 3. These can be rated between 3.7-11kW for a single-phase connection, and up to 22kW for a three-phase connection (WorkSafe NZ [2019]).

Table 2.1 List of EV Connector Types
Source: Energy Efficiency and Conservation Authority

Name	Technology	Description
Type 1	AC	Japanese standard for AC charging
Type 2	AC	European standard for AC charging
CHAdeMO	DC	Japanese standard for DC charging
Tesla Super-Charger	DC	Tesla standard for DC charging
Type 1 CCS	AC/DC	North American standard for DC charging
Type 2 CCS	AC/DC	European standard for fast charging

The most important considerations when modelling LV distribution networks are the maximum rate of charge and the battery capacity. In residential settings, AC to DC conversion takes place inside the car, and therefore, the maximum rate of charge is determined by the rating of the EVs inbuilt inverter.

Figure 2.10 shows a breakdown of the NZ EV fleet by the manufacturer. Some manufacturers have a range of EV models, and for some EV models, there are several generations. Table 2.2 shows the inverter rating and battery capacity for the most common EV models in NZ.

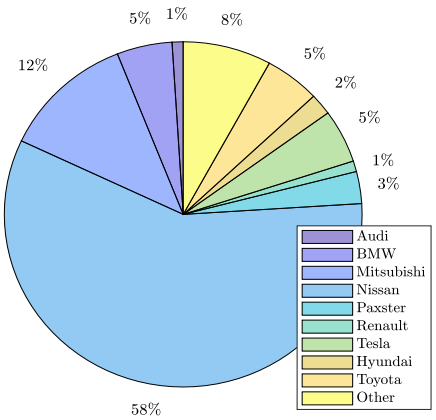

Figure 2.10 EV Fleet by Manufacturer, New Zealand 2019
Source: Energy Efficiency and Conservation Authority

Seven EV models make up more than 85% of the NZ EV fleet (Energy Efficiency and Conservation Authority [2019]); these are:

- Nissan Leaf
- Nissan eNV-200

- BMW i3
- Hyundai Ioniq
- Tesla Model S
- Mitsubishi Outlander
- Toyota Prius

The Nissan Leaf contributes the single largest share of any EV model; the majority of which have an inverter rating of 3.6kW (Energy Efficiency and Conservation Authority [2019]). Inverter ratings and battery capacities are typically higher for BEVs than PHEVs, and at present, BEVs comprise 76% of the NZ EV fleet. Premium EV models, including Audi, BMW, and Tesla have the highest inverter ratings and battery capacities; however, these models comprise only 11% NZ EV fleet.

Table 2.2 EV Model Specifications, New Zealand 2019
Source: Energy Efficiency and Conservation Authority

Manufacturer, Model	Classification	Inverter Rating (kW)	Battery Capacity (kWh)
Audi, A3 e-tron	PHEV	3.7	8.8
Audi, A3 e-tron	BEV	22	84
Audi, e-tron SUV	BEV	22	95
BMW, i3	BEV	7.4, 11	22, 33, 42
Honda, Urban	BEV	11	36
Hyundai, Ioniq	PHEV	3.3	8.9
Hyundai, Ioniq	BEV	6.6	28
Mercedes, EQ-C	BEV	7.4	85
Mitsubishi, Outlander	PHEV	3.7	12, 13.8
Nissan, Leaf	BEV	3.6, 6.6	24, 30, 40, 60
Nissan, E-NV200	BEV	6.6	40
Renault, Zoe	BEV	22	31
Tesla, Model S	BEV	22	60-100
Tesla, Model X	BEV	22	75-100
Toyota, Prius Prime	PHEV	2.2, 3.3	4.4, 8.8
Volvo, XC 40	BEV	11	78
VW, I.D. NEO	BEV	11	48

The EV charging strategy describes how EV load is scheduled, subject to the relevant constraints. On-arrival is the most common charging strategy and is that which EV owners are expected to adopt naturally. On-arrival charging is undesirable from an LV network perspective because of the correlation between EV arrivals and the residential

evening peak. As an alternative, charging can be delayed using the vehicles inbuilt timer function.

In the future, EV charging could be controlled by the DNO or some other third party intermediary. In NZ, a ripple injection system is currently used to manage peak loading via hot water cylinders and night store heaters (Orion [2017]). The system could equally be used to manage EV charging; however, it is expected that willingness to alter charging behaviour or to hand over control will vary among EV owners.

A report published in 2018 investigated the motivations behind different charging practices in NZ (Jake Roos Consulting [2018]). The report summarised the findings of a questionnaire completed by 77 EV owners. The participant responses were validated by two years worth of half-hour load data.

A significant number of participants charged on-arrival. Despite this, because of load diversity, the after-diversity peak load contribution was only between 0.5kW and 0.8 kW, for charger ratings between 2.5kW and 4 kW. Other participants delayed charging until later in the evening; typically around midnight. These customers were typically on day-night tariffs, and were, therefore, financially motivated to do so.

31% of participants claimed to always charge after 9 pm. Furthermore, 49% of participants claimed to typically charge after 9 pm. The questionnaire provided four possible reasons for charging after 9 pm. The participants were then asked to rank the importance of each. The participant responses can be seen in Figure 2.11. Cost-saving ranked highest; however, a significant number of participants also considered environmental and network benefits.

Participants who charged before 9 pm were also asked to provide their reasons for doing so. The responses can be seen in Figure 2.12. The most common response was convenience; some EV owners performed an initial charge when arriving home before using the vehicle later in the evening. For other participants, no cost-saving was the reason; these were customers who were not on day-night tariffs. Some EV owners charged during the day in order to maximise self-consumption from solar PV generation, while a small number of participants were not aware of delayed charging as an option.

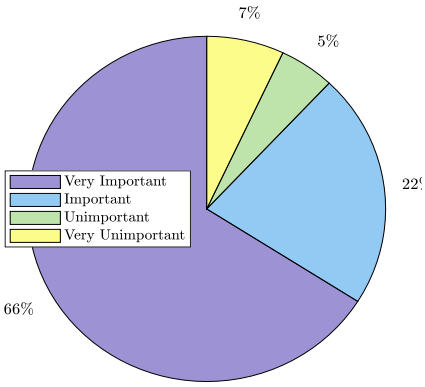

(a) Cost-Saving

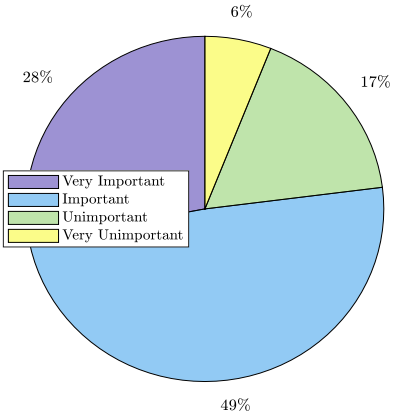

(b) Environmental Benefits

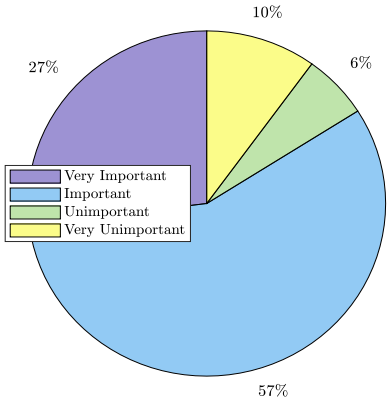

(c) Network Benefits

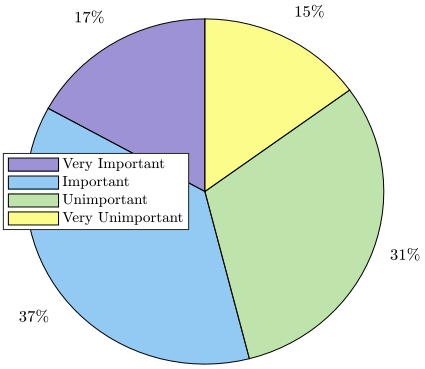

(d) Convenience

Figure 2.11 Importance of Different Reasons for Charging EV After 9pm
Source: Jake Roos Consulting

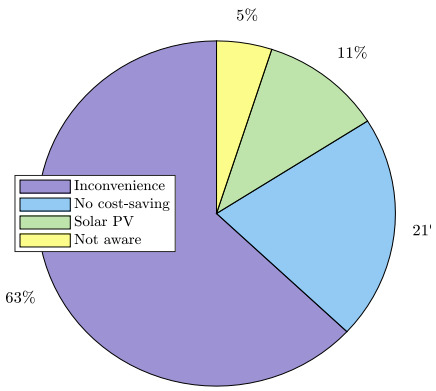

Figure 2.12 Reasons for Not Charging EV After 9pm
Source: Jake Roos Consulting

The questionnaire then introduced the idea of centralised control, explaining that rather than having to establish timing arrangements themselves, charging could be controlled by the DNO. The participants were asked how comfortable they would be with this arrangement; the responses can be seen in Figure 2.13a. The majority of participants said they would be either comfortable or very comfortable. The participants who were either uncomfortable or very uncomfortable stated that having control of their electricity at all times was crucial.

The participants were also provided six options for the level of monthly financial incentive they would require to hand over control; the responses can be seen in Figure 2.13b. Overall, it seems like there is a willingness among EV owners to alter their charging behaviour; however, this may reflect the small sample of early-adopters used in the study. As EVs become increasingly common, these attitudes may become less typical.

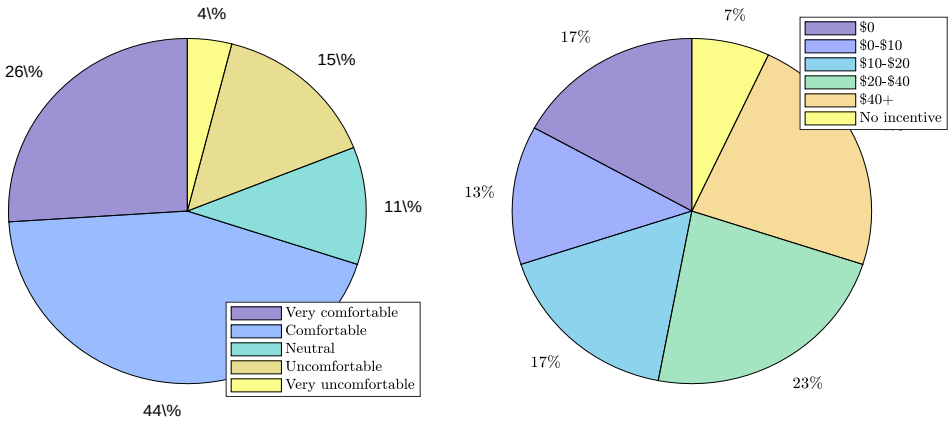

(a) Comfort Level (b) Monthly Financial Incentive

Figure 2.13 Comfort Level with Centralised Control
Source: Jake Roos Consulting

2.4 ELECTRICAL POWER SYSTEMS

The electrical power system, or electrical grid, is the network of components which supply, transfer and consume electric power. Electrical power systems provide power over an extended area, typically an entire country, or even continent. There are three primary components of the electrical power system: generation, transmission and distribution. Figure 2.14 provides an overview of the power system architecture; the voltage levels shown are specific to NZ.

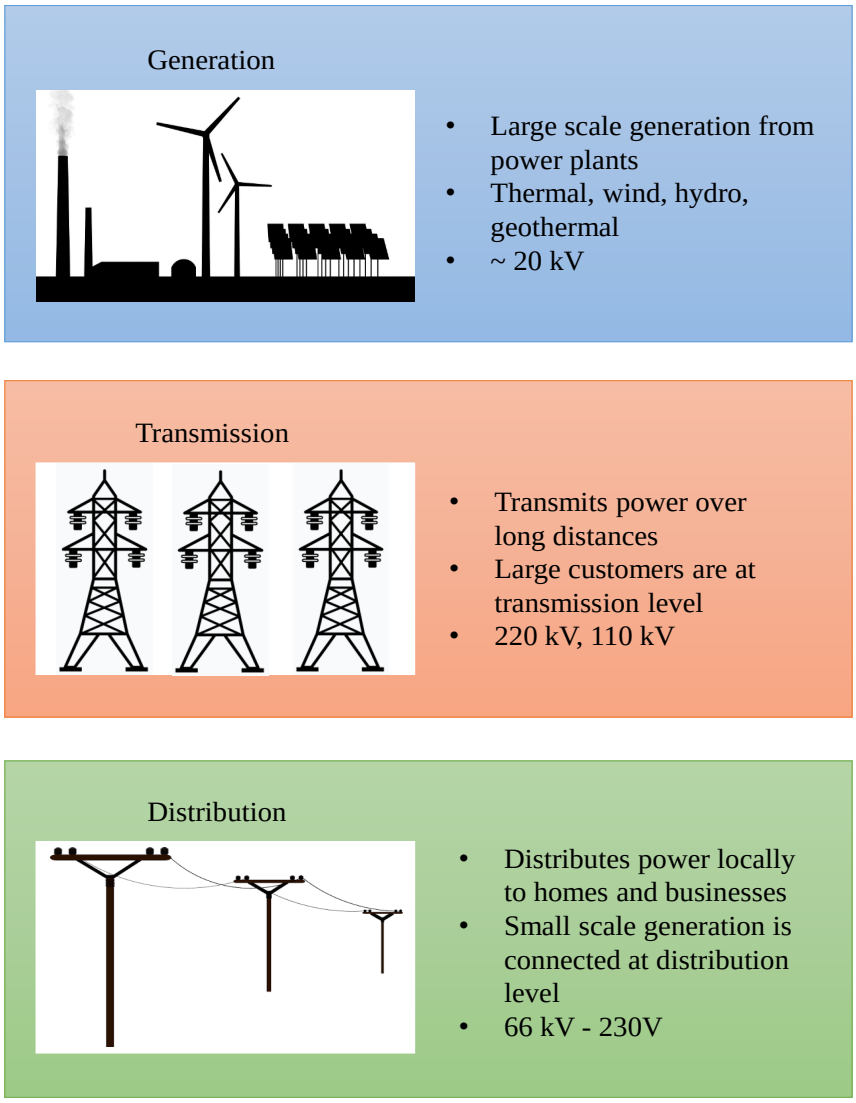

Figure 2.14 Overview of Electrical Power System Architecture

2.4.1 Electrical Power System Architecture

Generation refers to the power plants which generate electricity using some form of primary energy, typically coal, oil, natural gas, nuclear or renewables. At the generation stage, the output voltage is typically around 20kV, which is then stepped-up via a transformer to reduce transmission losses. Distributed generation (DG) refers to small-scale power plants which are embedded within distribution networks.

Transmission networks transmit power over long distances between generation and significant load centres. Transmission networks are characterised by high voltages as well as significant interconnectivity, redundancy and observability. In NZ, transmission voltages are 220kV and 110kV (WorkSafe NZ [2017]).

Transmission and distribution networks are connected via step-down substations. Distribution networks deliver power to end-users. Distribution typically incorporates high, medium and low voltage levels connected through a series of step-down transformers. In NZ, distribution voltages are 66kV, 50kV, 33kV, 22kV and 11kV and 230/400V. Depending on their size customers may be connected at each level. A small number of large customers may also be connected at the transmission level.

2.4.2 Impact of Electric Vehicle Charging in Low-Voltage Distribution Networks

LV distribution networks can be broadly classified as either city, residential, rural or industrial. In NZ, the majority of EV charging will take place in residential settings, and therefore, residential networks will be most severely impacted by EV charging (Watson et al. [2015]).

LV distribution networks are bound by operational limits for voltage, conductor loading and transformer loading, and are described as being constrained when these are violated. In NZ, the voltage magnitude at the point of supply must be within ±6% of the nominal 230V (Watson [2016]). Asset ratings determine the limits for conductor loading and transformer loading.

On-arrival charging will increase the evening peak load, and therefore, worsen network voltage drop. The general impact of EV charging on network voltage drop is illustrated in Figure 2.15. In radial distribution networks, the voltage decreases with distance from the LV transformer. In NZ, LV transformers typically provide a secondary line voltage of 415V or 1.0375 p.u.; this ensures that during peak load conditions, the end of line voltage remains within the statutory limits. When EV charging compounds the evening peak, the end of line voltage may exceed the -6% threshold. When such is the case, some form of mitigation is required. The most common mitigation option is network reinforcement; however, this is expensive, and the associated cost is ultimately passed on to customers.

The EV hosting capacity is defined as the maximum EV penetration level a network can accommodate before becoming constrained. Understanding the EV hosting capacity is the focus of this thesis.

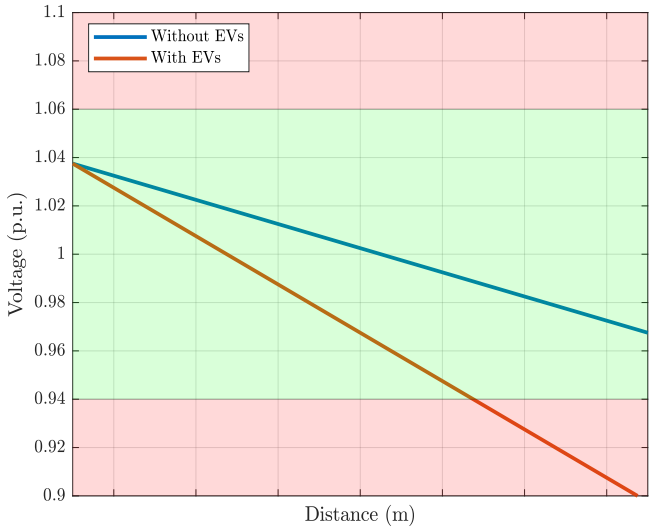

Figure 2.15 Impact of EV Charging on Voltage Drop in Radial Distribution Networks

Chapter 3

LITERATURE REVIEW

EVs will play a crucial role in reducing GHG emissions and fossil fuel dependence. Although NZ's energy landscape is well suited to the electrification of transport, EV integration will not be without challenges. One particular challenge is ensuring that power systems can handle the additional load due to EV charging.

In NZ, it is expected that the majority of EV charging will take place in residential settings, which are connected at LV. DNOs, therefore, need to understand the impact of EV charging on voltage, conductor loading and transformer loading in LV distribution networks. Load-flow simulations allow future scenarios to be assessed a priori.

In the literature, EV charging is assessed in a significant number of load-flow studies; however, these vary in their assumptions, analysis methods, and measures of performance. This chapter aims to provide a comprehensive review of the subject.

When modelling LV distribution networks, the residential and EV load components are typically treated separately. Residential load models are reviewed in Section 3.1, while EV load models are reviewed in Section 3.2.

In the literature, there are examples of both deterministic and stochastic load-flow simulations. When modelling LV distribution networks, a stochastic approach is appropriate, because customer loads are highly uncertain. Stochastic load-flow simulations are more common in recent literature. Stochastic load-flow simulations are reviewed in Section 3.3. The literature review is concluded in Section 3.4, by discussing gaps and limitations in the existing body of knowledge.

3.1 RESIDENTIAL LOAD MODELLING

Residential load models can be classified as either mathematical, data-driven, or after-diversity. Mathematical models use statistics to simulate customer load profiles based on occupancy, property type, appliance ownership and a range of temporal factors.

Data-driven models are based on real-life measurements; typically from SM data. After-diversity load models are based on aggregated load measurements; typically the maximum demand indication at the LV transformer.

3.1.1 Mathematical Models

There are numerous examples in the literature where residential load profiles are simulated by assuming that load variability is normally distributed (Kelly et al. [2009], Conti and Raiti [2007], Hatziargyriou et al. [1993], and Caramia et al. [2007]). In Kelly et al. [2009], load profiles are simulated for three customer classes: residential, office and retail. Each customer class is described by a normalised load curve and an associated standard deviation. The standard deviation describes the load variability during each hour of the day.

There are also numerous examples in the literature where residential load profiles are simulated using an activity-based approach. An activity-based approach is appropriate because residential load profiles are dependent upon domestic activities and the associated use of electrical appliances.

The activity-based approach in Richardson et al. [2010] uses patterns of active occupancy, daily activity diaries, and a library of individual load models for typical appliances. The simulated load profiles have 1-minute temporal resolution and were validated against real-life data measured at 22 properties. The validation process demonstrated that the simulated and measured data were statistically similar.

The activity-based approach in Bizzozero et al. [2016], uses a Markov-chain model based on time-use survey data. The model can simulate daily and diurnal load variations, and was again validated against real-life data. Johnson et al. [2014] uses a similar approach but provides an improved temporal resolution of 1 second. Furthermore, the model includes the effect of outdoor air temperature and solar irradiance.

Rahman and Arnob [2016] recognises that there are several factors which affect residential demand; including the number of occupants, occupant lifestyle, and working hours. When calculating the aggregate load, it is essential to capture the variation in these factors among customers. Residential load profiles are simulated using questionnaire data provided by 400 households. The questionnaire covered a range of topics, including household type, appliance ownership, usage times, and lighting. A series of cumulative distribution functions were fitted based on the usage times provided in the surveys; these describe the probability of performing a particular activity during each hour of the day.

In Jambagi et al. [2015], only the loads directly associated with human activities are modelled using time-use survey data; all other loads are modelled using a standard load profile. It is concluded that without this correction, the aggregate load of several households may be incorrect.

3.1.2 Data-Driven Models

There are numerous examples in the literature where residential loads are modelled using SM data. In Tijani and Butler-Purry [2019], a load-flow simulation was carried out on the IEEE 13 node test feeder. Loads were modelled using a SM dataset which provided a day worth of hourly averaged load data for 18 homes.

A real-life residential network was modelled in Lillebo et al. [2019]. The network contained both apartments and shared housing; which were aggregated as single loads. After aggregation, the total number of connections was 54. The distribution company provided SM data for each connection. The SM dataset provided a years worth of hourly averaged load data and was used to model the 'zero EV' base case; during that year, the surrounding region had only 13 registered EVs for a total population of 38,075.

Iwabuchi et al. [2014] recognises that SM data has considerable utility beyond automated billing and can be used to support system monitoring and control. The author proposes a state estimation method for assessing distribution network voltage using SM measurements. The aim is to reduce modelling errors due to line parameter uncertainties. Load-flow simulations are performed using SM data and are compared with voltage measurements in the real-life network. An optimisation algorithm is then applied, which estimates the actual distribution line parameters.

A similar state estimation method is proposed in Degefa et al. [2013]. The distribution network which is modelled consists of both MV and LV assets; a single primary transformer (110/20kV) feeds 16 secondary transformers (20/0.4kV) supplying a total of 1800 households. Loads are modelled using a SM dataset which provides a years worth of hourly averaged load data. Unlike in Lillebo et al. [2019], the corresponding connections for each SM are not known. Instead, SM load profiles are randomly assigned to individual connections within the simulated network. The load-flow simulation produced short term forecasts of the network state and was validated using real-life voltage measurements. The results show that SM data can be used to forecast customer voltages accurately.

3.1.3 After-Diversity Models

There are numerous examples in the literature where residential loads are modelled using an after-diversity load model. After-diversity load models are commonly used in MV

analysis; here, downstream voltage levels are modelled using lumped loads. Schneider et al. [2008] uses different after-diversity load profiles to reflect climatic differences in different locations.

Although less common, there are examples in the literature where after-diversity load profiles are used in LV analysis; here, individual customer loads are explicitly modelled. In Putrus et al. [2009], different after-diversity load profiles are used for summer and winter. The after-diversity load profiles are based on the aggregate load of 100 customers. The modelled network has four radial feeders, though only one of which is modelled in detail; all others are modelled as lumped loads. Shariff et al. [2016] uses a similar approach; here, a typical after-diversity load profile is scaled to match the maximum demand indication at the LV transformer.

In Tran-Quoc et al. [2012], different after-diversity load profiles are used for different customer classes; residential and industrial. The peak for the residential customer class occurs between 5 pm and 8 pm. On the other hand, the peak for the industrial customer class occurs at 7 am and is maintained until around 6 pm. The author recognises that the shape of these load profiles is similar in most countries. Two LV distribution networks were analysed; one rural and one urban. The number of residential loads was 10 and 71 for the rural and urban networks respectively. Similarly, the number of industrial loads was 2 and 1 for the rural and urban networks respectively.

3.2 ELECTRIC VEHICLE LOAD MODELLING

EV load models can also be classified as either mathematical or data-driven. In Lillebo et al. [2019], an EV load profile was derived using SM data from a household known to charge an EV using a 7.3 kW charger. The EV load profile was derived by subtracting an estimation of the residential load profile from the total reading. Two additional EV load profiles were then created by shifting the original forward and backward by one hour.

Although the EV load profiles are derived from real-life data, the method is limited. Firstly, the method is subject to error because the residential load profile is only an estimate. Secondly, while shifting the EV load profile adds a degree of load diversity, it is unclear whether this is a fair representation of EV load diversity in reality. Finally, it assumes that all EVs are charged using a 7.3 kW charger.

When modelling EV loads, measurement data is not always available or appropriate; therefore, mathematical models are the most common approach in the literature. This section provides a summary of the key considerations when modelling EV load.

3.2.1 Charging Availability

Although public charging infrastructure is being installed, it is expected that the majority of EV charging will take place in residential settings. Vehicles are typically away from home during the day, and therefore, the overnight window provides the best opportunity for charging. The charging availability is the time an EV is at home and hence available for charging.

In Putrus et al. [2009], the charging availability is modelled using the arrival time as the only variable. All EVs arrive home at 6 pm and are charged for 6 hours. The departure time is not required because all charging is completed long before the morning.

There are also numerous examples in the literature where the charging availability is modelled using both the arrival time and departure time as variables. In Tran-Quoc et al. [2012], both the arrival time and departure time are modelled as stochastic variables; both uniform and normal distributions are considered. For the arrival time, the uniform distribution has lower and upper bounds of 5 pm and 8 pm respectively. Similarly, the normal distribution has a mean of 6.30 pm and a standard deviation of 30 minutes. The distributions for the departure time were not described in detail. In Li and Crossley [2014], the arrival time is again modelled using a normal distribution with a mean of 6.30 pm, however here, the standard deviation is 1 hour.

In Papadopoulos et al. [2012] and Shariff et al. [2016], different distributions are used for winter and summer. In each case, the distribution is centred around the time at which the daily peak load occurs. During winter the peak load occurs at 5 pm, while in summer the daily the peak load occurs at 6 pm. In both winter and summer, the standard deviation is 2 hours. Papadopoulos et al. [2012] states that a normal distribution provides the best estimation of home arrival times in the UK, but recognizes that a log-normal distribution could also be used. Although the mean and standard deviation vary in the literature, the assumption that arrival and departure times are normally distributed is common.

In Zdraveski et al. [2019], arrival times are randomly sampled from a dataset containing 150,000 data points. The data comes from a nationwide survey conducted in Macedonia in 2017. Again, a histogram of the dataset suggests that a normal distribution provides a reasonable estimate.

In Farkas et al. [2011], the arrival time was modelled using a Poisson process. A Poisson process provides a good approximation because the number of EVs in the system is significant, the impact of a single EV on the system is minimal, and all EVs behave independently.

In Quirós-Tortós et al. [2015], the charging availability was modelled using the charging start time, rather than the arrival time. Charging start times were randomly sampled from a dataset which was obtained as part of the 'My Electric Avenue' project. The dataset contained the charging start times, initial states of charge, and final states of charge for 221 EVs over one year. The data showed that EV owners often completed a first charge in the morning, as well as a second charge in the evening; therefore the model included the possibility of multiple connections in a single day.

3.2.2 Charging Energy Requirement

The EV battery state of charge (SOC) is depleted each day; the extent of this depletion depends primarily on the total distance, terrain, and driving style. At night, EVs must be charged in order to recover the SOC lost during the day. The recovered energy is the charging energy requirement.

There are numerous examples in the literature where the charging energy requirement is modelled using the arrival SOC as the only variable. Here, the assumption is that EVs are recharged to full each night.

The simplest approach is in Schneider et al. [2008]. Here, EVs are fully discharged each day, and therefore, the charging energy requirement is equal to battery capacity. It is assumed that all EVs have a battery capacity of 10kWh.

In Tran-Quoc et al. [2012], the arrival SOC is modelled as a stochastic variable. The arrival SOC is uniformly distributed between 0% SOC and 80% SOC. The arrival time and arrival SOC are independent variables; that is to say, arriving home late at night is not necessarily indicative of travelling a greater distance. In Kelly et al. [2009], the arrival SOC is again uniformly distributed, however restricted to between 0% SOC and 50% SOC. In Papadopoulos et al. [2012] the upper and lower bounds are unclear.

In Leou et al. [2013], the arrival SOC is again modelled as a stochastic variable, however a normal distribution is assumed. The distribution has a mean of 50% SOC and a standard deviation of 10% SOC.

In Shariff et al. [2016], the assumption is that all EVs are charged to the 80% SOC, rather than to full. The author states that by charging to the 80% SOC, the EV battery life is preserved. The arrival SOC is normally distributed about a mean of 20% SOC; the standard deviation is unclear. In some cases, the departure time requires that EVs are disconnected before reaching the 80% SOC. Based on 1000 MC simulations, the probability of having to disconnect before the 76% SOC is 4%. Similarly, the probability of having to disconnect before the 70% SOC was negligible; indicating that the overnight

charging window is typically sufficient when using 3.6kW chargers. In Farkas et al. [2011] arrival SOC is again modelled as a Poisson process.

There are also examples in the literature where the charging energy requirement is modelled using both the arrival SOC and the departure SOC as variables. In Quirós-Tortós et al. [2015], both the arrival SOC and the departure SOC are randomly sampled from the 'My Electric Avenue' dataset. Different datasets were used for the first and second charging connections each day.

In Li and Crossley [2014], the charging energy requirement is modelled using the daily distance travelled as the only variable. The author recognises that BEVs and PHEVs have different characteristics; and therefore, different battery capacities and energy consumption coefficients are assumed in each case. The energy consumption coefficient is the distance per unit energy consumption. For BEVs and PHEVs, the energy consumption coefficients were 5.26 miles/kWh and 3.52 miles/kWh, respectively. The charging energy requirement is then calculated using the daily distance travelled and the corresponding energy consumption coefficient. The daily distance travelled follows a beta distribution with a mean of 18.7 miles and a maximum value of 100 miles.

A similar approach is used in Zdraveski et al. [2019]. Here, the daily distance travelled is sampled from the dataset based on the 2017 Macedonian survey. Comparing a histogram of the dataset to the beta distribution in Li and Crossley [2014], suggests that a beta distribution provides a good estimation of daily trip distances. Here, the energy consumption coefficients are classified by vehicle type: sedan, van, SUV, and pickup. The van and pickup have the lowest energy consumption coefficients, while the sedan has the highest. The percentage contribution of each vehicle type was again known from the survey data.

In the literature, the charging energy requirement is modelled using either the arrival SOC or the daily distance travelled. Either way, the charging energy requirement is calculated by assuming that EVs are recharged to full each night; or to some other predetermined SOC.

EV trial data suggests that among early adopters, EVs are rarely recharged each day (Jake Roos Consulting [2018]). Instead, EV owners decide whether or not to charge based upon their arrival SOC and predicted range requirement for the following day. Range anxiety describes an EV owners tendency to charge when not required to do so and reflects uncertainty when predicting journeys ahead of time. There are no examples in the literature where range anxiety is adequately captured in the EV load model. Ignoring range anxiety may misrepresent current charging practices in NZ.

3.2.3 Charger Ratings

The charger rating impacts the charge duration. From an EV owners perspective, higher-rated chargers can be beneficial for long or unplanned journeys; this is because the charging energy requirement can be achieved in a shorter time. On the other hand, higher-rated chargers are less desirable from an LV network perspective; especially when un-diversified.

There is a wide range of chargers available; these vary from non-dedicated charging circuits to wall-mounted chargers. In reality, the AC charging rate depends on both the charger rating and the EV model; however, in the literature, the charger rating is used synonymously with the AC charging rate. For consistency, the term charger rating is used throughout this thesis.

LV distribution networks will contain a mixture of different charger ratings. Despite this, there are numerous examples in the literature where a single charger rating is assumed for all EVs (Richardson et al. [2010], Putrus et al. [2009], Quirós-Tortós et al. [2015], Farkas et al. [2011]). The specific charger rating varies between publications, which may reflect differences in the assumed charger and EV models or the local supply voltage. The minimum charger rating was 2.3kW. Similarly, the maximum charger rating was 4.4kW.

There are also numerous examples in the literature where scenarios are defined in order to assess the impact of different charger ratings (Tran-Quoc et al. [2012], Schneider et al. [2008], Cundeva et al. [2018]). For each scenario, a single charger rating is assumed for all EVs.

In Tran-Quoc et al. [2012], load-flow results are compared for charger ratings of 2.1kW and 3kW. Similarly, in Schneider et al. [2008], load-flow results are compared for charger ratings of 1.8kW and 12kW. The author concludes that 12kW charging will require intelligent charging strategies in order to avoid network constraints at high penetration levels. In Cundeva et al. [2018], load-flow results are compared for charger ratings of 3.7kW and 7.4kW. Here, the author concludes that EV hosting capacity is higher when using 3.7kW chargers.

Because LV distribution networks will contain a mixture of different charger ratings, a more appropriate approach is to model the charger rating as a stochastic variable. In Li and Crossley [2014], Zdraveski et al. [2019], and Kelly et al. [2009], two possible charger ratings are considered.

In Li and Crossley [2014], the charger ratings are 2kW and 7kW; the corresponding probabilities are 80% and 20%. In Zdraveski et al. [2019], the charger ratings are again

2kW and 7kW; however, the corresponding probabilities are 70% and 30%. Here, 2kW chargers are single-phase, while 7kW chargers are three-phase.

In Kelly et al. [2009], the charger ratings are 1.4kW and 7.6kW. Here, the corresponding probabilities vary as the EV penetration is increased. At the 5% penetration level, the corresponding probabilities are 75% and 25%, while at the 25% penetration level, the corresponding probabilities are 90% and 10%.

In Papadopoulos et al. [2012], three possible charger ratings are considered. The charger rating is assigned based on vehicle type; either PHEV or BEVs. For all PHEVs, the charger rating is 3kW. For all BEVs, the charger rating can be either 3kW, 7kW, or 22kW; the corresponding probabilities are 70%, 20%, and 10%. It is assumed that PHEVs are twice as common as BEVs.

In Leou et al. [2013], each EV can use two different rates of charge; these are 1.9kW and 6.6kW. The rate of charge is selected based on the charging energy requirement; this ensures that the higher-rated chargers do not contribute unnecessarily to peak load, when not required to do so.

3.2.4 Battery Capacities

In the literature, the charging energy requirement is modelled using either the arrival SOC or the daily distance travelled. In both cases, the charging energy requirement is calculated by assuming that EVs are recharged to full each night; or to some other predetermined SOC. When using the arrival SOC, the charging energy requirement is directly proportional to the battery capacity; this is because the arrival SOC is expressed as a percentage of the battery capacity. On the other hand, when using the daily distance travelled, the charing energy requirement independent of the battery capacity because only the daily energy use is replenished.

While early PHEVs have relatively small batteries, modern BEVs have larger batteries. LV distribution networks will contain a mixture of EVs with different battery capacities. Despite this, there are again numerous examples in the literature where a single battery capacity is assumed for all EVs (Tran-Quoc et al. [2012],Schneider et al. [2008], Quirós-Tortós et al. [2015], Farkas et al. [2011]). The specific battery capacity varies between publications, which may reflect differences in the assumed EV model. The minimum battery capacity was 10kWh. Similarly, the maximum battery capacity was 30kWh.

There are also numerous examples in the literature where different battery capacities are assigned for PHEVs and BEVs (Kelly et al. [2009], Shariff et al. [2016], Papadopoulos et al. [2012], and Li and Crossley [2014]). Again the specific battery capacities vary

between publications; however, on average PHEV batteries are around one-third of the size of BEV batteries. The battery capacities for PHEVs were between 4.85kWh and 9kWh. Similarly, the battery capacities for BEVs were between 16.6kWh and 35kWh.

In Li and Crossley [2014], different battery capacities are again assigned for PHEVs and BEVs. Here, however, the battery capacity is modelled as a stochastic variable. The battery capacity for PHEVs is normally distributed with a mean of 16kWh and a standard deviation of 2kWh. The battery capacity for BEVs is normally distributed with a mean of 20kWh and a standard deviation of 2kWh.

In Zdraveski et al. [2019], different battery capacities are assigned by vehicle type: sedan, van, SUV, and pickup. The range is defined as the maximum distance, which can be covered by a single charge. The battery capacity is calculated using the range and the energy consumption coefficient for each vehicle type. For each vehicle type, there is a battery capacity for three different ranges; 48km, 64km, and 96km. Both the vehicle type and battery capacity are modelled as a stochastic variable.

3.2.5 Charging Strategies

The charging strategy describes how EV load is scheduled, subject to the relevant constraints. The most straightforward charging strategy is on-arrival charging. Here, charging begins on arrival and continues at rated capacity until either the battery is full or some other predetermined SOC is reached.

The on-arrival charging strategy is often referred to as passive charging and is the strategy which EV owners are expected to adopt naturally. The impact of EV charging in LV distribution networks may be reduced by adopting alternative charging strategies. Alternative charging strategies include delaying charging until later in the evening, as well as more sophisticated charging strategies which implement optimized routines via third party intermediaries.

There are numerous examples in the literature where the on-arrival charging strategy is used as the baseline against which alternative strategies are compared. In Putrus et al. [2009], the on-arrival charging strategy is compared with two alternatives. The first alternative imitates a simple day-night tariff structure; here, EV charging is delayed until 1 am. In the second alternative, EV charging is evenly staggered throughout the day. Four charging start times are assigned with equal probability; these are 11 pm, 5 am, 12 pm, and 6 am. The results show that network constraints are reduced when EVs charging is delayed until 1 am. However, staggering EV charging throughout the day provides the best performance.

Although the results provide some useful insights, they are in other ways limited. The second alternative charging strategy does not consider EV availability; because EVs are typically away from home during the day, this charging strategy will not be practically feasible.

In Leou et al. [2013], the on-arrival charging strategy is compared with a centrally controlled charging scheme. The charging scheme is triggered when an under-voltage is detected in the network. The charging schedule for each EV is then adjusted according to a priority index based on the battery SOC and the scheduled departure time.

Ovalle et al. [2018] proposes an optimized charging scheme based on dynamic programming. The arrival time, departure time, and charging energy requirement are provided for each EV. The objective function is the standard deviation of the transformer load profile. For each EV in turn, the optimal charging schedule is evaluated. The results show that the valley of the transformer load profile is effectively filled.

There are also numerous examples in the literature where the charging strategy is modelled as a stochastic variable. In Li and Crossley [2014], two possible charging strategies are considered; these are on-arrival and delayed. The corresponding probabilities are 70% and 30%. The delayed charging strategy is similar to that proposed in Putrus et al. [2009]; however, here, the delayed charging start time is also modelled as a stochastic variable. The delayed charging start time is normally distributed with a mean of 12 am and a standard deviation of 30 minutes. The stochastic approach is compared with a deterministic approach where all EVs are charged on arrival. The results show that the total number of constrained periods is reduced in the stochastic case; however, new constraints occur around the time when delayed charging begins. The author recognizes that more sophisticated charging strategies could reduce these new constraints.

A similar approach is used in Papadopoulos et al. [2012]; however, here, the probabilities for on-arrival and delayed charging are 84% and 16%, respectively. Furthermore, the stochastic approach is compared with centrally controlled charging scheme similar to that proposed in Leou et al. [2013].

The charging scheme is triggered if the limits for either voltage, conductor loading, or transformer loading are violated. When triggered, each EV is then assessed in turn. Charging is delayed until the following time interval if this does not interfere with the requirements of the EV owner. The load-flow equations are then re-solved before the next EV is assessed. The process is only repeated if the violations are not resolved. When compared to the stochastic case, the centrally controlled charging scheme eliminates all voltage violations at low EV penetration levels.

3.2.6 Electric Vehicle Placements

When modelling LV distribution networks, the locations of individual customer connections are typically known; however, when modelling future scenarios, it is often unknown which customers have EVs. The term EV placement describes the customers who have EVs and is a common source of uncertainty when modelling LV distribution networks. EV load placement can significantly impact load-flow results.

There are numerous ways in which this uncertainty is captured in the literature. In Putrus et al. [2009] and Schneider et al. [2008], EV loads are modelled using an after-diversity load profile. EV load placement is ignored because the aggregate load is averaged across all customer connections. Such an approach is the most straightforward; however, assuming perfectly balanced conditions may underestimate constraints.

There are other examples in the literature where scenarios are defined in order to describe several best and worst-case placements. Three scenarios were defined in Richardson et al. [2010]. In the first scenario, EVs are placed at the customers furthest away from the LV transformer, while in the second scenario, EVs are placed at the customers closest to the LV transformer. In both scenarios, EV placements are balanced across the phases. In the third scenario, EVs are only placed at customers on phase A. The author recognizes that although these scenarios are unlikely to occur, they provide an indication of the range between the best and worst-case placements.

In Li and Crossley [2014], a single, worst-case placement is compared with a single random placement; these are referred to as the unbalanced and balanced scenarios, respectively. In the balanced scenario, EV placements are assigned using a uniform distribution. In the unbalanced scenario, EV placements are assigned to customer connections on phase A only, beginning with those furthest away from the LV transformer. Once every customer on phase A has an EV, the process is repeated for phases B and C.

The results show that EV placement significantly impacts load-flow results. In the balanced scenario, voltages are within the statutory limits at each penetration level. In the unbalanced scenario, voltages drop below the statutory limits at the 50% penetration level. The author recognizes that when EV placements are re-sampled, the load-flow results may vary.

There are also numerous examples in the literaure where random EV placements are repeated (Tran-Quoc et al. [2012], Papadopoulos et al. [2012], Kelly et al. [2009], Leou et al. [2013], Cundeva et al. [2018], Shariff et al. [2016], Farkas et al. [2011], Quirós-Tortós et al. [2015], and Zdraveski et al. [2019]); this allows the distribution of possible load-flow results to be obtained. Tran-Quoc et al. [2012] concludes that EV placement significantly impacts phase imbalance and because of this, the load-flow results at the 10% penetration

level, are often worse than those at the 20% penetration level. The results show that repeating random EV placements is the most appropriate method.

3.3 STOCHASTIC LOAD-FLOW SIMULATIONS

Load-flow simulations can be broadly classified as either deterministic or stochastic. Deterministic simulations produce a single result and are prevalent in traditional planning practices. On the other hand, stochastic simulations produce probabilistic results. When modelling LV distribution networks, a stochastic approach is appropriate because customer loads are highly uncertain.

Despite this, there are examples of deterministic simulations in the earlier literature (Richardson et al. [2010], Putrus et al. [2009], Schneider et al. [2008]). In the more recent literature, however, there is a trend towards stochastic load-flow simulations. Stochastic load-flow simulations are reviewed in this section.

3.3.1 Simulation Time Horizon and Temporal Resolution

Load-flow simulations can also be classified as either steady-state (SS) or quasi-steady-state (QSS). SS simulations are typical in traditional planning practices and consider only a single time-period. On the other hand, QSS simulations capture time-dependent aspects, including the interactions between load, generation and control. The computational burden is lower for SS simulations; however, QSS simulations can be more informative.

There are numerous examples of SS simulations in the literature. In Watson et al. [2015], the load-flow equations are solved during the maximum demand time-period. The network maximum demand was known from an indication on the LV transformer. Customer load data was not available, and therefore, the transformer load was uniformly distributed between customer connections. Future scenarios were then assessed by superimposing EV loads based on an assumed charger rating.

A similar approach was used in Cundeva et al. [2018]; however, here, two time-periods were examined. The periods which were chosen reflected the maximum and minimum networks demands; these were 119 kVA and 68 kVA, respectively and occurred during the winter and summer. The transformer load was again uniformly distributed among customers; the corresponding loads per household were 747.5 W and 425 W.

In QSS simulations, the computational burden depends on both the time horizon and the temporal resolution. The most common time horizon in the literature is one day; this is because interactions between load and generation follow patterns which are repeated daily.

The temporal resolution, however, varies significantly; the most common resolutions are 1 minute (Quirós-Tortós et al. [2015] and Li and Crossley [2014]), 15 minutes (Farkas et al. [2011] and Zdraveski et al. [2019]) and 30 minutes (Papadopoulos et al. [2012], Kelly et al. [2009] and Shariff et al. [2016]). While in some cases there is a trade-off between temporal resolution and computational burden, the temporal resolution of the simulation is often limited by the resolution of available load data.

In Li and Crossley [2014], the author recognizes that sub-10-minute resolution is not required for network planning purposes because, in Europe, the statutory limits specify a 10-minute averaging period. Results obtained using higher-resolution data will, therefore, need to be averaged before being assessed.

3.3.2 Interpretation of Probabilistic Results

In stochastic simulations, the load-flow equations are solved repetitively using a Monte Carlo (MC) method. For each MC repetition, the stochastic variables are resampled, producing a distribution of possible results. Within the literature, there are numerous ways in which these probabilistic results are interpreted.

In Cundeva et al. [2018], the minimum network voltage is recorded for each MC repetition. Voltage violations are then assessed using the 10^{th} percentile of the recorded voltages. The author concludes that for their test case, the statutory limits are violated at the 100% penetration level.

In Shariff et al. [2016], both EV charging and DG are assessed. Here, the results show a histogram for transformer loading, network voltages, and power system losses. The results are limited because the exact meaning of these histograms is ambiguous. As an example consider network voltages; it is unclear whether the histogram describes the distribution of voltages across all customer connections, time intervals, and MC repetitions or whether the histogram describes the distribution of the minimum network voltages across all MC repetitions.

In Tran-Quoc et al. [2012], the results are the transformer load profile and the minimum network voltage profile. Again the results are limited because it is unclear how these load profiles were interpreted from the greater population of profiles produced by the MC simulation. There is a unique profile for each MC repetition, and therefore, the meaning of these load profiles is ambiguous. The author concludes that the transformer becomes overloaded above the 20% penetration level; however, no voltage violations are observed, even at the 100% penetration level.

In Kelly et al. [2009], the first result is the transformer load profile; however, it is clear how the result was interpreted from the greater population of profiles produced by the MC simulation. A plot shows the mean transformer load profile across all MC repetitions. Error bars indicate the minimum and maximum load values during each time step. The second result is a histogram of network voltages; more specifically, a histogram of the 6 pm voltages at the most heavily loaded bus. The results show that when the EV penetration is increased, the histogram shifts significantly towards lower voltages. The author concludes that voltage regulation may be required to accommodate future EV penetration levels.

In Leou et al. [2013], congestion indices are defined for both voltage drop and conductor loading. The congestion indices define the mean and maximum values, across both network locations and simulation time steps. The results show the mean value of the mean congestion index across all MC repetitions. Furthermore, the minimum and maximum values of the maximum congestion index are also shown. The congestion indices are used to compare the results from deterministic and stochastic load-flow simulations. The author concludes that deterministic simulations underestimate congestion due to load uncertainty and therefore, a stochastic approach is appropriate.

In Quirós-Tortós et al. [2015], the first result is the utilisation factor. For a particular asset, the utilisation factor is the maximum loading divided by the rated capacity. The utilisation factor is plotted as a function of the EV penetration level. At each penetration level, bars indicate the distribution of results across all MC repetitions. The second result is the percentage of customers with voltage violations. Both the mean and standard deviation are plotted as a function of the EV penetration level. Again both of these results are used to compare deterministic and stochastic load-flow simulations. The author concludes that deterministic simulations underestimate a small number of voltage violations which are observed in stochastic simulations.

In Li and Crossley [2014], both EVs and heat pumps are assessed. Here, the results are the voltage magnitude and unbalance factor profiles. Both are recorded at the end of a single feeder. Plots show the mean and fifth percentile profiles across all MC repetitions. The minimum daily voltage is significantly lower for the fifth percentile voltage profile. The author concludes that EV hosting capacity is significantly reduced when using the fifth percentile as an acceptability criteria.

In Papadopoulos et al. [2012], three operational states are defined: normal, alert, and emergency. For voltage, normal operation means the voltage at the most remote customer is between 0.95 p.u. and 1.09 p.u. Alert operation means the voltage at the most remote customer is between 0.94 p.u. and 0.95 p.u. or between 1.09 p.u. and 1.10 p.u. Emergency operation means the voltage at the most remote customer is either less than 0.94 p.u. or greater than 1.10 p.u.

The most vulnerable conductor in the network had been identified in previous research. For conductor loading, normal operation means the load in the most vulnerable conductor is between 0 p.u. and 1.00 p.u. Alert operation means the load in the most vulnerable conductor is between 1.00 p.u. and 1.45 p.u. Emergency operation means the load in the most vulnerable conductor is greater than 1.45 p.u. The operational states for transformer loading were similar; however, the upper threshold of the alert state was extended during the winter in order to account for the impact of ambient temperature.

Low, medium and high penetration levels are assessed; these correspond to 12.5%, 33.3%, and 70.8%, respectively. The results are the state probabilities at the various EV penetration levels. The results show that the network is constrained by transformer and conductor loading. At the low penetration level, the emergency state probability is significant for both conductor and transformer loading. On the other hand, the emergency state probability for voltage is low; however, it can be seen to increase with EV penetration.

3.3.3 Simulation Convergence

There are numerous examples in the literature where the number of MC repetitions is defined a priori (Leou et al. [2013], Quirós-Tortós et al. [2015], Cundeva et al. [2018] and Zdraveski et al. [2019]). The number of repetitions varies significantly; in Quirós-Tortós et al. [2015], only 100 repetitions are performed. On the other hand, in Cundeva et al. [2018], 10,000 repetitions are performed.

When the number of MC repetitions is defined a priori, the chosen number may be either too few or too many repetitions; when compared to the number required. When the chosen number is too few, the distribution of results may not have stabilised. On the other hand, when the chosen number is too many, the simulation run time is unnecessarily increased. Such risks can be mitigated by using an appropriate convergence criterion.

There are also examples in the literature where the MC simulation is terminated based on a convergence criterion. In Li and Crossley [2014], the author states that the MC simulation is repeated until convergence; however, the convergence criterion and tolerance are not explicitly stated. Similarly, in Kelly et al. [2009], 350 MC repetitions are performed. The author states that the value was chosen based on a convergence analysis; however, the criterion and tolerance are again not stated.

In Tran-Quoc et al. [2012], the mean voltage and transformer loading are plotted as a function of the number of MC repetitions. The author states that both are stable by 500 repetitions; however, the tolerance is again not clear.

In Papadopoulos et al. [2012], the author states that, for convergence, the standard error of nodal voltages during each time-step should be below 0.001%. This is a common criterion used in load-flow software packages; however, it refers to the convergence of the iterative method used to solve the load-flow equations, and not the distribution of results across all MC repetitions.

3.4 LIMITATIONS

In the literature, EV charging is assessed in a significant number of load-flow studies; however, these vary in their assumptions, analysis methods and measures of performance.

There are examples of both deterministic and stochastic load-flow simulations. Deterministic simulations produce a single result and are prevalent in traditional planning practices. On the other hand, stochastic simulations produce probabilistic results. When modelling LV distribution networks, a stochastic approach is appropriate because customer loads are highly uncertain. Furthermore, results show that when modelling LV distribution networks, deterministic simulations often underestimate constraints.

The concept of hosting capacity is commonly cited in the literature when assessing the impact of DERs (Hes et al. [2019] and Maduranga et al. [2019]). The EV hosting capacity is the maximum EV penetration level a network can accommodate before becoming constrained. With deterministic load-flow simulations, each LV network has a single EV hosting capacity. With stochastic load-flow simulations, each LV network has a distribution of EV hosting capacities; that is to say, the EV hosting capacity is uncertain because of the uncertainty in customer loads.

The results in Papadopoulos et al. [2012] demonstrate uncertainty in the EV hosting capacity. At the low EV penetration level, the normal state probability for voltage is high. Similarly, at the high EV penetration level, the emergency state probability for voltage is high. At the medium EV penetration level, however, there is a reasonable probability of either the normal, alert or emergency state; because of this, the EV hosting capacity is uncertain.

When interpreting stochastic load-flow results, it is important to consider:

- The definition of a more extreme result
- The probability of a more extreme result
- The severity of more extreme results

When operational limits for voltage, conductor loading or transformer load are violated, it is important to consider both the magnitude and duration, because, together, these

provide a clearer indication of severity. In the current literature, there are no examples where EV hosting capacity is assessed when taking into account both the magnitude and duration. This thesis presents a framework for assessing EV hosting capacity using flexible criteria, which overcomes this limitation.

Chapter 4

STOCHASTIC EV LOAD MODEL

The NZ EV fleet has doubled in each of the last three years (Energy Efficiency and Conservation Authority [2019]). In the future, networks may become constrained because of the additional load associated with EV charging. Load-flow simulations allow future scenarios to be assessed a priori and require appropriate models for both residential and EV load.

This chapter describes the stochastic EV load model. Variable time indexing is discussed in Section 4.1. Section 4.2 introduces the model variables, including the relationships between them.

The charging strategy describes how EV load is scheduled, subject to the relevant constraints. While some EV owners charge on arrival, others delay charging until later in the evening. Three charging strategies are considered in this thesis: on-arrival (OA), day-night tariff (DNT) and by-morning (BM). Each of these is described in Section 4.3.

The model includes seven stochastic variables:

- Arrival time
- Departure time
- Daily distance travelled
- Battery Capacity
- Charger rating
- Range Anxiety
- Charging strategy

Section 4.4 describes the distributions from which these are sampled.

The model simulates EV load data for each customer in the typical residential network. The stochastic variables are re-sampled for each EV, which allows a diverse range of charging behaviours to be captured. Section 4.5 provides examples of the simulated EV load profiles.

4.1 TIME INDEXING

The model simulates weekly EV load profiles with 30-minute temporal resolution. 30-minute temporal resolution was chosen to provide consistency with the SM data used to model residential loads.

Variables change during the simulation; for some variables, the temporal resolution is one day, while for others, the temporal resolution is 30 minutes. Variables are indexed using either the day index, d, or the time index, t. The day index, d, is the day of the week; numbered from Monday through to Sunday. The time index, t, is the half-hour interval; numbered from 00:00-00:30 on Monday through to 23:30-00:00 on Sunday. Both time indices can be seen in Table 4.1, for the first two days of the week.

Table 4.1 Examples of Day and Time Indices

dd/mm/yy	18/06/12				19/06/12			
day index (d)	1				2			
hh:mm	00:00-00:30	00:30-01:00	...	23:30-00:00	00:00-00:30	00:30-01:00	...	23:30-00:00
time index (t)	1	2	...	48	49	50	...	96

4.2 MODEL DESCRIPTION

EVs depart home in the morning and return in the evening. The departure and arrival times are denoted δ_d and α_d, respectively. For both variables, the units are time index, and the subscript indicates the day of the week.

Charging cannot begin until after α_d. Similarly, charging must be completed before δ_{d+1}. The availability window, μ_d, is the length of time where charging can take place and is calculated using Equation 4.1. The availability window overlaps successive days and, therefore, the convention is that, μ_d, is the availability window beginning on the d^{th} day.

$$\mu_d = \delta_{d+1} - \alpha_d - 1 \tag{4.1}$$

The entire availability window is not always used. Instead, the load schedule is defined by the charging start and end times, $\underline{\lambda}_d$ and $\overline{\lambda}_d$, respectively. The charging strategy determines how these are calculated. Different charging strategies are discussed in Section 4.3.

$\underline{S}$ and $\overline{S}$ are the minimum and maximum permissible SOCs; these are calculated using Equations 4.2 and 4.3, respectively, where C is the battery capacity. The battery is charged between 0% and 80% SOC, which is a common assumption because regularly charging above 80% SOC can reduce the battery lifetime (Shariff et al. [2016]).

$$\underline{S} = C \times 0 \tag{4.2}$$

$$\overline{S} = C \times 0.8 \tag{4.3}$$

Both journeys and charging events impact the battery SOC; journeys take place during the day while charging events take place at night. The driving energy requirement, β_d, is calculated using Equation 4.4, where ϕ_d is the daily distance travelled. The assumed rate of energy consumption is 0.2 kWh/km; this value was chosen to provide consistency with previously published reports in New Zealand (Concept Consulting [2018]). In reality, this is a simplification and the rate of consumption will vary depending on the vehicle type (PHEV or BEV), vehicle model, terrain, and driving style (Zdraveski et al. [2019]).

$$\beta_d = \phi_d \times 0.2 \tag{4.4}$$

$\ddot{S}_d$ and $\dot{S}_d$ are the departure SOC and arrival SOC, respectively. These are related through the driving energy requirement, as seen in Equation 4.5. It is assumed that on the first day of the week, the EV departs home with the maximum permissible SOC; that is to say, $\ddot{S}_d = \overline{S}$.

$$\dot{S}_d = \ddot{S}_d - \beta_d \tag{4.5}$$

A curtailed journey event, θ_d, is recorded when the departure SOC is insufficient to cover the driving energy requirement. In such case, the arrival SOC is 0%; the arrival time is unaffected. Curtailed journey events are calculated using Equation 4.6.

$$\theta_d = \begin{cases} 0, & \text{if } \ddot{S}_d \geq \beta_d \\ 1, & \text{if } \ddot{S}_d < \beta_d \end{cases} \tag{4.6}$$

Charging events relate the arrival SOC on a given day, $\dot{S}_d$, to the departure SOC the following day, $\ddot{S}_{d+1}$. A target SOC, $\hat{S}_{d+1}$, is defined for every charging event. EVs are not necessarily recharged every day; instead, EV owners decide whether or not to charge based upon their arrival SOC and predicted driving energy requirement for the following day. Range anxiety describes the tendency to charge when not required to do so and reflects uncertainty when predicting, β_{d+1}, ahead of time.

The range anxiety factor, F, is a dimensionless variable which can take values between 0 and 1. The range anxiety factor is used to calculate the threshold SOC, $\tilde{S}_d$, as seen in Equation 4.7.

$$\tilde{S}_d = F \times (\overline{S} - \beta_{d+1}) + \beta_{d+1} \tag{4.7}$$

The EV is only charged if the arrival SOC is less than the threshold SOC. The decision regarding whether or not to charge is implemented through the target SOC, as seen in Equation 4.8.

$$\hat{S}_{d+1} = \begin{cases} \overline{S}, & \text{if } \dot{S}_d < \tilde{S}_d \\ \dot{S}_d, & \text{if } \dot{S}_d \geq \tilde{S}_d \end{cases} \tag{4.8}$$

When the arrival SOC is less than the threshold SOC, the target SOC is set to the maximum permissible SOC; this ensures that the EV charges to the maximum permissible SOC when possible. When the arrival SOC is greater than the threshold SOC, the target SOC is set to the arrival SOC; this ensures that the EV is not charged.

In the literature review, it was stated that when using the daily distance travelled, the charging energy requirement is independent of the battery capacity because only the daily energy use is replenished each day. When range anxiety is captured, this is no longer the case because having a higher battery capacity allows an EV to go a more significant number of days without being recharged. For days between charges, the charging energy requirement will be zero. On the other hand, the charging energy requirement will be more significant for days when the EV is charged.

In some cases, the target SOC cannot be achieved given the availability window and charger rating. The maximum departure SOC, $\overline{\ddot{S}}_{d+1}$, is calculated using Equation 4.9. R is the charger rating and Δt is the simulation time step expressed in hours. The departure SOC is then calculated using Equation 4.10.

$$\overline{\ddot{S}}_{d+1} = \dot{S}_d + (R \times \Delta t \times \mu_d) \tag{4.9}$$

$$\ddot{S}_{d+1} = \min(\overline{\ddot{S}}_{d+1},\ \hat{S}_{d+1}) \tag{4.10}$$

An incomplete charge event, η_d, is recorded when the maximum departure SOC is less than the target SOC. Incomplete charge events are calculated using Equation 4.11.

$$\eta_d = \begin{cases} 0, & \text{if } \overline{\ddot{S}}_{d+1} \geq \hat{S}_{d+1} \\ 1, & \text{if } \overline{\ddot{S}}_{d+1} < \hat{S}_{d+1} \end{cases} \tag{4.11}$$

The charging energy requirement, γ_d, is the stored energy gained during the availability window and is calculated using Equation 4.12.

$$\gamma_d = \ddot{S}_{d+1} - \dot{S}_d \tag{4.12}$$

Ω_t is the EV charging load during the t^{th} time interval. The availability window, charger rating, and charging energy requirement all place constraints on the EV charging load.

The availability window constraint can be seen in Equation 4.13. Charging must be completed before δ_d, and charging cannot begin until after α_d.

$$\Omega_t = 0, \qquad \forall t \in \{\delta_d, ..., \alpha_d\},\ \forall d \tag{4.13}$$

The charger rating constraint can be seen in Equation 4.14. Bidirectional capability is not considered and charging occurs at rated capacity only. This is commonly referred to as unidirectional, on/off charging.

$$\Omega_t = 0 \vee R, \qquad \forall t \in \{\alpha_d + 1, ..., \delta_{d+1} - 1\},\ \forall d \tag{4.14}$$

The charging energy requirement constraint can be seen in Equation 4.15; this ensures that the departure SOC is met.

$$\Delta t \sum_{t=\alpha_d+1}^{\delta_{d+1}-1} \Omega_t = \gamma_d,\ \forall d \tag{4.15}$$

Each constraint is implemented when calculating the charging start and end times, $\underline{\lambda}_d$ and $\overline{\lambda}_d$, respectively. This process is described in Section 4.3. The EV load profile is then constructed using Equation 4.16.

$$\Omega_t = \begin{cases} 0, & \forall t \in \{\overline{\lambda}_{d-1} + 1, ..., \underline{\lambda}_d - 1\},\ \forall d \\ R, & \forall t \in \{\underline{\lambda}_d, ..., \overline{\lambda}_d\},\ \forall d \end{cases} \tag{4.16}$$

On the first day of the week, Equation 4.16 is replaced by 4.17; this is because the charging end time from the previous day, $\overline{\lambda}_{d-1}$, is not known.

$$\Omega_t = \begin{cases} 0, & \forall t \in \{0, ..., \underline{\lambda}_d - 1\},\ \forall d \\ R, & \forall t \in \{\underline{\lambda}_d, ..., \overline{\lambda}_d\},\ \forall d \end{cases} \tag{4.17}$$

4.3 EV CHARGING STRATEGIES

The charging strategy defines how EV load is scheduled, subject to the relevant constraints. Three charging strategies are considered in this thesis: on-arrival (OA), day-night tariff (DNT) and by-morning (BM). These were chosen because they can be implemented using a non-dedicated charging cable, and by the majority of EV models.

4.3.1 On-Arrival Charging

The OA charging strategy is depicted in Figure 4.1a. OA is the strategy which EV owners are expected to adopt naturally. The charging start and end times are calculated using Equations 4.18 and 4.19 respectively. Charging cannot begin until after α_d; therefore, charging starts at the subsequent time index. The charging end time depends on the charging energy requirement and charger rating.

$$\underline{\lambda}_d = \alpha_d + 1 \tag{4.18}$$

$$\overline{\lambda}_d = \underline{\lambda}_d + \frac{\gamma_d}{\Delta t \times R} - 1 \tag{4.19}$$

4.3.2 Day-Night Tariff Charging

Electricity retailers offer day-night tariffs to incentivise appliance usage overnight. The night tariff start time varies between electricity retailers; however, typical start times include 9 pm, 11 pm, and midnight. Here, the night tariff start time is midnight. ζ_d is the night tariff start time on the d^{th} day of the week. The units for ζ_d are the time index t.

The DNT charging strategy is depicted in Figure 4.1b. The charging start time is calculated using Equation 4.20. Ordinarily, charging starts at the night tariff start time; however, if the EV arrives after the night tariff start time, the strategy defaults to OA.

$$\underline{\lambda}_d = \begin{cases} \zeta_d, & \text{if } \alpha_d < \zeta_d \\ \alpha_d + 1, & \text{if } \alpha_d \geq \zeta_d \end{cases} \tag{4.20}$$

Equation 4.9 is no longer valid because the entire availability window cannot be utilised. Instead, the maximum departure SOC is calculated using Equation 4.21. The charging end time is then calculated using Equation 4.19.

$$\overline{\ddot{S}}_{d+1} = \dot{S}_d + (R \times \Delta t \times (\delta_{d+1} - \zeta_d)) \tag{4.21}$$

4.3.3 By-Morning Charging

The BM strategy is depicted in Figure 4.1c. The charging start and end times are calculated using Equations 4.23 and 4.22 respectively. Charging is delayed until the latest possible time while ensuring that the departure SOC is reached. The majority of EV models can implement the BM strategy. The vehicles onboard charger calculates the charging start time based on the battery SOC and the departure time, as set by the EV owner.

$$\overline{\lambda}_d = \delta_{d+1} - 1 \tag{4.22}$$

$$\underline{\lambda}_d = \overline{\lambda}_d - \frac{\gamma_d}{\Delta t \times R} + 1 \tag{4.23}$$

4.3.4 Load Magnitude Correction to Account for Temporal Resolution

For each charging strategy, the load schedule is defined by the charging start and end times, $\underline{\lambda}_d$ and $\overline{\lambda}_d$, respectively. The charge duration depends on the charging energy requirement, γ_d, and the charger rating, R. The charge duration is rounded upwards to the nearest integer value; this is necessary because non-integer values violate the temporal resolution of the model. The load magnitude is then adjusted to ensure that only the charging energy requirement is supplied. To demonstrate this process, consider the variable values in Table 4.2. Let us also assume the OA charging strategy.

Table 4.2 Example Variable Values to Demonstrate Load Magnitude Correction

Variable	Value
γ_d	7 kWh
R	4 kW
$\underline{\lambda}_d$	10

The charging end time, $\overline{\lambda}_d$, is calculated using Equation 4.19. The calculated value is 12.5, which is rounded up to 13. The load magnitude during $\overline{\lambda}_d$ is reduced to $\frac{R}{2}$; this ensures that the energy supplied to the battery matches charging energy requirement.

4.4 STATISTICAL DISTRIBUTIONS

Many of the variables which describe the EV load model cannot be precisely predicted. For example, the daily distance travelled, ϕ_d, will vary for each day of the week. Furthermore, the daily distance travelled will vary for each EV. When variables cannot be precisely predicted, a stochastic approach is appropriate; here, variables are assumed to follow a random probability distribution. The EV load model has seven stochastic variables. The stochastic variables are presented in Table 4.3, alongside the distributions from which they are sampled. The arrival time, departure time, and daily distance travelled are re-sampled for each day of the week. On the other hand, the battery capacity, charger rating, range anxiety factor, and charging strategy are sampled once, at the beginning of the week.

The chosen probability distributions reflect, where possible, statistics and information which is available on EV charging in New Zealand. For some of the variables however, no statistics or useful information was available; for these, the distributions were chosen based on the literature review. Sections 4.4.1 -4.4.6 provide justifications for the probability distributions which were chosen.

Even for those variables where the necessary statistics are available, it is important to recognize that these describe EV charging practices at present. The EV landscape is continuously evolving and EV charging practices are likely to change in the future. As an example, let us consider the EV charger rating. The EV charger rating is sampled from a multinomial distribution which produces three discrete ratings: 2kW, 4kW, and 8kW. These ratings, and the associated probabilities, were chosen based on ownership statistics for various EV and charger models in New Zealand. In the future, the contribution of different EV and charger models will change as new products are released. Any uncertainty

regarding future charging practices can be assessed by performing sensitivity studies. An example of a sensitivity study is presented in Section 6.4 where the appropriate probability distributions are adjusted to reflect:

- Using lower-rated chargers
- Reducing range anxiety
- Using an even mix of charging strategies

In the future, the most appropriate adjustments will be able to be made once insights into future charging practices become clearer.

4.4.1 Arrival and Departure Times

Arrival and departure times are sampled from a normal distribution. The arrival time distribution has a mean of 6 pm and a standard deviation of one hour. Similarly, the departure time distribution has a mean of 8 am and a standard deviation of one hour; it is assumed that there is no correlation between arrival and departure times. All samples are converted to units of time index, based on the time intervals in Table 4.1.

Arrival and departure time data was not available for NZ, and therefore these distributions were assumed. Despite this, the literature suggests that a normal distribution reasonably approximates arrival and departure times in other countries (Papadopoulos et al. [2012], Tran-Quoc et al. [2012] Shariff et al. [2016], and Li and Crossley [2014]).

Table 4.3 List of Stochastic Variable Distributions

Variable	Type	Parameters
Departure Time	Normal	μ=8am, σ=1h
Arrival Time	Normal	μ=6pm, σ=1h
Daily Distance	Gamma	a=1.65, b=19.5 km
Battery Capacity	Multinomial	P(20, 30, 40 kWh)=[0.15, 0.70, 0.15]
Charger Rating	Multinomial	P(2, 4, 8 kW)=[0.15, 0.70, 0.15]
Range Anxiety	Multinomial	P(0.1, 0.5, 0.9 p.u.)=[0.10, 0.20, 0.70]
Charging Strategy	Multinomial	P(OA, DNT, BM)=[0.80, 0.10, 0.10]

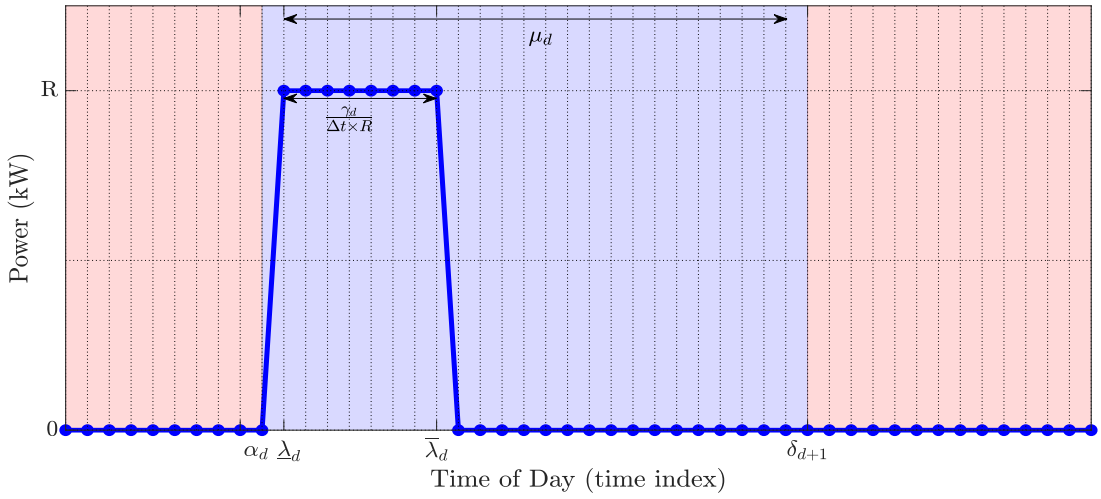

(a) On-Arrival

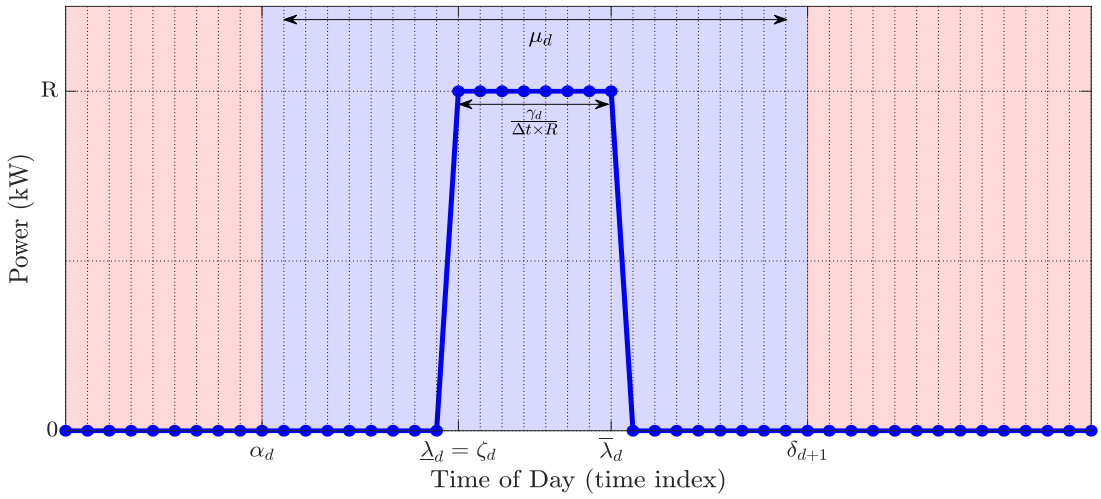

(b) Day-Night Tariff

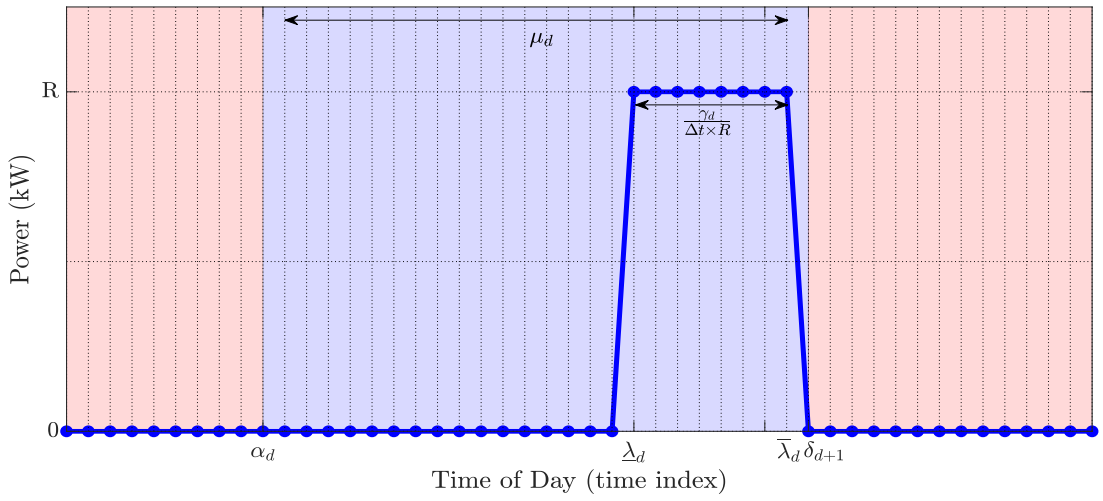

(c) By-Morning

Figure 4.1 EV Load Profile Examples for Each Charging Strategy

4.4.2 Daily Distance Travelled

The daily distance travelled is sampled from a gamma distribution with shape and scale parameters of 1.65 and 19.5, respectively. The distribution was fitted to data from the NZ Ministry of Transport and provides a mean daily distance travelled of 31.7 km (Concept Consulting [2018]).

4.4.3 Battery Capacity

The battery capacity is sampled from a multinomial distribution which produces three discrete capacities: 20kWh, 30kWh and 40kWh. These were chosen to reflect the range of battery capacities in Table 2.2. Some EV models have capacities of up to 100kWh; however, these are significantly less common and were therefore not considered.

4.4.4 Charger Rating

The charger rating is sampled from a multinomial distribution which produces three discrete ratings: 2kW, 4kW, and 8kW. These reflect not only the AC ratings in Table 2.2 but also the charging cables used in NZ. While some EV models have AC ratings of up to 22kW, in NZ, the majority of residential charging is conducted using a non-dedicated circuit, and therefore, the charging rate is limited by the cable (Energy Efficiency and Conservation Authority [2019]).

4.4.5 Range Anxiety

The range anxiety factor is sampled from a multinomial distribution which produces three discrete values: 0.1, 0.5 and 0.9. These reflect low, medium and high range anxiety, respectively. Although trials suggest that EVs are only charged every 2-3 days, this may be a reflection of current EV owners are early adopters (Jake Roos Consulting [2018]). The chosen distribution represents relatively high range anxiety throughout the EV fleet.

4.4.6 Charging Strategy

The charging strategy is sampled from a multinomial distribution which produces either OA, DNT, and BM. The OA strategy is generally considered the most convenient (Jake Roos Consulting [2018]). Furthermore, not all electricity retailers offer day-night tariffs; therefore, some customers have no incentive to delay charging. The chosen distribution favours the OA strategy; in comparison, the DNT and BM strategies occur with relatively low probability.

4.5 EV LOAD SIMULATION

The EV load model is used to simulate weekly EV load profiles for each customer in the typical residential network. The stochastic variables are re-sampled for each customer in order to capture EV load diversity. Four examples of the simulated EV load profiles can be seen in Figure 4.2, for the first day of the week.

Customers one and three both charge using a 4kW charger; however, they differ in charging strategy and charge duration. Customer one charges using the OA strategy, for a total of three hours between 17:30 and 20:30. Customer three charges using the BM strategy, for a total of four hours between 04:30 and 08:30. Customer two charges using an 8kW charger and the DNT charging strategy. The higher-rated charger is the reason for the shorter charge duration when compared to the other customers. Customer four also charges using the OA strategy; however, arrives later in the evening than customer one. Customer four also uses a lower-rated, 2kW charger.

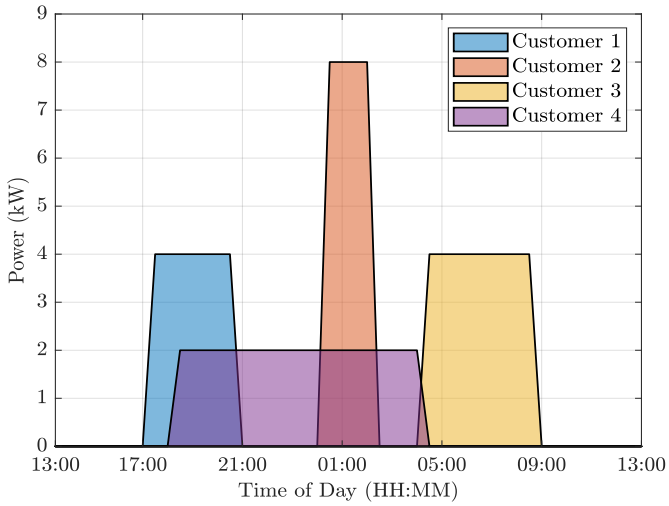

Figure 4.2 Four Examples of EV Load Profiles

Chapter 5

STOCHASTIC LOAD-FLOW SIMULATION

LV distribution networks are bound by operational limits for voltage, conductor loading and transformer loading, and are described as being constrained when these limits are violated. Networks may become constrained because of the additional load due to EV charging. The EV hosting capacity is the maximum EV penetration level a network can accommodate before becoming constrained. EV hosting capacity can be assessed using load-flow modelling, which allows planning and investment to be allocated ahead of time. This chapter describes the stochastic load-flow simulation.

In NZ, the majority of EV charging will take place in residential settings and therefore, residential distribution networks will be most significantly impacted by EV uptake (Energy Efficiency and Conservation Authority [2019]). A typical residential network was modelled in OpenDSS. The network topology is described in Section 5.1.

In science and engineering, black-box systems are described by their inputs and outputs, without any knowledge of the system internal workings. In this thesis, OpenDSS may be considered a black-box. The inputs are the customer load profiles, which are comprised of residential and EV load components. Residential loads are sampled from a SM dataset while EV loads are generated using the stochastic EV load model. Customer load profiles are constructed by superimposing the residential and EV load components, with an appropriate adjustment to account for the EV penetration level. This process is described in Section 5.2.

Although not essential, a basic understanding of OpenDSS is useful; a brief overview is provided in Section 5.3. Using the customer load profiles provided as input, OpenDSS performs a week-long QSS load-flow simulation and outputs a series of network monitors which record voltages, conductor loading, and transformer loading during the simulation; these are described in Section 5.4.

Voltage, conductor loading and transformer loading vary during the week. Furthermore, at any given time, voltage and conductor loading vary throughout the network. In the

literature, constraints are assessed using hard criteria where, all voltages, conductor loadings and transformer loadings must be within the specified limits. This thesis proposes flexible criteria, where a small number of violations are permitted depending on the violation magnitude. Section 5.5 describes how constraints are assessed from the network monitors using both hard and flexible criteria.

The stochastic load-flow simulation is based on a Monte Carlo (MC) method. MC methods are computational algorithms which produce probabilistic results based on repeated random sampling. A flow chart of the stochastic load-flow simulation can be seen in Figure 5.1. Each repetition of the Monte Carlo loop is referred to as a MC repetition. For each MC repetition, residential loads are re-sampled from the SM dataset while EV loads are re-generated using the stochastic EV load model. Multiple EV penetration levels are then assessed within the penetration loop. For each MC repetition, the EV hosting capacity is assessed using the constraint assessments at each penetration level; this process is described in Section 5.6.

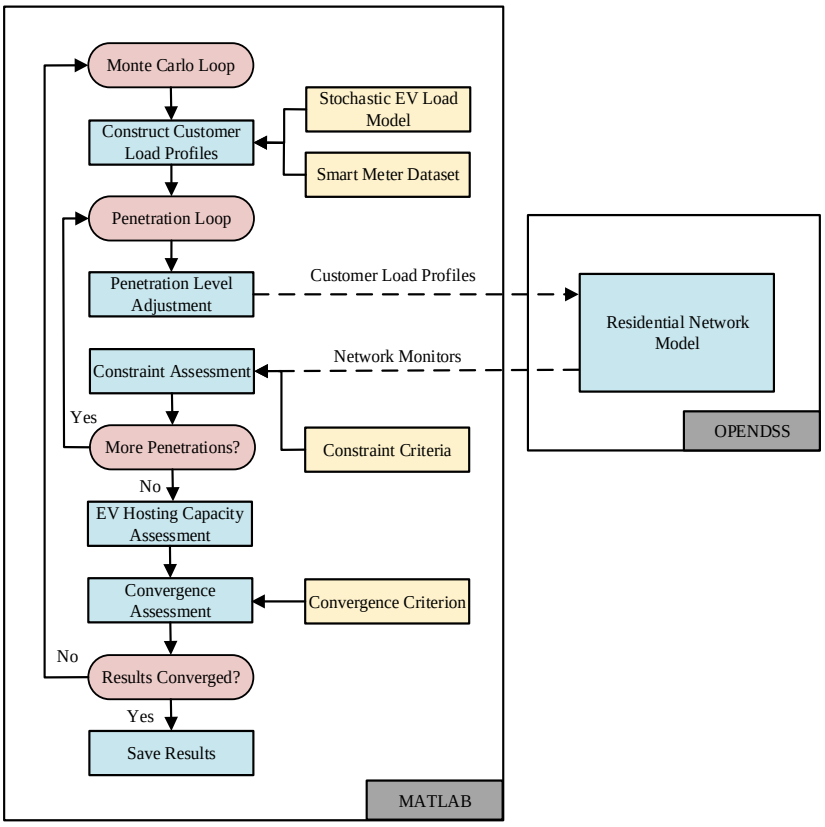

Figure 5.1 Flowchart of Stochastic Load-Flow Simulation

The EV hosting capacity will vary for successive MC repetitions depending on sampling. The distribution of EV hosting capacities can be obtained by performing a significant

number of MC repetitions; however, because the Monte Carlo loop could continue ad infinitum, it is necessary to show that for a finite number of MC repetitions, the distribution has converged. The convergence criterion is described in Section 5.7. When the convergence criterion is satisfied, the MC simulation is terminated, and the significant results are saved. Section 5.8 provides a summary of the results which are saved.

5.1 TYPICAL RESIDENTIAL NETWORK

A typical residential network was modelled in OpenDSS; this section describes the network topology including the MEN system used in NZ.

5.1.1 Network Topology

LV distribution networks can be broadly classified as either city, residential, rural or industrial. Cluster analysis allowed 10,558 networks in NZ to be classified (Watson et al. (2018)). The network in Figure 5.2 is the median of the residential cluster, and therefore, provides a typical residential network.

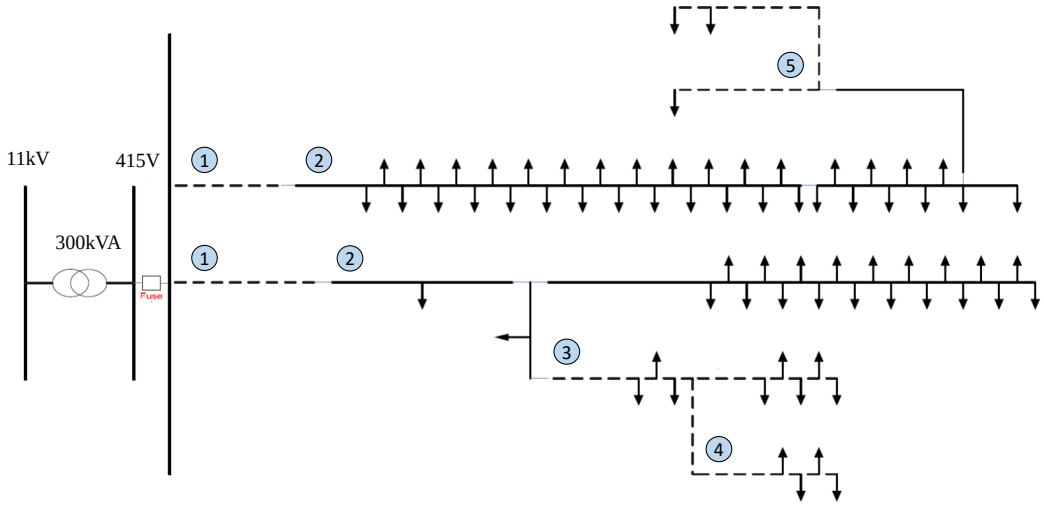

Figure 5.2 Typical Residential Low-Voltage Distribution Network

The network has 71 customer connections in total, which are assumed to be evenly distributed between the phases. The network contains a mixture of overhead lines and underground cables, which are depicted by solid and dashed lines respectively. Both overheads lines and underground cables are comprised of 3 phase conductors and a neutral. The distribution transformer provides a secondary line voltage of 415V, which

equates to 1.037 p.u. in a 400/230V LV system. The conductor specifications are provided in Table 5.1.

Both overhead lines and underground cables were modelled using the self impedance. Furthermore, the neutral conductor was assumed to have the same self impedance as the phase conductors, which is a common assumption when modelling four identically sized and uniformly spaced conductors. The mutual impedance was neglected because cross arm geometries and cable spacing were unknown (Kersting [2002]). Shunt admittance was also neglected, which is a common assumptions when modelling LV distribution networks because conductors are relatively short (Ciric et al. [2003]).

Table 5.1 Conductor Specifications for Typical Residential Low-Voltage Distribution Network

Key	Description	Rating (A)	Self Impedance (Ω/km)
1	Aluminum, XLPE, 185XN	265	0.164+0.072j
2	Copper, Stranded, 19/14	310	0.265+0.268j
3	Copper, XLPE, 185PN	344	0.099+0.072j
4	Copper, XLPE, 25XN	114	0.727+0.081j
5	Copper, PVC, 25PN	108	1.15+0.11j

5.1.2 Multiple Earthed Neutral

When modelling LV distribution networks, the current return path is important because phase imbalance is often significant. In NZ, LV distribution networks are MEN systems, where the neutral conductor is earthed at the LV transformer and each customer throughout the network. The purpose of the MEN system is to provide improved earthing during faults; during normal operation, the majority of the current returns through the neutral wire.

When modelling LV distribution networks, different approximations are often made regarding neutral grounding. The extreme ends of these approximations are the isolated and perfectly grounded neutral. In reality, the earthing impedances at the LV transformer and at each customer are finite, placing the true connectivity somewhere between these extremes (Urquhart and Thomson [2013]). Understanding the true connectivity is important when modelling neutral voltage rise due to unbalanced currents. This section describes how the MEN system was modelled in OpenDSS.

The earthing system at the transformer typically provides a better connection to ground. At the transformer, earthing is provided by an earth grid or mat. At each customer, earthing is provided by an earth stake. Earth stakes may also be used at the transformer; however, these are larger and provide a lower earthing resistance. At the transformer, the earthing system is required to have a maximum resistance to earth based upon its rating.

The earthing requirements at each customer are specified in AS/NZS 3000 [2018]. The standard does not state a maximum earthing resistance, but instead the required depth, L, and stake diameter, d; these are 1.8m and 20mm, respectively. The resistance to earth is calculated using Equation 5.1, which provides a value of 52Ω. ρ is the earth resistivity and is assumed to have a value of 100Ωm.

$$R = \frac{\rho}{2\pi L} \ln\left(\frac{4L}{d}\right) \tag{5.1}$$

Earthing resistance is variable depending on the local soil and weather conditions; therefore, the calculated value provides only an approximation. In the network model, the neutral conductor is connected to earth at each customer via a 52Ω resistance. At the transformer, the neutral conductor is connected to earth via a 15Ω resistance; this value was taken from the design standard used by a NZ distribution company. Earthing resistances can be considered in parallel since customers are generally spaced by more than $\frac{L}{4}$, and thus current flows do not interfere (IEEE Std 80 [2013]).

5.2 CUSTOMER LOAD PROFILES

5.2.1 Residential Load Component

The SM dataset is denoted $\boldsymbol{\Theta}$ and contains a week's worth of half-hour load data for 400 customers. $\boldsymbol{\Theta}$ was extracted from a larger dataset containing a years's worth of half-hour load data for 2216 customers in the Canterbury region, NZ. Figure 5.3 shows a histogram of the annual energy consumptions in the original dataset.

The customers in $\boldsymbol{\Theta}$ are those centered around the median of the distribution and therefore represent 400 average sized households. The data comes from the week beginning Monday 18th June 2012; this was the week that contained the annual peak that year. Figure 5.4 shows an example of a daily load profile within the SM dataset. The SM data is discretized and has a power resolution of 200W.

$\boldsymbol{\Theta}$ is indexed using the SM index, k, and the time index, t. $\Theta_{k,t}$ is the real power load of the k^{th} SM during the t^{th} time interval. The customer index, j, identifies customers within the typical residential network. A SM index, k, is randomly sampled for each customer. SM indices are sampled without replacement, which means that the same SM cannot be assigned to more than one customer. The variable $\boldsymbol{\Upsilon}$ contains the SM assignments for each customer; Υ_j is the SM index assignment for the j^{th} customer. $\boldsymbol{\Upsilon}$ is re-sampled at the beginning of each MC repetition.

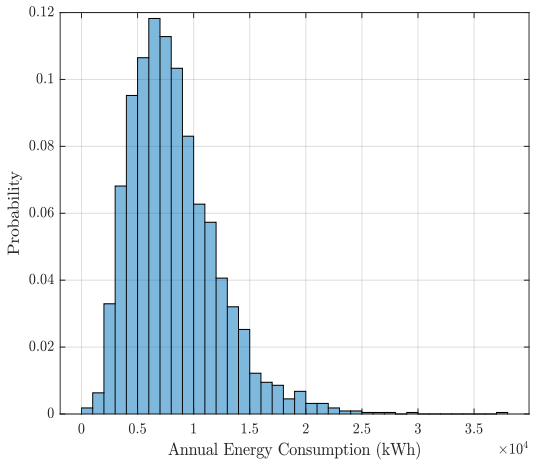

Figure 5.3 Histogram of Annual Energy Consumption in Original Smart Meter Dataset

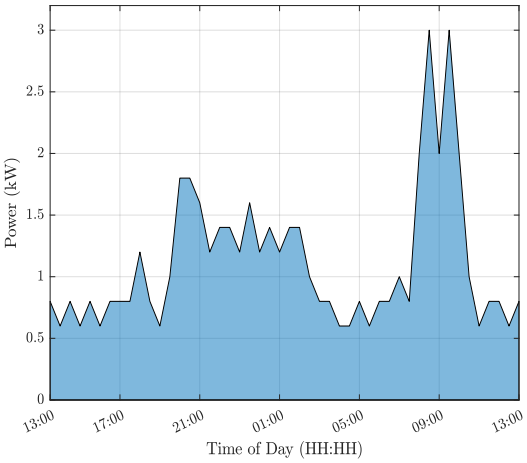

Figure 5.4 Example of Smart Meter Daily Load Profile

5.2.2 EV Load Component

EV load data is generated using the stochastic EV load model. The EV load data is denoted $\boldsymbol{\Omega}$, and is indexed using the customer index, j, and the time index, t. $\Omega_{j,t}$ is the real power EV load for the j^{th} customer during the t^{th} time interval. Again, $\boldsymbol{\Omega}$ is re-generated at the beginning of each MC repetition.

5.2.3 Superposition And Penetration Level Adjustment

Customer load profiles are constructed by superimposing the residential and EV load components. The customer load profiles are denoted $\boldsymbol{P}$, and are indexed using the customer index, j, and the time index, t. $P_{j,t}$ is the real power load for the j^{th} customer during the t^{th} simulation time-step. $P_{j,t}$ is calculated using Equation 5.2, which includes an adjustment to account for the EV penetration level.

The EV penetration level can be expressed as either the number of EVs or the percentage of customers with an EV; these are denoted, Ψ and $\hat{\Psi}$, respectively. For each MC repetition, 11 EV penetration levels are assessed within the penetration loop. For

penetration levels which are less than 100%, the EV load component is ignored for specific customers.

There are 71 customers in the typical residential network. At each penetration level, Ψ numbers between 1 and 71 are randomly generated. These numbers are denoted, $\mathbf{\Phi}$, and describe the customers with EVs. The EV load component is only superimposed for customers in $\mathbf{\Phi}$. The numbers in $\mathbf{\Phi}$ generated without replacement, which this means that each customer can only be generated once.

$$P_{j,t} = \begin{cases} \Theta_{\Upsilon_{j,t}} + \Omega_{j,t} & \text{if } j \in \mathbf{\Phi} \\ \Theta_{\Upsilon_{j,t}} & \text{if } j \notin \mathbf{\Phi} \end{cases} \quad \forall j, t \tag{5.2}$$

An important point to note is how the EV locations are generated for successive penetration levels. As an example, let us consider three penetration levels: 33%, 67%, and 100%. $\mathbf{\Phi}_{33\%}$, $\mathbf{\Phi}_{67\%}$, and $\mathbf{\Phi}_{100\%}$, are the EV locations at the corresponding penetration levels. Similarly, $\Psi_{33\%}$, $\Psi_{67\%}$, and $\Psi_{100\%}$, are the number of EVs at the corresponding penetration levels. At the 67% penetration level, the first $\Psi_{33\%}$ elements in $\mathbf{\Phi}_{67\%}$ are equal to $\mathbf{\Phi}_{33\%}$. Similarly, at the 100% penetration level, the first $\Psi_{67\%}$ elements in $\mathbf{\Phi}_{100\%}$ are equal to $\mathbf{\Phi}_{67\%}$. Generating EV locations in this way is representative of how EVs are added to a network in reality. for each MC repetition, $\mathbf{\Phi}$ is re-generated to provide different EV locations.

A load power factor of 0.95 lagging is assumed for the residential load component; this is a simplification because, in reality, the load power factor varies depending on the appliance composition (Roy and Mather [2019]). A load power factor of 0.99 lagging is assumed for the EV load component; again, this is a simplification because, in reality, the load power factor varies with charge rate. 0.99 is the power factor for a Nissan Leaf when charging at rated capacity (Idaho National Laboratory [2012]). The customer load profiles - including both the real and reactive components - are the inputs to OpenDSS.

5.3 OPENDSS

OpenDSS models the distribution network using a system admittance matrix, which allows for three-phase, unbalanced load-flow simulations. The system admittance matrix defines the network impedance and topology. Both the system admittance matrix and modelling of individual circuit elements are covered extensively in the literature, which the reader is encouraged to consult for more comprehensive coverage on the topic (Roger C. Dugan [2020]). This section provides only a brief overview of the modelling procedure, within the particular context of the stochastic load-flow simulation.

5.3.1 Buses and Nodes

Circuit elements include sources, transformers, conductors and loads. All circuit elements are connected to buses. Each bus has five nodes; one for each conductor and one for ground. An example of a network bus is depicted in Figure 5.5.

5.3.2 Power Delivery Elements

Adjacent buses are connected via power delivery elements. Examples of power delivery elements include: overhead lines, underground cables and transformers; these are linear elements and are modelled using a primitive admittance matrix. Figure 5.6 depicts a power delivery element connecting two adjacent buses.

5.3.3 Power Conversion Elements

Loads and generators are examples of power conversion elements; these are connected to a single network bus. An example of a power conversion element is depicted in Figure 5.7. In NZ, residential customers receive a single-phase connection; power conversion elements are connected between a single-phase and neutral.

Linear loads are modelled using a primitive admittance matrix. On the other hand, non-linear loads are modelled using a Norton equivalent circuit which contains a primitive admittance matrix and a parallel injection current.

Both the residential and EV load components are modelled using a constant power load model. For each customer, the primitive admittance matrix is calculated using the assigned load and the nominal voltage. The injection current compensates for any deviation from the nominal voltage and ensures that the assigned load is supplied.

5.3.4 Source

The source is a Thevenin equivalent circuit used to model all components upstream of the distribution transformer. The circuit is comprised of three phase voltages which are equal in magnitude and displaced by 120°. The source impedance is low, and hence load variation does not significantly impact the distribution transformer primary voltages; this is often referred to as a stiff source. The source is a unique power conversion element and allows the solution process to be initialized.

5.3.5 System Y Matrix

There is a primitive admittance matrix for each circuit element. These matrices provide the building blocks for the larger, system admittance matrix. A list of all bus connections

describes the network topology. The system admittance matrix is then constructed using a sparse matrix solver; this allows the network to be modelled using a standard nodal admittance formulation, as seen in Figure 5.8.

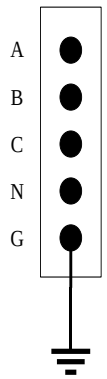

Figure 5.5 OpenDSS Bus and Associated Nodes

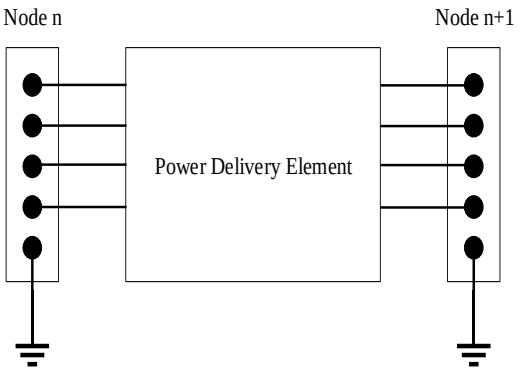

Figure 5.6 OpenDSS Power Delivery Element

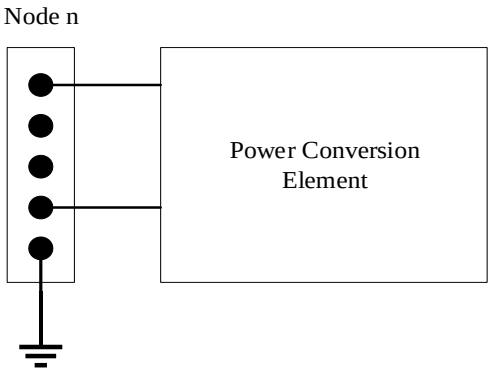

Figure 5.7 OpenDSS Power Conversion Element

5.3.6 Load Flow Solution Method

The load-flow equations are solved using a fixed point iterative method, as seen in Equation 5.3. The system admittance equation is solved directly to provide an initial guess for the bus voltages, $\boldsymbol{V}_{bus,0}$; loads are modelled using their primitive admittance matrix with no injection currents. The initial guess for the bus voltages is often close to the converged solution.

The first iteration begins by calculating the injection currents for each load, $\boldsymbol{I}$, using the initial guess of the bus voltages $\boldsymbol{V}_{bus,0}$. The load-flow equations are then solved using these new injection currents, providing the next guess at the bus voltages $\boldsymbol{V}_{bus,1}$. This process is repeated until the bus voltages converge within 0.0001 p.u.

$$\boldsymbol{V}_{bus,n+1} = [\boldsymbol{Y}_{system}]^{-1}\, \boldsymbol{I}(\boldsymbol{V}_{bus,n}), \qquad n = 0, 1, 2, ... \tag{5.3}$$

When performing quasi-steady-state (QSS) load-flow simulations, the assigned loads are updated for each time-step. Furthermore, the converged solution provides the initial guess at the bus voltages for the next time-step. The system admittance matrix, $\boldsymbol{Y}_{system}$, is not recalculated unless there is a significant change in load; this reduces the computation time.

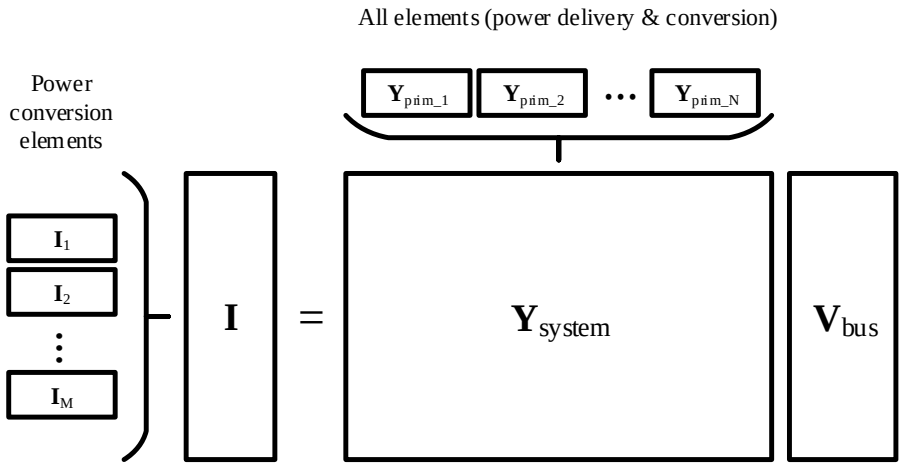

Figure 5.8 System Admittance Matrix Formulation

5.4 NETWORK MONITORS

OpenDSS performs a week-long QSS load-flow simulation and outputs a series of network monitors which record voltages, conductor loading and transformer loading during the simulation. This section describes the monitor variables which are exported from OpenDSS.

5.4.1 Customer Voltage Profiles

The monitor variable $\boldsymbol{V}$ contains the weekly customer voltage profiles. $V_{j,t}$ is the voltage at the j^{th} customer during the t^{th} time-step. All measurements are of the phase to neutral voltage and are expressed as a percentage of the 230V nominal voltage.

5.4.2 Conductor Loading Profiles

The monitor variable $\boldsymbol{I}$ contains the conductor loading profiles. $I_{l,t}$ is the loading of the l^{th} conductor during the t^{th} time-step. All measurements are of the most heavily loaded phase - including the neutral - and are expressed as a percentage of the conductors per phase continuous Ampere rating.

5.4.3 Transformer Loading Profile

The monitor variable $\boldsymbol{S}$ contains the transformer loading profile. S_t is the transformer loading during the t^{th} simulation time-step. All measurements are of the most heavily

loaded phase and are expressed as a percentage of the transformers per phase continuous kVA rating.

5.5 CONSTRAINT ASSESSMENT

LV distribution networks are described as being constrained when operational limits for voltage, conductor loading or transformer loading are violated. These limits protect both customer equipment and network assets. In the literature, constraints are assessed using hard criteria where, all voltages, conductor loadings and transformer loadings must be within the specified limits, during all of the time. In order to demonstrate hard criteria, let us consider voltage as an example.

Voltages depend on residential demand and are typically lower during peaks—peaks occur twice per day, once in the morning and a second time in the evening. Voltages also vary throughout the network and are lower towards the end of radial feeders. The statutory limits are unlikely to be violated during low demand. Furthermore, the statutory limits are unlikely to be violated for customers near the start of radial feeders. Constraints are therefore assessed using the minimum voltage across all customers and time intervals. The minimum voltage is compared to a single voltage threshold; this is typically the lower bound of the statutory limits. If the minimum voltage is above the threshold, then voltage is guaranteed to be within statutory limits for all customers, during all of the time. The benefit of using hard criteria is that EV hosting capacity is assessed in a customer-centric way.

On the other hand, the downside of using hard criteria is that neither the magnitude nor duration of violations is considered. Hard criteria cannot distinguish between minor and major under-voltages because only a single threshold is considered. The under-voltage duration is unclear because constraints are assessed using the minimum voltage. Statutory limits often include flexibility to allow for a small number of minor voltage violations. In the EU for example, voltages between -10% and -15% are permitted for 5% of the 10-minute readings in a week. When using hard criteria, this flexibility cannot be accounted for, which may restrict EV hosting capacity.

This thesis proposes a framework for assessing constraints using flexible criteria where, a small number of voltage, conductor loading and transformer loading violations are permitted. The number of permitted violations depends on the violation magnitude. In order to demonstrate flexible criteria, let us again consider voltage as an example.

Voltage constraints are assessed using the number of under-voltage hours per week, for the worst affected customer. The number of under-voltage hours is calculated using two different magnitude thresholds, which allows minor and major under-voltages to

be explicitly defined. For each magnitude threshold, there is an associated duration threshold. Constraints are assessed by comparing the number of under-voltage hours to the corresponding duration threshold.

An alternative approach is to mirror the SAIDI and SAIFI measures used for system reliability (Electricity Authority [2014]). The System Average Interruption Duration Index (SAIDI) is the average interruption duration for a group of customers, supplied by the power system. The System Average Interruption Frequency Index (SAIFI) – is the average interruption frequency for a group of customers. Mirroring this approach, voltage constraints could be assessed using the average number of under-voltage hours per week, for a group of customers. This approach was discounted because the majority of the under-voltage hours per week are likely to be contributed by a small number customers at the remote end of radial feeders; therefore, using the average significantly underestimates the number of under-voltage hours for the worst affected customer.

When using the proposed flexible criteria, the EV hosting capacity is still assessed in a customer-centric way, because voltages are assessed for the worst affected customer. The benefit however, is that EV hosting capacity can be significantly increased. The proposed framework provides flexibility because the magnitude and duration thresholds can be adjusted to reflect the statutory limits in different countries. The following sections describes how constraints are assessed from the monitor variables, using both hard and flexible criteria.

5.5.1 Hard Criteria

Table 5.2 provides an overview of the nomenclature used to describe the hard constraint criteria. For each monitor variable, constraints are assessed by comparing the critical variable to the corresponding constraint threshold.

The critical variable for $\boldsymbol{V}$ is the minimum voltage, across all customers, j, and time indices, t. The minimum voltage is used because under-voltage is the dominant concern regarding EV charging. The constraint threshold is 0.94p.u., which corresponds to the lower bound of the steady-state voltage limits in NZ. The constraint criterion is breached when the minimum voltage is less than 0.94p.u..

The critical variable for $\boldsymbol{I}$ is the maximum conductor loading, across all conductors, l, and time indices, t. Similarly, the critical variable for $\boldsymbol{S}$ is the maximum transformer loading, across all time indices, t. In each case, the constraint threshold is 1.00p.u., which corresponds to the per phase continuous rating. For $\boldsymbol{I}$ and $\boldsymbol{S}$, the constraint criterion is breached when the critical variable is greater than 1.00p.u..

Table 5.2 Constraint Nomenclature: Hard Criteria

Monitor Variable	Critical Variable	Constraint Threshold	Constraint Criterion
$\boldsymbol{V}$	$\min_{j,t} \boldsymbol{V}$	0.94 p.u.	$\min_{j,t} \boldsymbol{V} < 0.94$ p.u.
$\boldsymbol{I}$	$\max_{l,t} \boldsymbol{I}$	1.00 p.u.	$\max_{l,t} \boldsymbol{I} > 1.00$ p.u.
$\boldsymbol{S}$	$\max_{t} \boldsymbol{S}$	1.00 p.u.	$\max_{t} \boldsymbol{S} > 1.00$ p.u.

5.5.2 Flexible Criteria

Table 5.3 provides an overview of the nomenclature used to describe the flexible constraint criteria.

Table 5.3 Constraint Nomenclature: Flexible Criteria

Monitor Variable	Critical Variable	Magnitude Thresholds	Duration Thresholds	Constraint Criterion
$\boldsymbol{V}$	$\frac{1}{2}\max_{j}\sum_{t}\mathfrak{V}^{\mathcal{V}}$	$\mathcal{V}_1$, $\mathcal{V}_2$	$\Gamma_{\mathcal{V}_1}$, $\Gamma_{\mathcal{V}_2}$	$\frac{1}{2}\max_{j}\sum_{t}\mathfrak{V}^{\mathcal{V}_1} > \Gamma_{\mathcal{V}_1} \vee \frac{1}{2}\max_{j}\sum_{t}\mathfrak{V}^{\mathcal{V}_2} > \Gamma_{\mathcal{V}_2}$
$\boldsymbol{I}$	$\frac{1}{2}\max_{l}\sum_{t}\mathfrak{I}^{\mathcal{I}}$	$\mathcal{I}_1$, $\mathcal{I}_2$	$\Gamma_{\mathcal{I}_1}$, $\Gamma_{\mathcal{I}_2}$	$\frac{1}{2}\max_{l}\sum_{t}\mathfrak{I}^{\mathcal{I}_1} > \Gamma_{\mathcal{I}_1} \vee \frac{1}{2}\max_{l}\sum_{t}\mathfrak{I}^{\mathcal{I}_2} > \Gamma_{\mathcal{V}_2}$
$\boldsymbol{S}$	$\frac{1}{2}\sum_{t}\mathfrak{S}^{\mathcal{S}}$	$\mathcal{S}_1$, $\mathcal{S}_2$	$\Gamma_{\mathcal{S}_1}$, $\Gamma_{\mathcal{S}_2}$	$\frac{1}{2}\sum_{t}\mathfrak{S}^{\mathcal{S}_1} > \Gamma_{\mathcal{S}_1} \vee \frac{1}{2}\sum_{t}\mathfrak{S}^{\mathcal{S}_2} > \Gamma_{\mathcal{S}_2}$

The critical variable for $\boldsymbol{V}$ is the number of under-voltage hours per week for the worst affected customer in the network. $\mathfrak{V}^{\mathcal{V}}$ is a binary variable with the same dimensions as $\boldsymbol{V}$ and is evaluated using Equation 5.4. The term, $\max_{j}\sum_{t}\mathfrak{V}^{\mathcal{V}}$, is the number of under-voltage half-hour intervals per week for the worst affected customer in the network. The multiplication by $\frac{1}{2}$ is required to convert the units from half-hour intervals to hours.

The critical variable is evaluated using two magnitude thresholds, $\mathcal{V}_1$ and $\mathcal{V}_2$; these are referred to as the minor and major magnitude thresholds, respectively. For each magnitude threshold, there is an associated duration threshold, $\Gamma_{\mathcal{V}_1}$ and $\Gamma_{\mathcal{V}_2}$. $\Gamma_{\mathcal{V}_1}$ is the number of hours per week the voltage at the worst affected customer is allowed to be below $\mathcal{V}_1$. Similarly, $\Gamma_{\mathcal{V}_2}$ is the number of hours per week the voltage at the worst affected customer is allowed to be below $\mathcal{V}_2$.

By establishing appropriate thresholds, it is possible to permit a small number of minor under-voltages, while rejecting major under-voltages, even if infrequent. The

constraint criterion has two clauses; the first clause is breached by a large number of minor under-voltages while the second clause is breached by a small number of major under-voltages.

As an example, consider that $\mathcal{V}_1$ and $\mathcal{V}_2$ are 0.94p.u. and 0.90p.u., respectively. Similarly, consider that $\Gamma_{\mathcal{V}_1}$ and $\Gamma_{\mathcal{V}_2}$ are 5 hours and 0 hours, respectively. The constraint criterion is breached if, for the worst affected customer:

- The number of under-voltage hours per week below 0.94p.u. is greater than 5; or,
- The number of under-voltage hours per week below 0.90p.u. is greater than 0.

The critical variable for $\boldsymbol{I}$ is the number of overload hours per week for the worst affected conductor in the network. Similarly, the critical variable for $\boldsymbol{S}$ is the number of overload hours per week for the transformer. $\mathfrak{I}^{\mathcal{I}}$ and $\mathfrak{S}^{\mathcal{S}}$ are binary variables with the same dimensions as $\boldsymbol{I}$ and $\boldsymbol{S}$, respectively; these are calculated using Equations 5.5 and 5.6.

$$\mathfrak{V}_{j,t}^{\mathcal{V}} = \begin{cases} 1, & \text{if } V_{j,t} < \mathcal{V} \\ 0, & \text{if } V_{j,t} \geq \mathcal{V} \end{cases} \tag{5.4}$$

$$\mathfrak{I}_{l,t}^{\mathcal{I}} = \begin{cases} 1, & \text{if } I_{l,t} > \mathcal{I} \\ 0, & \text{if } I_{l,t} \leq \mathcal{I} \end{cases} \tag{5.5}$$

$$\mathfrak{S}_{t}^{\mathcal{S}} = \begin{cases} 1, & \text{if } S_{t} > \mathcal{S} \\ 0, & \text{if } S_{t} \leq \mathcal{S} \end{cases} \tag{5.6}$$

Table 5.4 details the magnitude and duration thresholds which are used in this thesis. Voltages between 0.94 p.u. and 0.90 p.u. are defined as minor under-voltages. Voltages below 0.90 p.u. are defined as major under-voltages. Conductor or transformer loadings between 1.00 p.u. and 1.20 p.u. are defined as minor overloads. Conductor or transformer loadings above 1.20 p.u. are defined as major overloads. Minor violations are permitted for up to 5 hours per week, while major violations are not permitted at all.

Table 5.4 List of the Magnitude and Duration Thresholds Used in This Thesis

Monitor Variable	Magnitude Thresholds		Duration Thresholds	
$\boldsymbol{V}$	$\mathcal{V}_1$=0.94 p.u.	$\mathcal{V}_2$=0.90 p.u.	$\Gamma_{\mathcal{V}_1}$=5 hours	$\Gamma_{\mathcal{V}_2}$=0 hours
$\boldsymbol{I}$	$\mathcal{I}_1$=1.00 p.u.	$\mathcal{I}_2$=1.20 p.u.	$\Gamma_{\mathcal{I}_1}$=5 hours	$\Gamma_{\mathcal{I}_2}$=0 hours
$\boldsymbol{S}$	$\mathcal{S}_1$=1.00 p.u.	$\mathcal{S}_2$=1.20 p.u.	$\Gamma_{\mathcal{S}_1}$=5 hours	$\Gamma_{\mathcal{S}_2}$=0 hours

5.6 EV HOSTING CAPACITY ASSESSMENT

Multiple EV penetration levels are assessed for each MC repetition; this can be seen in the flowchart in Figure 5.1. In this thesis, 11 EV penetration levels between 0% and 100% are assessed. Each penetration level is treated sequentially in OpenDSS. The network monitor variables $\boldsymbol{V}$, $\boldsymbol{I}$ and $\boldsymbol{S}$ are exported for each penetration level. The dimensions of these variables are $[71 \times 336]$, $[7 \times 336]$ and $[1 \times 336]$, respectively.

At the constraint assessment stage, the number of results is significantly reduced. For each monitor variable, constraints are recorded as a single binary indicator. A binary 1 indicates a breach of the constraint criterion. After the final EV penetration level has been assessed, the results are a $[3 \times 11]$ binary matrix, which indicates whether or not the constraint criterion was breached for each monitor variable, at each penetration level.

The number of results is further reduced at the EV hosting capacity assessment stage. The EV hosting capacity is the maximum EV penetration level a network can accommodate before becoming constrained by either voltage, conductor loading or transformer loading and is calculated using the $[3 \times 11]$ binary constraint matrix. A single EV hosting capacity is produced for each MC repetition; the variable H_m is the EV hosting capacity for the m^{th} MC repetition. The units of H_m are the same as the EV penetration level $\hat{\Psi}$; that is % of customers with an EV.

Because of the stochastic elements in the residential and EV load models, the EV hosting capacity varies for successive MC repetitions. The variable $\boldsymbol{H}$ is the set of EV hosting capacities across all MC repetitions. The EV hosting capacity CDF is calculated using Equation 5.7.

$F(\hat{\Psi})$ is the probability of an EV hosting capacity less than or equal to the penetration level $\hat{\Psi}$. $\boldsymbol{\mathcal{H}}^{\hat{\Psi}}$ is a binary variable with the same dimensions as $\boldsymbol{H}$ and is calculated using Equation 5.8. Due to the upper bound on the penetration levels assessed, $F(\hat{\Psi})$ is equal to 1 at the 100% penetration level.

$$F(\hat{\Psi}) = \frac{1}{M} \sum_{m=1}^{M} \mathcal{H}_m^{\hat{\Psi}} \tag{5.7}$$

$$\mathcal{H}_m^{\hat{\Psi}} = \begin{cases} 1, & \text{if } H_m \leq \hat{\Psi} \\ 0, & \text{if } H_m > \hat{\Psi} \end{cases} \tag{5.8}$$

5.7 CONVERGENCE CRITERION

The Monte Carlo loop could continue ad infinitum; because of this, it is necessary to show that for a finite number of MC repetitions, the EV hosting capacity CDF has stabilised. $F(\hat{\Psi})$ is assessed for convergence after multiples of 100 MC repetitions. Convergence is assessed using the KS statistic, Λ, which is calculated using Equation 5.9.

$F_m(\hat{\Psi})$ is the value of $F(\hat{\Psi})$, when evaluated after m repetitions. The sup function is the supremum of the set of distances and provides the maximum difference between the CDFs evaluated on the m^{th}, and $m - 100^{th}$ repetitions. Convergence requires that the KS statistic is less than 0.005 for five successive evaluations.

$$\Lambda = \sup_{\hat{\Psi}} |F_m(\hat{\Psi}) - F_{m-100}(\hat{\Psi})| \tag{5.9}$$

5.8 SAVING SIGNIFICANT RESULTS

The stochastic load-flow simulation generates a significant number of results. In performing 1000 MC repetitions, the load-flow equations are solved over 3.5 million times. Rather than save the monitor variables for every MC repetition, a smaller number of more meaningful results are saved; these are the critical variables and EV hosting capacities. The critical variables are catalogued by MC repetition and EV penetration level. The EV hosting capacities are catalogued by MC repetition only.

Chapter 6

RESULTS

This chapter presents the results of the stochastic load-flow simulations. In Section 6.1, the EV hosting capacity is assessed using hard constraint criteria. Similarly, in Section 6.2, the EV hosting capacity is assessed using flexible constraint criteria. In both sections, the following results are presented:

- Critical variable distributions
- Constraint breach probabilities
- EV hosting capacity CDF

The differences between the results are then discussed, and based on this; it is argued that using flexible criteria is appropriate for assessing EV hosting capacity in stochastic load-flow simulations.

The MC simulation is terminated when the convergence criterion is satisfied. In Section 6.3, the KS statistic is plotted as a function of the number of MC repetitions. The plot shows that the convergence criterion is satisfied on the 2700^{th} MC repetition.

The EV hosting capacity depends on the charging practices adopted by EV owners. Examples of more favourable charging practices include:

- Using lower-rated chargers
- Reducing range anxiety
- Using an even mix of charging strategies

Different charging scenarios can be examined by altering the statistical distributions from which the stochastic variables are sampled. The distributions in Chapter 4 define the baseline charging scenario. The baseline charging scenario describes the charging practices which EV owners are expected to adopt naturally. An alternative charging scenario is defined in Section 6.4, which describes a range of more favourable charging practices. The EV hosting capacities are compared for the baseline and alternative charging scenarios.

6.1 EV HOSTING CAPACITY ASSESSMENT: HARD CRITERIA

6.1.1 Critical Variable Distributions

When using hard criteria, the critical variables are as follows:

- Minimum voltage
- Maximum conductor loading
- Maximum transformer loading

These values are plotted in Figure 6.1. At each penetration level, a histogram shows the distribution of values across all MC repetitions; this is the uncertainty due to the stochastic variables. The distribution of weekly minimum customer voltages is left-skewed; that is to say, the mean result is lower than the median because of a small number of exceptionally low voltages. On the other hand, the distributions for the weekly maximum conductor loading and the weekly maximum transformer loading are right-skewed. Here, the mean result is higher than the median because of a small number of exceptionally high loads.

The lowest voltages and highest loads are referred to as extreme results. MC repetitions which produce more extreme results are referred to as unfavourable repetitions. On the other hand, MC repetitions which produce less extreme results are referred to as favourable repetitions. There are examples of both favourable and unfavourable MC repetitions at each penetration level; however, despite this, clear trends can still be observed. As the EV penetration level increases, the level of the minimum voltage distributions decrease. Conversely, the level of the maximum conductor loading and the maximum transformer loading distributions increase as the EV penetration level increases.

There are two reasons why some MC repetitions produce more extreme results than others; these are temporal coincidence and load placement. In order to demonstrate these, let us consider the 0% penetration level as an example; the mechanisms are the same, whether or not EVs are included.

Figure 6.2 shows the distribution of customer loads, at both at 7 pm and 3 am; these correspond to the evening peak and overnight low, respectively. The data comes from the SM dataset $\mathbf{\Theta}$ and is for the first day of the week. At 7 pm, there is a mixture of both high and low loads. There is also a mixture of high and low loads at 3 am; however, higher loads are significantly less probable.

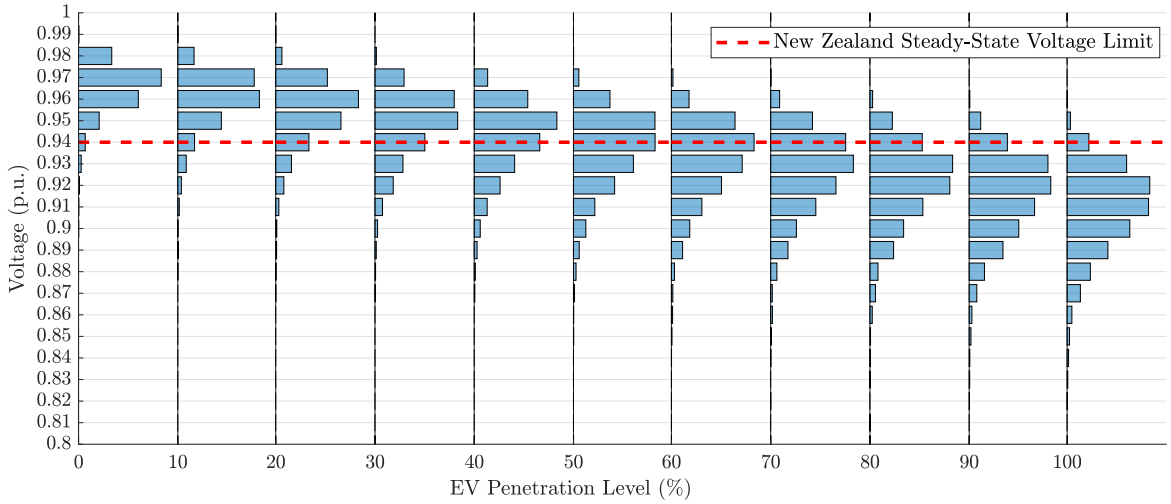

(a) Weekly Minimum Customer Voltage

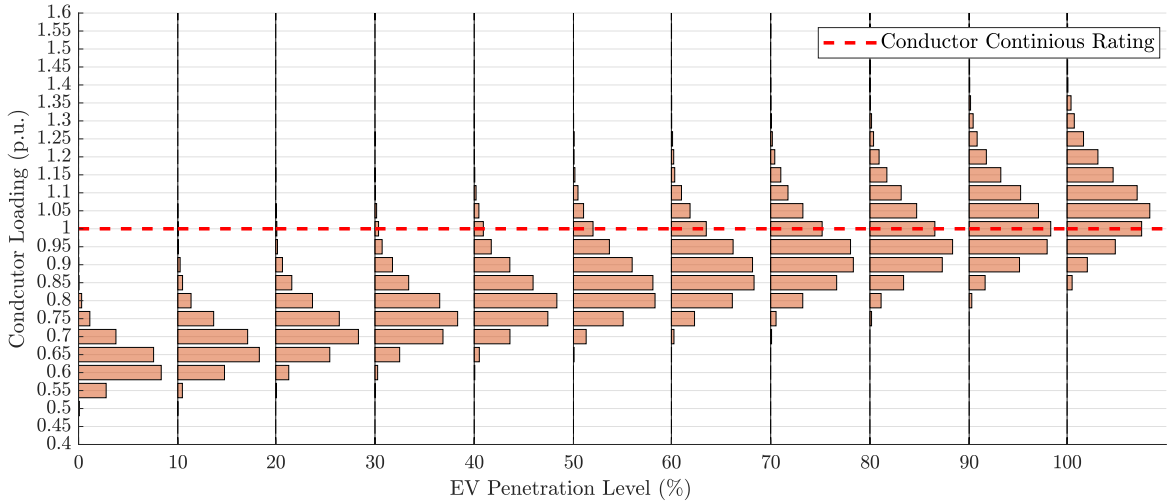

(b) Weekly Maximum Conductor Loading

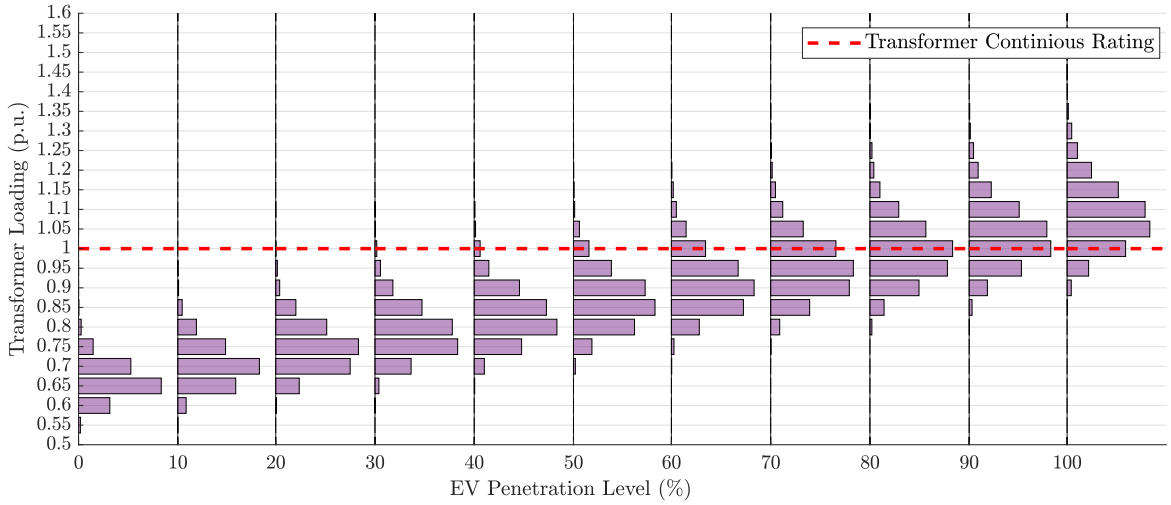

(c) Weekly Maximum Transformer Loading

Figure 6.1 Critical Variable Distributions: Hard Criteria

When residential loads are sampled from the SM dataset, there will be a mixture of both high and low loads during each time-step. Some MC repetitions will produce a more significant number of high loads than others; such repetitions are described as having high temporal coincidence. Temporal coincidence impacts each of the critical variables.

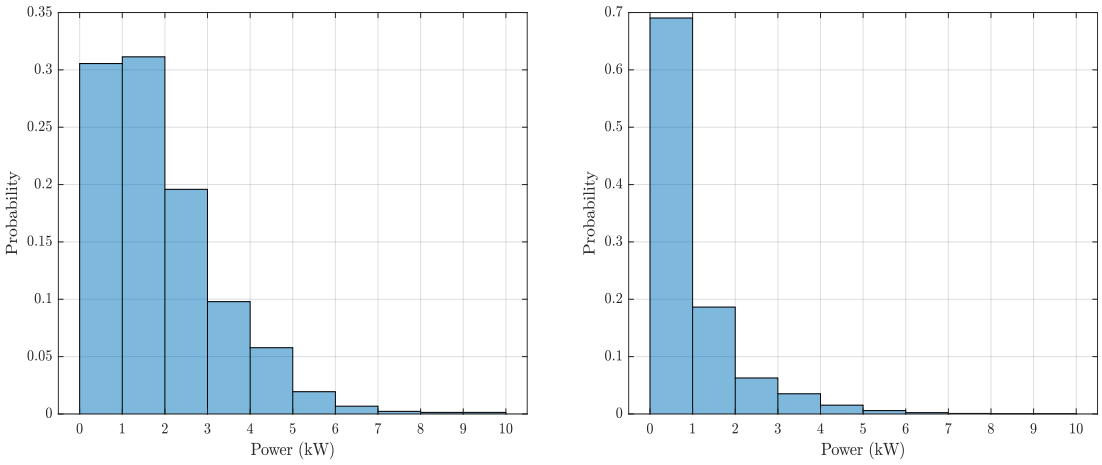

(a) 7pm (b) 3am

Figure 6.2 Histogram of Customer Loads: 0% EV penetration

For a given aggregate load, there are three ways in which load placement impacts load-flow results:

- Feeder imbalance
- Phase imbalance
- Longitudinal imbalance

To understand feeder imbalance, consider a network with two radial feeders. For simplicity, assume that both feeders have an equal number of customers. For some MC repetitions, the feeders will receive an equal allocation of high and low loads. For other MC repetitions, one feeder will receive a skewed sample of high loads; this increases the conductor loading and subsequent voltage drop along that particular feeder. When feeder imbalance is significant, the weekly maximum conductor loading is typically higher. Similarly, the weekly minimum customer voltage is typically lower.

Phase imbalance works similarly. To understand phase imbalance, consider a single radial feeder. For simplicity, assume that each phase is assigned an equal number of customers. For some MC repetitions, the phases will receive an equal allocation of high and low loads. For other MC repetitions, one phase will receive a skewed sample of high loads; this increases the loading and subsequent voltage drop along that particular phase.

When phase imbalance is significant, both the weekly maximum conductor loading and the weekly maximum transformer loading are typically higher. Similarly, the weekly minimum customer voltage is typically lower. Customer voltages are also influenced by neutral voltage displacement, which is more significant when the phases are unbalanced.

To understand longitudinal imbalance, consider a single phase radial feeder. For some MC repetitions, high and low loads will be evenly distributed along the length of the feeder. For other MC repetitions, a more significant number of high loads will be placed towards the end of the feeder. When a more significant number of high loads are placed towards the end of the feeder, the weekly minimum customer voltage is lower because a more significant proportion of the total feeder current flows through a more significant proportion of the total phase impedance.

The weekly maximum conductor loading may also be higher because conductors towards the end of radial feeders typically have lower ratings than those towards the beginning; this can be seen in Figure 5.2. When a more significant number of high loads are placed towards the end of the feeder, a more significant proportion of the total feeder current flows through these smaller conductors. The reader is encouraged to consult the unpublished works in Appendix A for a more detailed description of how load-flow results are impacted by load placement.

6.1.2 Constraint Breach Probabilities

In Figure 6.1, the constraint threshold is indicated for each Critical variable. The constraint threshold for voltage is 0.94 p.u. which corresponds to the lower bound of the NZ steady-state voltage limits. The constraint threshold for conductor loading and transformer loading is 1.00 p.u. which corresponds to the per-phase continuous rating.

At each penetration level, the constraint breach probability for voltage can be interpreted as the percentage of the histogram below the 0.94 p.u. threshold. Similarly, the constraint breach probabilities for conductor loading and transformer loading can be interpreted as the percentage of the histograms above the 1.00 p.u. threshold.

The constraint breach probabilities for voltage, conductor loading and transformer loading are plotted in Figures 6.3a, 6.3c and 6.3e, respectively. At each penetration level, the constraint breach probability is highest for voltage, which indicates that for this particular network, voltage is the constraining factor.

There is a small chance of a voltage constraint breach, even at the 0% penetration level; these occur for a small number of the most unfavourable MC repetitions. On the other hand, the chance of a voltage constraint breach at the 100% penetration level is very high. Here, even some of the most favourable MC repetitions produce constraint breaches.

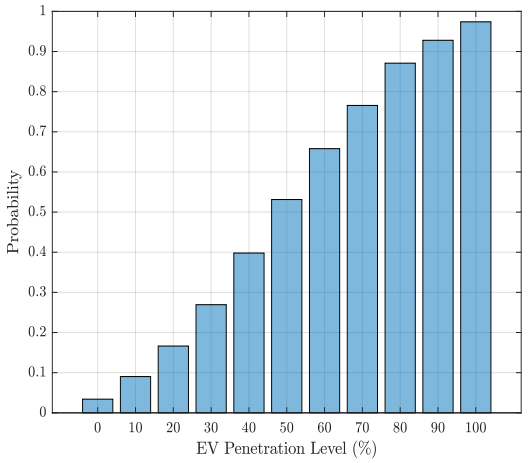

(a) Voltage: Hard Criteria

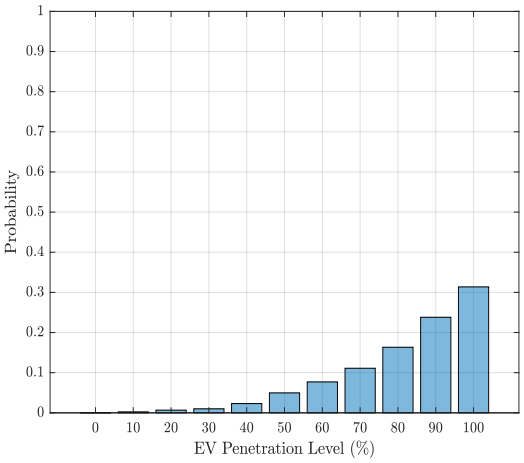

(b) Voltage: Flexible Criteria

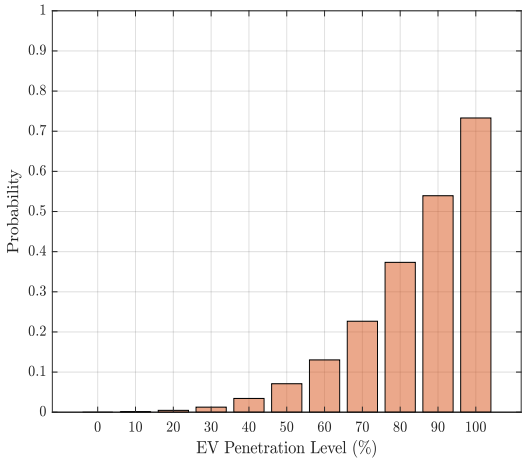

(c) Conductor Loading: Hard Criteria

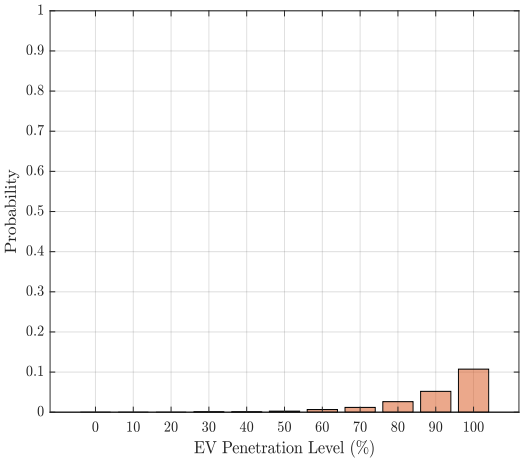

(d) Conductor Loading: Flexible Criteria

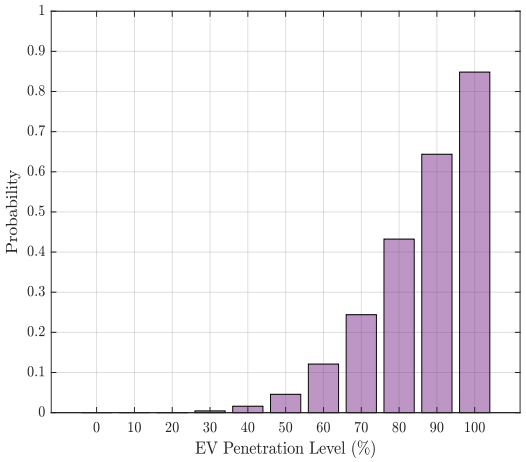

(e) Transformer Loading: Hard Criteria

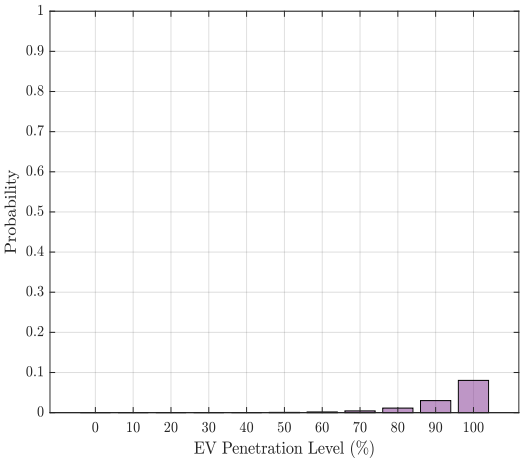

(f) Transformer Loading: Flexible Criteria

Figure 6.3 Constraint Breach Probabilities

One can be relatively confident when considering the 0% and 100% penetration levels; however, there is significant uncertainty at moderate penetration levels. At the 50% penetration level, the constraint breach probability for voltage is 0.54; it is, therefore, unclear whether or not a voltage constraint will occur.

This result was also seen in Papadopoulos et al. [2012]; however, an acceptable constraint breach probability was not defined. Without defining an acceptable constraint breach probability, it is difficult to interpret these results meaningfully.

6.1.3 EV Hosting Capacity CDF

The EV hosting capacity is the maximum EV penetration level a network can accommodate before becoming constrained. While deterministic load-flow simulations produce a single EV hosting capacity, stochastic load-flow simulations produce a distribution of EV hosting capacities. The EV hosting capacity is uncertain because of the uncertainty in customer loads. The EV hosting capacity CDF can be seen in Figure 6.4a.

The x-axis shows the range of EV hosting capacities. The minimum possible EV hosting capacity is <0%; this means that the network is constrained at the 0% penetration level, before any EVs are added. The maximum possible EV hosting capacity is 100%; this means that the network is not constrained, even at the 100% penetration level. The maximum possible EV hosting capacity is 100%, because penetration levels between 0% and 100% were assessed within the penetration loop. The y-axis shows the probability of an EV hosting capacity less than or equal to the value on the x-axis.

The CDF shows that the EV hosting capacity varies between the minimum and maximum possible values. For the most unfavourable repetitions, the EV hosting capacity is <0%. On the other hand, for the most favourable repetitions, the EV hosting capacity is 100%. A single EV hosting capacity can be assigned by choosing an appropriate percentile value; this process is equivalent to choosing an acceptable constraint breach probability. The question is then, what is an appropriate percentile value?

The 50^{th} percentile - or P50 - provides an expected EV hosting capacity. The P50 can be interpreted as the intersection of the CDF and a horizontal line at 0.5. The P50 EV hosting capacity is 40%; this does not mean that constraint breaches will not occur at the 40% penetration level, but rather, for the worst week of the year, there is at least a 50% chance that constraint breaches will not occur.

Using the P50 produces a relatively high EV hosting capacity and therefore allows network reinforcement to be deferred until moderate penetration levels. On the other hand, there is a significant constraint breach probability at the assigned EV hosting

capacity. The probability of an EV hosting capacity less than or equal to 30% is 0.42; this is the constraint breach probability at the 40% penetration level.

Choosing a lower percentile value produces a lower EV hosting capacity; however, the constraint breach probability is also lower. The P5 EV hosting capacity is 0%, indicating that network reinforcement is required to accommodate even low penetration levels. The probability of an EV hosting capacity less than 0%, however, is only 0.03; this is the constraint breach probability at the 0% penetration level. If EV hosting capacity is assigned using the P5, networks may be reinforced prematurely and the associated costs are ultimately passed on to customers.

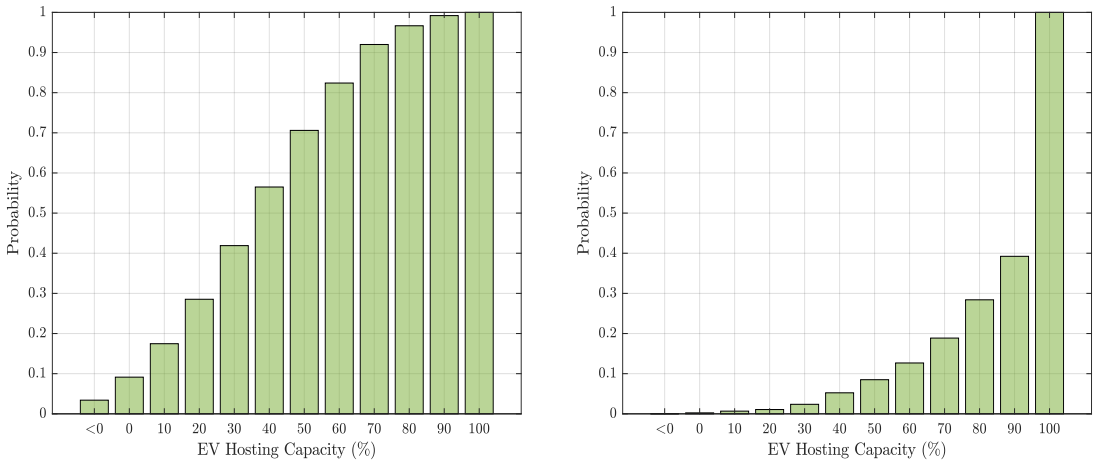

(a) Hard Criteria

(b) Flexible Criteria

Figure 6.4 EV Hosting Capacity CDF

6.2 EV HOSTING CAPACITY ASSESSMENT: FLEXIBLE CRITERIA

6.2.1 Critical Variable Distributions

When using the proposed flexible criteria, the critical variables are as follows:

- Number of under-voltage hours per week for the worst affected customer
- Number of overload hours per week for the worst affected conductor
- Number of overload hours per week for the transformer

These values are plotted in Figure 6.5, using the minor magnitude thresholds $\mathcal{V}_1$, $\mathcal{I}_1$ and $\mathcal{S}_1$. Similarly, these values are plotted in Figure 6.6, using the major magnitude thresholds $\mathcal{V}_2$, $\mathcal{I}_2$ and $\mathcal{S}_2$. At each penetration level, a histogram shows the distribution of values for all MC repetitions; again, this is the uncertainty due to the stochastic variables.

Voltages between 0.94p.u. and 0.90p.u. are significantly more likely than voltages below 0.90p.u.; this can be seen by comparing Figures 6.5a and 6.6a. At the 0% penetration level, voltages between 0.94p.u. and 0.90p.u. do occur; however, it is not until moderate penetration levels where these begin to occur for a significant number of hours per week. Even at high penetration levels, voltages below 0.90p.u. are unlikely to occur for a significant number of hours per week. The distributions are right-skewed; this is because the minimum duration is 0 hours, by definition.

The same trends can be seen for conductor loading and transformer loading. Overloads between 1.00p.u. and 1.20p.u. are significantly more likely than overloads above 1.20p.u.; this can be seen by comparing Figures 6.5b and 6.5c to Figures 6.6b and 6.6c, respectively. Overloads between 1.00p.u. and 1.20p.u. do occur; however, it is not until high penetration levels where these begin to occur for a significant number of hours per week. Even at high EV penetration levels, overloads above 1.20p.u. are unlikely to occur for a significant number of hours per week.

6.2.2 Constraint Breach Probabilities

In Figures 6.5 and 6.6, the corresponding duration thresholds are also indicated. Minor violations are permitted for up to 5 hours per week. Major violations are not permitted at all. At each penetration level, the constraint breach probabilities can be interpreted as the percentage of the histograms above the corresponding duration threshold. The constraint breach probabilities for voltage, conductor loading and transformer loading are plotted in Figures 6.3b, 6.3d and 6.3f, respectively. These can be compared with those in Figures 6.3a, 6.3c and 6.3e, respectively, for when using hard criteria.

When using flexible criteria, the constraint breach probabilities are significantly lower; this is the case for each monitor variable and at each penetration level. When using hard criteria, the constraint breach probability for voltage increases sharply with EV penetration level. When using flexible criteria, the constraint breach probability for voltage increases only a little until moderate EV penetration levels. Again, the constraint breach probability is highest for voltage, indicating that voltage is the constraining factor.

6.2.3 EV Hosting Capacity CDF

The EV hosting capacity CDF can be seen in Figure 6.4b. This can be compared with the CDF in Figure 6.4a, for when using hard criteria. When using flexible criteria, the CDF is significantly lower at each penetration level, indicating that higher EV hosting capacities occur with greater probability.

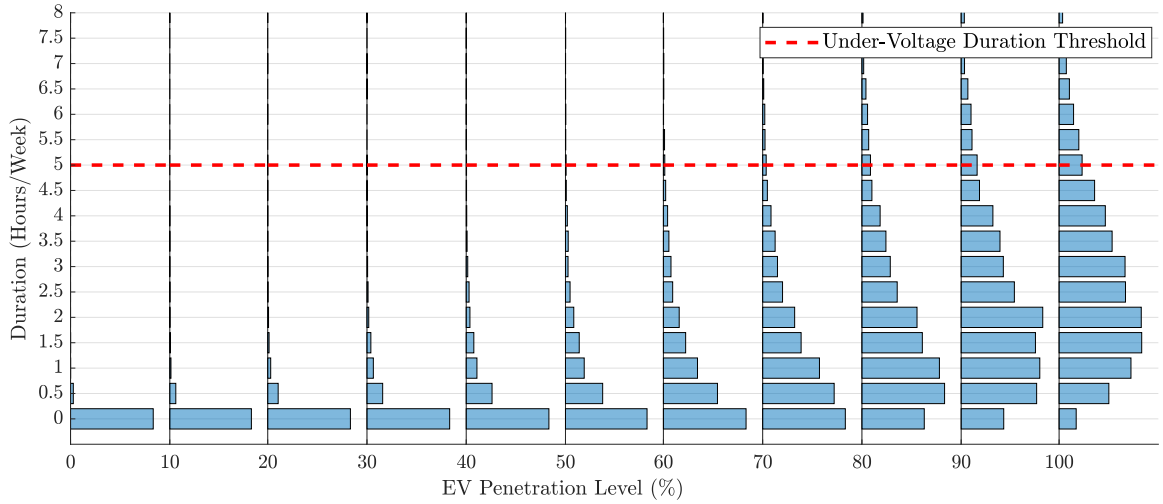

(a) Worst Affected Customer Under-Voltage Hours Per Week: $\mathcal{V} = \mathcal{V}_1$=0.94 p.u.

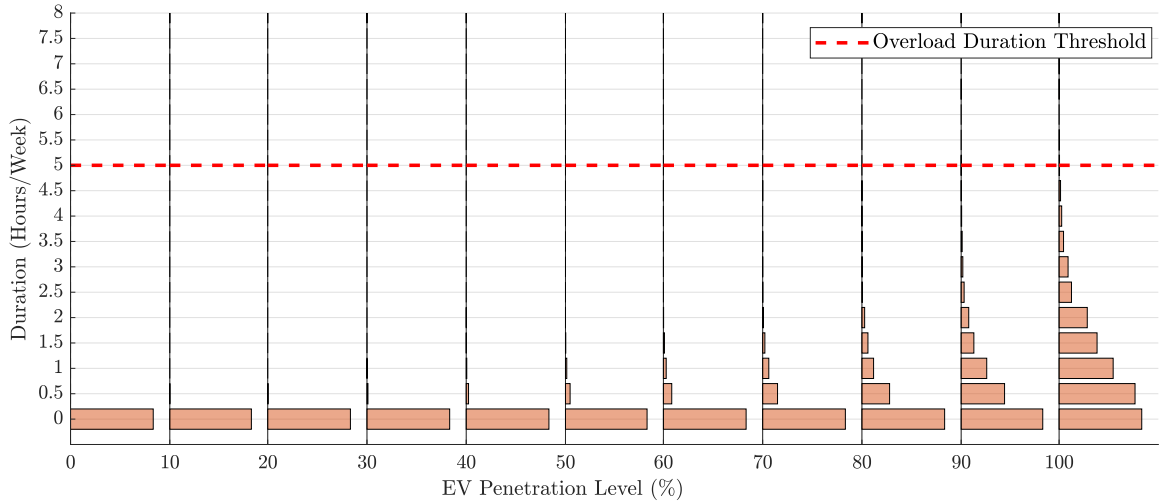

(b) Worst Affected Conductor Overload Hours Per Week: $\mathcal{I} = \mathcal{I}_1$=1.00 p.u.

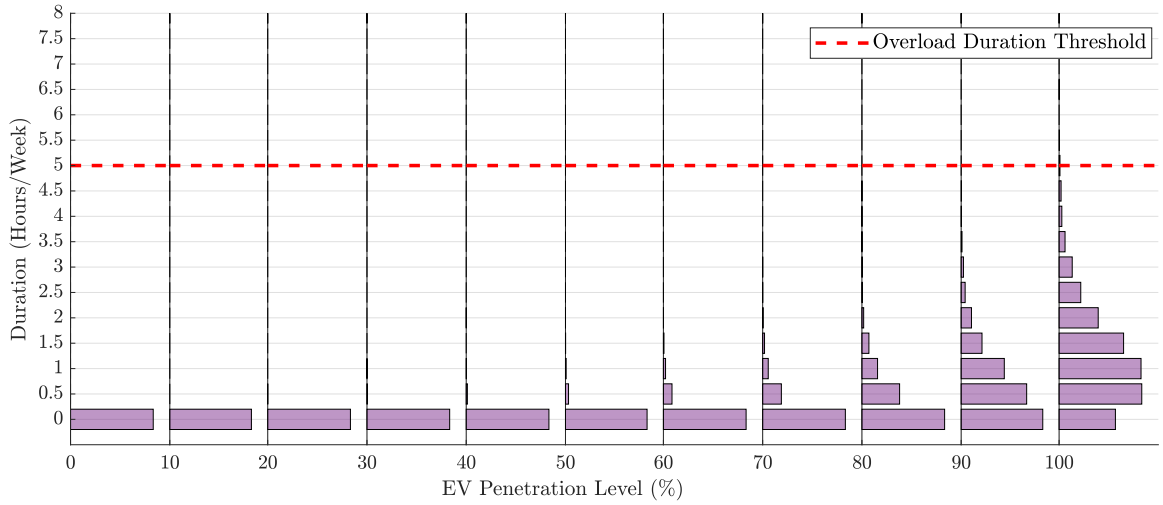

(c) Transformer Overload Hours Per Week: $\mathcal{S} = \mathcal{S}_1$=1.00 p.u.

Figure 6.5 Critical Variable Distributions: Flexible Criteria, Minor Magnitude Threshold

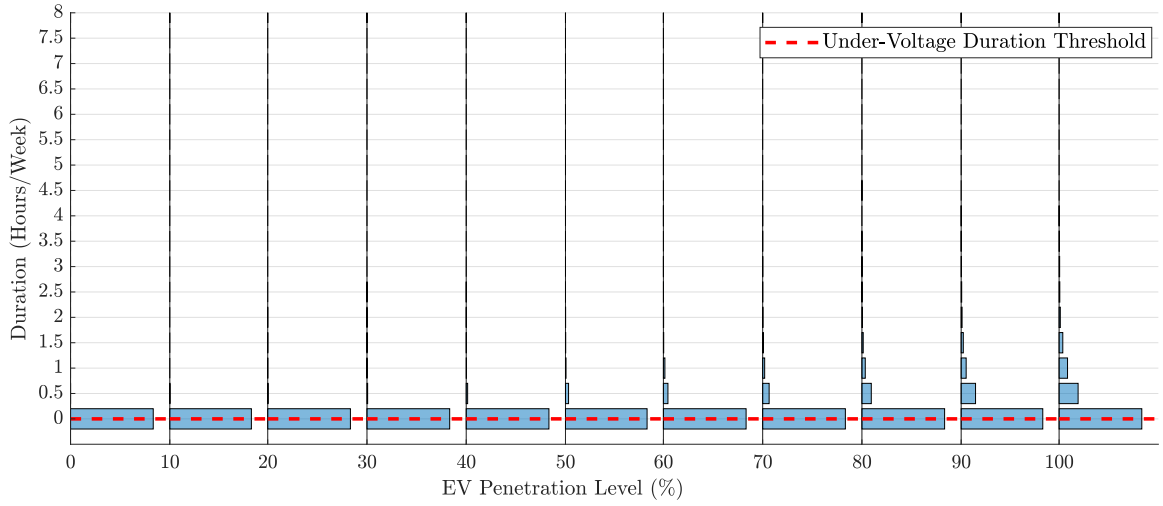

(a) Worst Affected Customer Under-Voltage Hours Per Week: $\mathcal{V} = \mathcal{V}_2$=0.90 p.u.

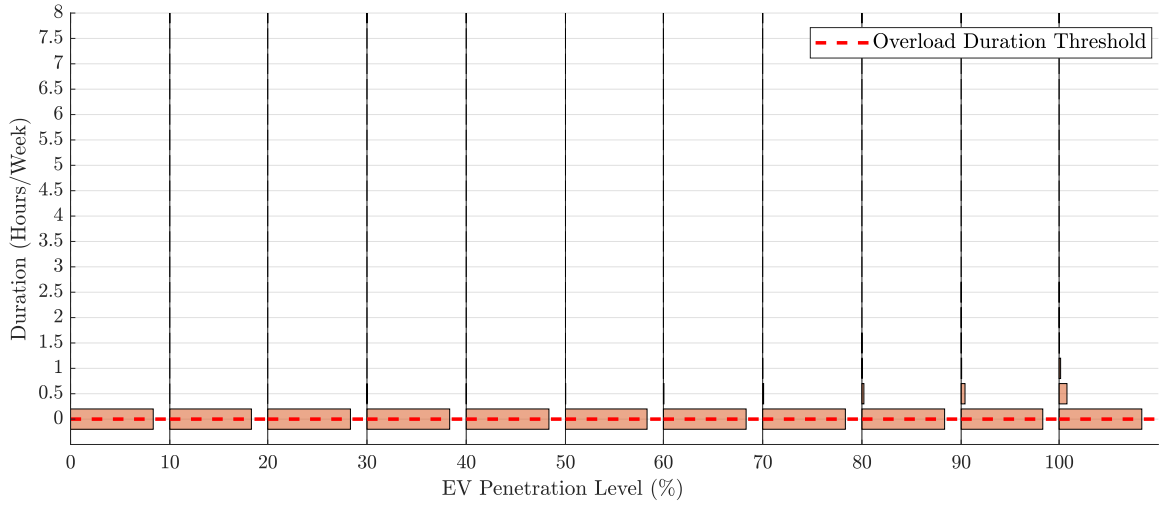

(b) Worst Affected Conductor Overload Hours Per Week: $\mathcal{I} = \mathcal{I}_2$=1.20 p.u.

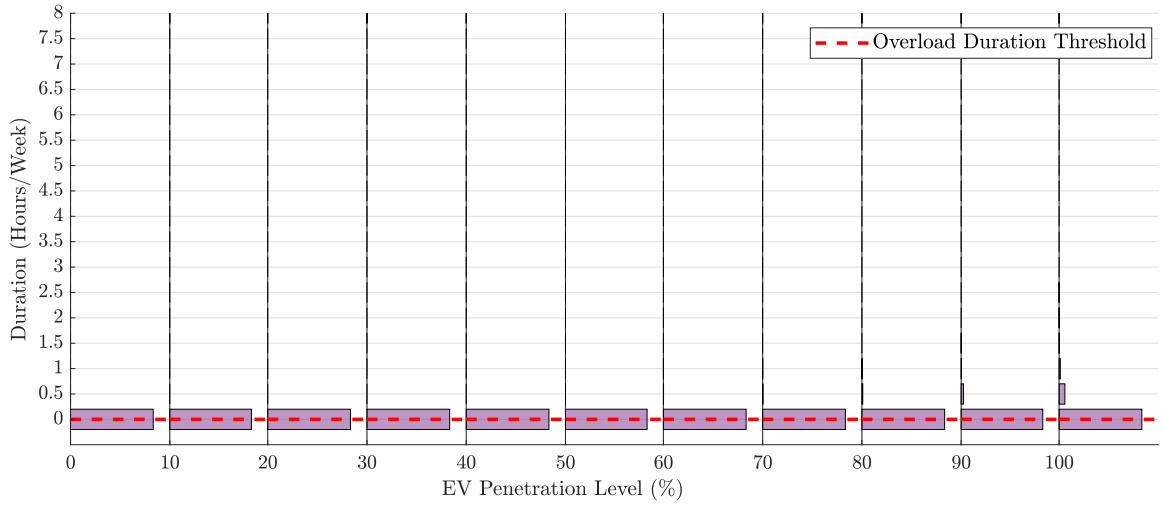

(c) Transformer Overload Hours Per Week: $\mathcal{S} = \mathcal{S}_2$=1.20 p.u.

Figure 6.6 Critical Variable Distributions: Flexible Criteria, Major Magnitude Threshold

When using flexible criteria, the P5 EV hosting capacity increases from 0% to 40%. Similarly, the P50 EV hosting capacity increases from 40% to 100%.

6.2.4 Discussion

Stochastic load-flow simulations produce a distribution of EV hosting capacities because of the uncertainty in customer loads. A single EV hosting capacity can be assigned by choosing an appropriate percentile of the EV hosting capacity distribution. Choosing a higher percentile value produces a higher EV hosting capacity assignment; however, the constraint breach probability at the assigned EV hosting capacity is also higher.

A higher EV hosting capacity allows network reinforcement to be deferred and is, therefore, preferable. However, there needs to be a compromise between deferring reinforcement and the possibility of violating operational limits. When operational limits are violated, both the magnitude and duration together, provide a clearer indication of the severity.

When using hard criteria, neither the magnitude nor duration of violations is explicitly captured. For example, the network is constrained if a customer experiences a single under-voltage of 0.93p.u. Equally, the network is constrained if a customer experiences numerous under-voltages between 0.85p.u. and 0.93p.u. When using hard criteria, these two cases cannot be differentiated, which makes understanding the necessary compromise difficult.

The EV hosting capacity can be significantly increased by using flexible criteria. Furthermore, because both the magnitude and duration of violations are explicitly captured, the necessary compromise is more clearly understood. For a particular EV hosting capacity assignment, both the confidence level and the severity of potential violations are explicitly stated. The confidence level depends on the percentile value, while the severity of potential violations depends on both the magnitude and duration thresholds. When using the thresholds in Table 5.4, the P5 EV hosting capacity is 40%; this can be interpreted as follows:

At the 40% EV penetration level, one can be 95% confident that:

- For all customers in the network:
  - The number of weekly under-voltage hours below 0.94p.u. will not exceed 5; and
  - The number of weekly under-voltage hours below 0.90p.u. will not exceed 0
- For all conductors in the network:
  - The number of weekly overload hours above 1.00p.u. will not exceed 5; and
  - The number of weekly overload hours above 1.20p.u. will not exceed 0
- For the transformer:

– The number of weekly overload hours above 1.00p.u. will not exceed 5; and
– The number of weekly overload hours above 1.20p.u. will not exceed 0

In this thesis, voltages between 0.94p.u. and 0.90p.u. are defined as minor under-voltages, while voltages below 0.90p.u. are defined as major under-voltages. Similarly, overloads between 1.00p.u. and 1.20p.u. are defined as minor overloads, while overloads above 1.20p.u. are defined as major overloads. Minor violations are permitted for 5 hours per week, while major violations are not permitted at all.

The magnitude and duration thresholds can be adjusted as appropriate. Adjusting the magnitude thresholds changes the definition of minor and major violations. Adjusting the duration thresholds changes the number of permitted violations. The magnitude and duration thresholds can be adjusted independently for each monitor variable; this may be appropriate if overloads are deemed to be more of a concern than under-voltages.

Figure 6.7 shows the impact of the duration thresholds on the P5 EV hosting capacity. In this example, the duration thresholds are equal for each monitor variable. The x-axis shows the minor violation duration threshold, while each plot represents a different value for the major violation duration threshold.

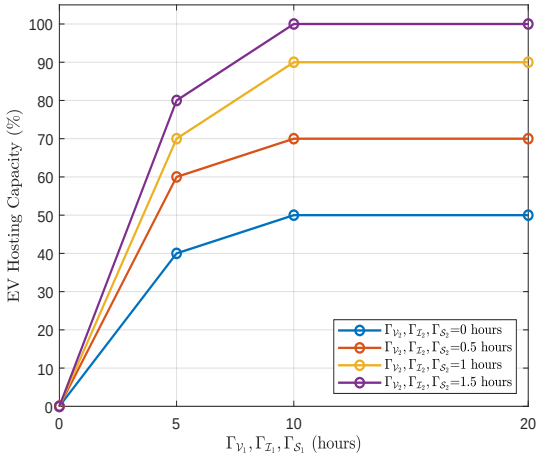

Figure 6.7 P5 EV Hosting Capacities for Various Duration Thresholds

Let us first consider the blue plot. Here, the major violation duration threshold is 0 hours, that is to say, major violations are not permitted at all. For the first point on the plot, the minor violation duration threshold is also 0 hours. This point corresponds to the EV hosting capacity when using hard criteria because neither minor nor major violations are permitted for any length of time. The second point on the blue plot corresponds to the thresholds in Table 5.4. As the minor violation duration threshold increases, the EV

hosting capacity also increases. A maximum EV hosting capacity of 50% is reached for a minor violation duration threshold of 10 hours. At this point, increasing the minor violation duration threshold no longer increases the EV hosting capacity; this indicates that the network is constrained by a small number of major violations, rather than a large number of minor violations.

The EV hosting capacity can only be increased by increasing the major violation duration threshold; this can be seen by comparing each of the plots. This graph allows the nature of violations to be more clearly understood. Here, the EV hosting capacity is restricted by a small number of major under-voltages.

6.3 SIMULATION CONVERGENCE

In Figure 6.8, the KS statistic is plotted as a function of the number of MC repetitions. The tolerance threshold is also indicated. The result shown here is the KS statistic for when using flexible criteria; however, the same trends are observed when using hard criteria.

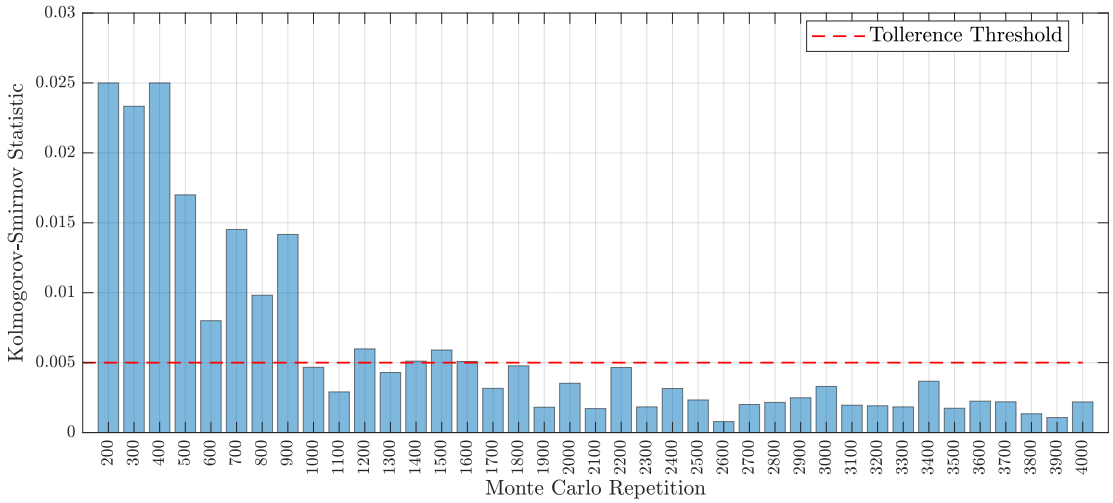

Figure 6.8 Demonstration of Simulation Convergence Criterion

The KS statistic decreases as the simulation proceeds, indicating a stabilising of the EV hosting capacity CDF. While overall, the KS statistic is decreasing, it is relatively volatile; for successive evaluations, it can be seen to both increase and decrease.

On the 1000^{th} MC repetition, the KS statistic drops below the tolerance threshold for the first time. On the 1200^{th} MC repetition, it then increases above the tolerance threshold.

For convergence, the KS statistic is required to stay below the tolerance threshold for five successive evaluations. The convergence criterion is satisfied on the 2700^{th} MC repetition. At this point, the MC simulation would ordinarily be terminated; however, additional repetitions are shown here for demonstration purposes. It can be seen that the KS statistic continues to decrease as the simulation proceeds. Reducing the tolerance threshold increases the number of repetitions required for convergence. A tolerance threshold of 0.005 was deemed appropriate for this thesis; however, this can be varied as required.

In contrast, the number of repetitions required by the brute force approach can be considered almost infinite. Let us consider the 0% penetration level as a example. Recall that there are 71 customer connections within the typical residential network and that for each customer, the residential load component is sampled from a SM dataset containing 400 customers. The number of ways in which 400 loads can be assigned to 71 customer connections can be calculated using Equation 6.1; this is a permutations problem where order is important and repetition is not permitted.

$$\frac{400!}{(400-71)!} = 7.48 \times 10^{181} \tag{6.1}$$

Order is important because it matters to which specific customers the various loads are assigned. Repetition is not permitted because each load can be assigned only once. It can be seen that the number of repetitions required by the brute force approach is significantly higher than the 2700 required by the MC approach. If we now consider all other penetration levels, where for each customer there are seven stochastic variables to be sampled, the number of repetitions required for the brute force approach can be considered almost infinite.

6.4 IMPACT OF EV CHARGING PRACTICES

The EV hosting capacity depends on the charging practices adopted by EV owners. Examples of more favourable charging practices include:

- Using lower-rated chargers
- Reducing range anxiety
- Using an even mix of charging strategies

Different charging scenarios can be examined by altering the statistical distributions from which the stochastic variables are sampled. The distributions in Table 4.3 define the baseline charging scenario. The baseline charging scenario describes the charging practices which EV owners are expected to adopt naturally. On the other hand, more

favourable charging practices may require increased public engagement, or some form of incentive, financial or otherwise.

The transformer load profile for the baseline charging scenario can be seen in Figure 6.9a. This is the mean transformer load profile across all MC repetitions, for the first day of the week. The residential and EV load contributions are indicated separately.

The transformer load profile provides a qualitative assessment of different charging scenarios. Network assets are sized for peaks, and therefore, a high average to peak load ratio is desirable. There are two peaks in the residential load component; the morning peak is at 9:30 am, while the evening peak is at 7.30 pm. There are also valleys during the day; the first occurs in the early hours of the morning between 3 am-7 am, and the second during business hours between 11 am-3 pm. From an LV network perspective, more favourable charging practices minimize the contribution to peaks, and also fill the valleys where possible.

In the baseline charging scenario, EV charging significantly compounds the residential evening peak; this is because the majority of customers use the OA charging strategy. Furthermore, the majority of EV charging is completed before the overnight valley. The small number of customers that use the DNT and BM strategies provide the small EV load contribution during the overnight valley.

The area between the residential load profile and a horizontal line at the residential peak is the theoretical charging energy which could be supplied without affecting network peak. By adopting more favourable charging practices, it may be possible to accommodate high EV penetration levels without significantly increasing peak demand.

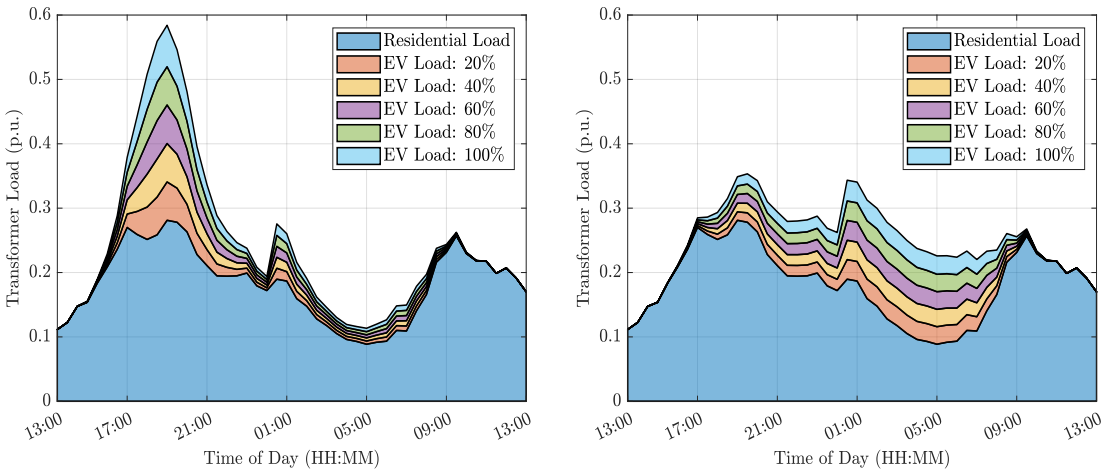

(a) Baseline Charging Scenario

(b) Alternative Charging Scenario

Figure 6.9 Mean Transformer Load Profile

The alternative charging scenario is defined in Table 6.1. Relative to the baseline charging scenario, there are three key differences. Firstly, lower-rated chargers occur with significantly higher probability; the vast majority of EVs are charged using a 2kW charger. Using lower-rated chargers reduces the magnitude of the aggregate EV load profile. Furthermore, the charge duration is increased, meaning that charging extends until later in the overnight valley.

Table 6.1 Stochastic Variable Distributions for Baseline and Alternative Charging Scenarios

Scenario	Distribution Parameters		
	Charger Ratings P(2, 4, 8 kW)	Range Anxiety P(0.1, 0.5, 0.9 p.u.)	Charging Strategies P(OA, BM, DNT)
Baseline	[0.15, 0.70, 0.15]	[0.10, 0.20, 0.70]	[0.80, 0.10, 0.10]
Alternative	[0.95, 0.025, 0.025]	[0.95, 0.025, 0.025]	[0.33, 0.33, 0.33]

Secondly, range anxiety is significantly reduced; for the vast majority of EVs, the range anxiety factor is 0.1. Reducing range anxiety impacts the aggregate EV load profile in a similar way to reducing charger ratings. The magnitude of the aggregate EV load profile is reduced because only a subset of the entire fleet is charged each day. Furthermore, EVs are discharged more deeply, meaning that charging extends until later in the overnight valley.

Finally, there is a more even mix of charging strategies; the OA, DNT and BM strategies occur with equal probability. Using a more even mix of charging strategies reduces the peak load contribution because a significant proportion of the EV charging load is delayed until later in the evening.

The transformer load profile for the alternative charging scenario can be seen in Figure 6.9b. When compared to the baseline charging scenario, the peak load contribution is significantly reduced. Furthermore, the overnight valley is more effectively utilized, and as a result, the average to peak load ratio is significantly improved.

While the transformer load profiles provide a qualitative comparison of the baseline and alternative charging scenarios, the EV hosting capacities provide a quantitative comparison. The EV hosting capacities for the baseline and alternative charging scenarios are compared in Figure 6.10. The plot shows the P5 EV hosting capacities when using both hard and flexible criteria. When using hard criteria, the P5 EV hosting capacity is 30% higher for the alternative charging scenario. When using flexible criteria, the P5 EV hosting capacity is 60% higher for the alternative charging scenario.

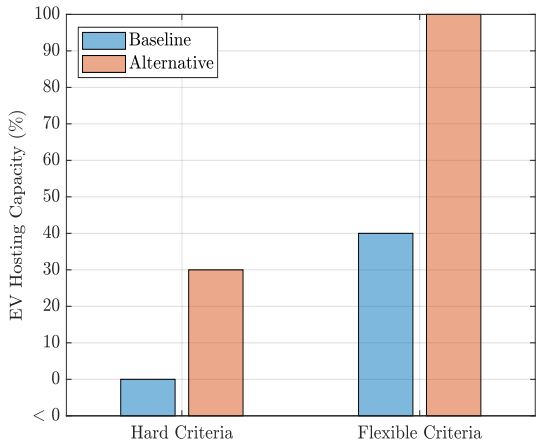

Figure 6.10 P5 EV Hosting Capacities

While the alternative charging scenario is more favourable from an LV network perspective, it is essential to consider the impact on EV owners, since these charging practices represent a move away from the behaviours which would be adopted naturally. The impact on EV owners can be analysed using the incomplete charge and curtailed journey probabilities; these are plotted in Figures 6.11 and 6.12, respectively.

An incomplete charge event is recorded when the target SOC cannot be reached; this is only the case for charging events with large charging energy requirements and narrow availability windows. For each EV, the number of weekly incomplete charge events can be between 0 and 7. Figure 6.11 shows the probability of between 1 and 7 incomplete charge events, for both the baseline and alternative charging scenarios. The probabilities are calculated using the results for all EVs and across all MC repetitions.

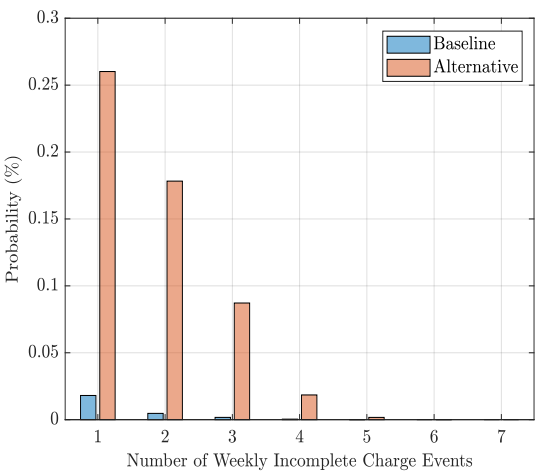

Figure 6.11 Incomplete Charge Probabilities

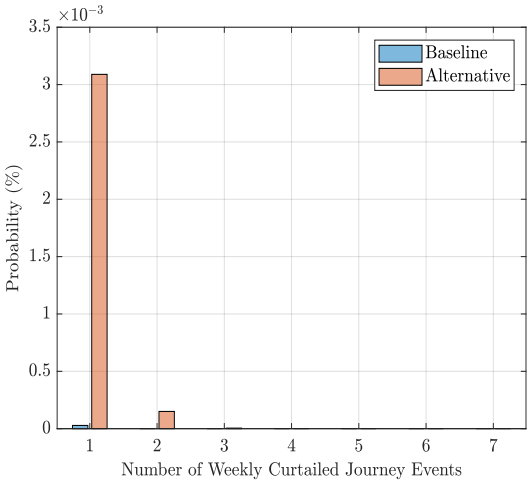

Figure 6.12 Curtailed Journey Probabilities

The incomplete charge probabilities are significantly higher for the alternative charging scenario; the reasons for this are as follows:

- Lower-rated chargers require more time to reach the target SOC
- When range anxiety is reduced, EVs are discharged more deeply
- The entire availability window cannot be utilised when using the DNT charging strategy

Although the probability of a single incomplete charge event is relatively high, the probability of multiple incomplete charge events decreases significantly. Furthermore, not all incomplete charge events impact EV end-use; this can be seen by comparing the incomplete charge and curtailed journey probabilities.

A curtailed journey event is recorded when, because of an incomplete charge event, the departure SOC is insufficient to cover the driving energy requirement. Again, for each EV, the number of weekly curtailed journey events can be between 0 and 7. Figure 6.12 shows the probability of between 1 and 7 curtailed journey events, for both the baseline and alternative charging scenarios.

The probability of a single curtailed journey event is negligible, even for the alternative charging scenario; this indicates that for most incomplete charge events, the departure SOC is not far from the intended target. EV owners are therefore not significantly impacted by the proposed changes in charging practices.

Chapter 7

CONCLUSIONS

In the past, DNOs have designed their networks based on assumptions of after-diversity demand. In the time that has passed since many networks were built, demand has changed significantly and EV charging is just one example of how demand will change in the future. DNOs have limited observability in their LV networks. While transformer maximum demand indications are typically available, network voltages and conductor loading are unknown. DNOs are required by law to ensure that customer voltages are kept within the steady-state voltage limits specified in government legislation. Conductor overloading must also be avoided to ensure that conductors do not overheat. The limited observability in LV networks means that distribution companies have little way of knowing whether or not violations are occurring. Voltage assessment is typically limited to manual assessments at particular locations, often in response to customer complaints. As EV ownership is expected to increase, DNOs need to understand how changes in demand will impact their networks. This will allow planning and investment to be allocated ahead of time.

Stochastic load-flow simulations allow future scenarios to be assessed while taking into account the uncertainty in customer-level loads. Unlike the simpler deterministic calculations which would have been performed historically, the results of stochastic load-flow simulations need to be interpreted using statistical methods. This thesis has presented a due diligence framework which DNOs can use to assess network voltages and asset loading for a range of future scenarios. The methodology allows different EV charging practices to be assessed which will allow DNOs to quantify the potential benefits of encouraging more positive behaviors. DNOs will be able to fully understand both the probability and severity of potential violations. The severity of violations is defined by the magnitude and duration thresholds, which can be adjusted to reflect the power quality standards used in different countries. The probability of violations is obtained by performing a significant number of MC repetitions. Ultimately, when assessing EV hosting capacity, there is a necessary compromise between deferring network reinforcement and the possibility of violating operational limits. The proposed framework allows this compromise to be fully understood, meaning that DNOs can then make

informed decisions regarding future investments.

The motivation for this research was established in Chapter 2. Reducing GHG emissions will be one of the critical challenges for the 21st century, and as part of this, the electrification of transport will play a crucial role. NZ is particularly well suited for the electrification of transport because of its unique energy landscape.

The NZ EV fleet has doubled in each of the last three years, and in the future, LV distribution networks may become constrained because of the additional load due to EV charging. Load-flow simulations allow future scenarios to be assessed a priori, allowing planning and investment to be allocated ahead of time.

When modelling LV distribution networks, individual customer loads are explicitly modelled. At the level of individual customers, loads are highly uncertain, and therefore, a stochastic approach is suitable. When repeated, sampling causes some load-flow results to be more extreme than others; using a MC method allows the range of possible outcomes to be quantified. Unlike deterministic load-flow simulations which produce a single EV hosting capacity, stochastic load-flow simulations produce a distribution of EV hosting capacities. The primary research question was, therefore, as follows:

"How can we interpret stochastic load-flow results in order to make meaningful conclusions regarding EV hosting capacity?"

A review of the relevant literature was presented in Chapter 3. The review was broken down into three sections: residential load modelling, EV load modelling and stochastic load-flow simulations. Gaps and limitations in the existing body of knowledge were also discussed.

The stochastic EV load model was described in detail in Chapter 4. The model simulates weekly EV load profiles with half-hour resolution and incorporates seven stochastic variables:

- Arrival time
- Departure time
- Daily distance travelled
- Battery capacity
- Charger rating
- Range anxiety
- Charging strategy

The stochastic variables allow unique load profiles to be simulated for each customer. Different charging practices were compared by altering the statistical distributions from which the stochastic variables are sampled.

The stochastic load-flow simulation was described in Chapter 4, including the typical residential network which was modelled in OpenDSS. The inputs to OpenDSS are the weekly customer load profiles. The outputs are a series of network monitors which record voltage, conductor loading and transformer loading during the simulation.

Constraints were assessed from the exported monitor variables using both hard and the newly proposed flexible criteria. When using hard criteria, all voltages must be within the statutory limits. Similarly, all conductor and transformer loadings must be within their continuous rating. On the other hand, when using flexible criteria, a small number of minor violations are permitted, where the permitted duration depends on the violation magnitude. This approach more reasonably reflects the needs of network assets and customer equipment.

The EV hosting capacity is the maximum EV penetration level a network can accommodate before becoming constrained. A CDF described the distribution of EV hosting capacities across all MC repetitions. The MC simulation was terminated, when after a significant number of MC repetitions, the CDF stabilised.

The results from the stochastic load-flow simulation were presented in Chapter 6. The critical variable distributions, constraint breach probabilities, and EV hosting capacity CDFs were compared for when using hard and flexible criteria. The differences were then discussed, highlighting the limitations of using hard criteria, and the extent to which these can be overcome by using flexible criteria. It was also demonstrated how EV hosting capacity is significantly increased by adopting more favourable charging practices.

7.1 REVIEW OF SECONDARY RESEARCH QUESTIONS

7.1.1 Research Question 1

"What are the stochastic variables required to model EV load?"

There are numerous stochastic EV load models in the literature, and the number of variables is indicative of the level of detail. The specific variables can vary; however, in general, the model must account for the following:

- Charging availability
- Charging energy requirement
- Rate of charge
- Battery capacity
- Charging strategy

Charging availability describes the time when an EV is at home and hence available for charging. Charging availability is typically modelled using the arrival time and departure time; however, in simpler models only the arrival time is used. When using only the arrival time, there is an implicit assumption that charging is completed before departure. The model presented in this thesis uses both the arrival and departure time. The departure time allows the number of incomplete charges to be captured. Furthermore, the by-morning (BM) charging strategy requires that the departure time is known. EV trial data suggests that arrival and departure times can be reasonably approximated by a normal distribution.

The charging energy requirement depends on the driving demands of the EV owner. The charging energy requirement is typically modelled using the arrival SOC, and by assuming that EVs are recharged to full each night. The arrival SOC is sampled from a statistical distribution, typically normal or uniform. Alternatively, the charging energy requirement can be modelled using the daily distance travelled. The arrival SOC is then calculated using the departure state of charge earlier that day, and an assumed energy consumption coefficient.

In the literature, it is assumed that all EVs are recharged to full each night; or to some other predetermined SOC. Despite this, EV trial data suggests that EVs are rarely recharged each day, and instead, EV owners decide whether or not to charge based upon their arrival SOC and predicted range requirement for the following day. Range anxiety describes the tendency to charge when not required to do so and reflects uncertainty when predicting journeys ahead of time. The EV load model presented in this thesis provides an improvement on those in the literature by including an additional stochastic variable to capture range anxiety.

The rate of charge depends on both the charger and EV model. The rate of charge will, therefore, vary among customers. In order to capture this variation, the charger rating can be sampled from a multinomial distribution. Similarly, the battery capacity also depends on the EV model, and therefore, a multinomial distribution is again appropriate.

The EV charging strategy describes how EV load is scheduled, subject to the relevant constraints. Simple charging strategies can be modelled using the charging start time, charging end time, and charger rating. More sophisticated charging strategies are modelled using the arrival time, departure time, and load trajectory. In the case of more sophisticated charging strategies, the rate of charge can be modulated and can start and stop several times during the availability window.

The charging strategy of choice will vary among customers. In order to capture this variation, the charging strategy can again be sampled from a multinomial distribution.

Three EV charging strategies were considered in this thesis: on arrival (OA), day-night tariff (DNT) and by morning (BM). These strategies were chosen because they can be implemented using a non-dedicated charging cable, and by the majority of EV models.

7.1.2 Research Question 2

"How to determine the uncertainty in EV hosting capacity?"

A stochastic approach is appropriate when modelling LV distribution networks because customer loads are highly uncertain; this uncertainty propagates through the LV network model and is reflected in the EV hosting capacity CDF. Although LV distribution networks are bound by operational limits for voltage, conductor loading and transformer loading, one of the three is typically the constraining factor. For the typical residential network, voltage is the constraining factor. When using hard criteria, voltage violations are rare at low penetration levels and occur for only the most unfavourable MC repetitions. Voltage violations are significantly more common at high penetration levels; however, despite this, for some of the most favourable MC repetitions, there are no violations even at the 100% penetration level. For this reason, the EV hosting capacity can vary between <0% and 100%, which are the minimum and maximum possible values, based on the EV penetration levels assessed.

For the network under study, the probability of an EV hosting capacity <0% is 0.03. On the other hand, the probability of an EV hosting capacity >90% is 0.01. The EV hosting capacity is low when temporal coincidence is high, and when load placements result in significant feeder, phase and longitudinal imbalance. On the other, the EV hosting capacity is high when temporal coincidence is low, and when load placements result in less significant feeder, phase and longitudinal imbalance.

7.1.3 Research Question 3

"How many MC repetitions are required?"

In the literature, the number of MC repetitions is often defined a priori. Less often, the simulation is repeated until convergence; however, the convergence criterion is not always clear. Here, convergence was assessed using the KS statistic.

The EV hosting capacity CDF is re-evaluated after every 100 MC repetitions. The KS statistic is the maximum change in the CDF, and therefore, provides a measure of stability. For convergence, the statistic is required to be within the specified tolerance for five successive evaluations. For the network under study and with a tolerance of 0.005, convergence was achieved by 2700 MC repetitions. Using a lower tolerance value produces a more stable CDF, but requires a more significant number of MC repetitions.

7.1.4 Research Question 4

"What are the limitations of using hard constraint criteria?"

A single EV hosting capacity can be assigned by choosing a percentile of the EV hosting capacity distribution. A higher percentile value produces an higher EV hosting capacity; however, the constraint breach probability at the assigned EV hosting capacity is also higher. For the network under study, when using hard criteria the P50 EV hosting capacity is 40% and the constraint breach probability is 0.42. Similarly, the P5 EV hosting capacity is 0% and the constraint breach probability is 0.03. Both of these are the constraint breach probabilities for the worst week of the year; that is, the week that contained the annual peak load.

If a low percentile value is chosen, network reinforcement is required to accommodate even low EV penetration levels; the costs of which are ultimately passed on to customers. If a high percentile value is chosen, network reinforcement can be deferred; however, the probability of a constraint breach increases.

In reality, customer equipment can handle a small number of minor under-voltages. Similarly, network assets can handle a small number of minor overloads. When operational limits are violated, it is important to consider both the magnitude and duration, because together, these provide a clearer indication of severity.

When assigning EV hosting capacity, there is a necessary compromise between deferring network reinforcement and the possibility of severely violating operational limits. When using hard criteria, the magnitude and duration of violations are not explicitly captured. The network is constrained if a customer experiences a single minor under-voltage, or if a customer experience numerous major under-voltages. When using hard criteria, these two cases cannot be differentiated, which makes understanding the necessary compromise difficult.

7.1.5 Research Question 5

"To what extent can these limitations be overcome by using flexible constraint criteria?"

When using flexible criteria, the severity of violations is explicitly defined. The proposed structure of the flexible criteria is as follows: voltages between 0.94p.u. and 0.90p.u. are defined as minor under-voltages, while voltages below 0.90p.u. are defined as major under-voltages. Similarly, overloads between 1.00p.u. and 1.20p.u. are defined as minor overloads, while overloads above 1.20p.u. are defined as major overloads. Minor violations are permitted for 5 hours per week, while major violations are permitted for 0 hours per week.

The magnitude and duration thresholds can be tightened or loosened as required. The definition of minor and major violations can be changed by altering the corresponding magnitude thresholds. The permitted number of violations can be changed by altering the duration thresholds. The magnitude and duration thresholds may also be tightened across one or more monitor variables; this may be appropriate if overloads are deemed to be more of a concern than under-voltages.

The EV hosting capacity can be significantly increased by using flexible criteria. When using hard criteria, the P5 EV hosting capacity is 0%; this is increased to 40% when using flexible criteria. Furthermore, both the confidence level and the severity of potential violations are fully understood. The confidence level depends on the chosen percentile value, while the severity of potential violations depends on the magnitude and duration thresholds.

7.1.6 Research Question 6

"To what extent can the EV hosting capacity be increased by alternative charging practices?"

Different charging practices can be examined by altering the statistical distributions from which the stochastic variables are sampled. The distributions in the baseline charging scenario reflect the charging practices which EV owners are expected to naturally adopt. In the baseline charging scenario, EV charging compounds the residential evening peak and is completed before the start of the overnight valley.

The distributions in the alternative charging scenario reflect a range of more favourable charging practices; these include:

- Using lower-rated chargers
- Reducing range anxiety
- Using a more even mix of charging strategies

In the alternative charging scenario, EV charging contributes significantly less towards the evening peak and the overnight valley is more effectively utilised. For the network under study, when using hard criteria the P5 EV hosting capacity is increased from 0% to 30%. Similarly, when using the proposed flexible criteria, the P5 EV hosting capacity is increased from 40% to 100%.

7.2 CRITIQUES AND FUTURE WORK

The primary contribution of this thesis is a framework for assessing EV hosting capacity using flexible criteria. The proposed framework goes some way in addressing the primary

research question and therefore contributes to the existing body of knowledge. On the other hand, the work in this thesis is not without limitations and there are various avenues for future work.

When assessing EV hosting capacity, establishing appropriate constraint criteria is crucial; however it is ultimately a philosophical decision. No criteria is without limitations. Using hard criteria is limited because the magnitude and duration of violations are not explicitly captured. The flexible criteria proposed in this thesis are able to overcome this limitation; however, there are still blind spots. Let us consider voltage as an example. The proposed criterion considers the number of under-voltage hours per week, for the worst affected customer; the number of hours for all other customers is not considered. One could argue that a more comprehensive measure would consider voltages throughout the network. The worst affected customer was chosen because it provides the maximum number of under-voltage hours. All other customers will have a fewer number of under-voltage hours per week; however, the extent to which this is the case is unclear.

In this thesis, only under-voltages were assessed. The reason for this is because under-voltage is the primary concern with regards to EV charging. On the other hand, over-voltage can become a concern in distribution networks with distributed generation. In New Zealand, there is little correlation between EV charging and PV generation. It is therefore possible that some networks could experience both over-voltages and under-voltages, during different periods of the day. Distributed generation was beyond the scope of this thesis; however, the proposed criterion could be adapted to include over-voltage assessment. In New Zealand, the EEA guidelines state that steady-state voltage shall be assessed using 99^{th} and 1^{st} percentiles of 10-minute averaged r.m.s. voltages over a period of one week. Here, both under-voltages and over-voltages are permitted for 1% of the time in a week. The proposed framework could easily be adapted to include this type of assessment. The constraint criterion would instead consider both the number of under-voltage hours per week, and the number of over-voltage hours per week. Both of these would be compared against a uniform duration threshold equal to 1% of the number of hours in a week.

The EV hosting capacity is sensitive to the probability distributions provided as inputs. Where possible, these distributions were chosen to reflect data which was available for New Zealand. When such data was not available, the wider literature was consulted. In practice, the EV hosting capacity will depend on the charging practices adopted by EV owners. Even at present, EV charging practices in New Zealand are not fully understood. Although nationwide studies provide significant insights into vehicle models and charging technologies, any understanding of charging strategies and range anxiety is based on questionnaires completed by small sample groups. Understanding how EV charging practices are likely to evolve in the future is even more difficult. The

contribution of this thesis is not the specific EV hosting capacities which were presented, but rather framework for assessing EV hosting capacity. DNOs can adjust the probability distributions to reflect their own assumptions regarding EV charging practices and can be updated as new data becomes available. Alternatively sensitivity studies can be performed to quantify the impact of any uncertainty on the EV hosting capacity; an example of one such sensitivity study was presented in Section 6.4. Performing additional sensitivity studies is a possible avenue for future work.

The framework presented in this thesis can be used to identify the point at which networks will experience voltage and thermal loading violations. At this point, some form of mitigation is required. Assessing different mitigation options was beyond the scope of this thesis; however, it would be remiss not to discuss some of the possible options. Conventional reinforcement involves up-sizing existing network assets, and can be used to mitigate both voltage and thermal loading violations. Conventional reinforcement is expensive and is often considered a last resort. As was the case with the typical residential network considered in this thesis, voltage is often the dominant constraint and thankfully there are various alternative options for mitigating voltage violations.

Reactive power control has been used to limit over-voltages due to PV generation and it is possible that such an approach could equally be used to limit under-voltages due to EV charging. Studies show that because reactive power control is only activated at customers with high voltage, the increase in PV hosting capacity is minimal; however, extreme over-voltages are substantially reduced. This would likely be the case with EV charging as well, where reactive power would only be activated at customers with low voltages; typically these are those towards the end of radial feeders. In New Zealand, the R/X ratio in LV distribution networks is typically around 1.0 (Watson et al. [2016]). A high R/X ratio reduces the effectiveness of reactive power in regulating voltage magnitude and therefore reactive power alone may not be sufficient to mitigate voltage violations. Furthermore, it is worth noting that reactive power capabilities would require the use of a dedicated wall mounted charger which are significantly less common in New Zealand due to the associated cost.

Another option is to increase the secondary voltage of the distribution transformer. In New Zealand, distribution transformers typically provide off-load tap settings of $\pm$ 2.5%. Under-voltages could be mitigated by increasing the secondary voltage by 2.5%. It is worth remembering, however, that the transformer nameplate is 11kV/415V, which already equates to 1.037 p.u. in a 400V system. Further increasing the secondary voltage may risk over-voltages during low load periods, especially in networks with PV generation. Because off-load tap settings cannot be changed over the course of the day, the risk of both under-voltage and over-voltage should be considered when adjusting tap settings. Single phase loads result in voltage magnitude and phase angle unbalance between the

phases. This unbalance gives rise to negative and zero sequence components which cannot be mitigated by adjusting the transformer tap settings.

Line drop compensation at the MV level can also be used. In New Zealand, DNOs can regulate voltage by applying line drop compensation at the zone substation (Watson et al. [2016]). Using line drop compensation, it is possible to provide a lower network voltage at times of low load and a higher voltage at time of high load. These voltages are typically 10.9kV and 11.2kV, respectively. The line drop compensation settings could be adjusted to manage the risk of both under-voltages due to EV, and over-voltages due to distributed generation. The framework presented in this thesis will allow various mitigation options to be assessed; this remains a possible avenue for future work.

Statutory limits often specify the necessary averaging period for voltage measurements. While this varies between countries, 10-minute averaging is the most common. In this thesis, the stochastic load-flow simulation has half-hour temporal resolution and therefore, the number of voltage violations will be underestimated. The temporal resolution of the simulation is limited by the resolution of the SM data and could easily be adapted if high-resolution load data becomes available in the future.

Future scenarios were assessed by increasing the EV penetration level; however, the residential load component was not altered. It is unclear how residential demand will change in the future. While new devices may increase residential demand, efficiency gains may cause a reduction. A possible solution would be to scale the SM data at each EV penetration level. Alternatively, the simulations could be repeated, as and when more recent load data becomes available.

EVs charge at a reduced rate as the battery approaches fully charged (Concept Consulting [2018]). In this thesis, it was assumed that EVs are charged between 0% and 80% SOC, and therefore, all charging is at rated capacity. The impact of ignoring these second-order effects remains unquantified, and may be an area for future work.

The model assumes that EV charing is 100% efficient; because of this, the charging energy requirement will be underestimated. In reality, the efficiency depends on a number of factors including the vehicle model and rate of charge. the model could be improved by including efficiency; however, the impact is not expected to be significant.

The stochastic EV load model presented here provides an improvement on those in the literature by including a stochastic variable to capture range anxiety. When range anxiety is high, EVs are recharged each day, independent of the arrival SOC. When range anxiety is low, EVs are charged less frequently; only when the arrival SOC relatively low. While providing an improvement, the model is still limited. EVs are either charged to

full or not charged at all. In practice, some EV owners may choose to perform a short, top-up, charge. Furthermore, in some cases, EV owners may perform multiple top-up charges per day. Human behavior in this context requires more investigation.

In the future, public charging infrastructure will become more common. As a result, EV charging will be shared between residential and public settings. In this thesis, it is assumed that all EV charging is takes place at home, and therefore, the results may overestimate the impact of EV charging in residential networks. Understanding how EV charging will be shared between residential and commercial settings is an area for future work. The stochastic EV load model may be updated to take into account charging away from the home.

Results were only presented for a single residential network. Although the chosen network is typical, LV distribution networks vary significantly in terms of size, topology and strength. Future work will look to assess a greater number of LV networks using the flexible criteria proposed in this thesis.

Appendix A

UNPUBLISHED WORKS

The Significance of Load Diversity on Voltage Assessment in Low Voltage Distribution Networks

Euan McGill
Electric Power Engineering Centre (EPECentre)
University of Canterbury
Christchurch 8041
Email: euan.mcgill@pg.canterbury.ac.nz

***Abstract*— Low voltage distribution networks in New Zealand are experiencing an increasing penetration of disruptive technologies such as electric vehicles and photovoltaics. There are concerns among distribution companies regarding the impacts these technologies may have on steady state voltage levels. Load flow simulations provide a means to assess these impacts. Load diversity describes variation in the coincident loading of individual consumers. A common simplifying assumption within modelling is to assume uniform load distribution throughout the network. Whilst frequently applied, this simplification is rarely reflected in reality. Failure to account for the true load diversity may result in inaccurate load flow results. Within this work, Smart Meter data is used to assess the impact of load diversity on steady state voltage drop for radial distribution networks. Two scaling factors are defined to relate the voltage drop equations for the uniformly distributed and diversified cases. These scaling factors describe load diversity along the length of feeders, and across the phases. A Monte Carlo method is implemented in order to derive empirical distributions for the scaling factors. Results demonstrate that neglecting load diversity can result in both underestimation and overestimation of the true voltage drop. The extent of these inaccuracies is found to decrease with increasing aggregation scale. It is concluded that in order to avoid masking potential statutory limit voltage violations in future impact studies, load diversity should be considered in the analysis.**

I. Introduction

Electric vehicles (EVs) and photovoltaics (PVs) are two emerging technologies which will impact low voltage (LV) distribution networks. Whilst modest at present, their penetration is forecast to significantly increase in the near future [1], [2]. Consequently there are concerns regarding how these will affect steady state (SS) voltage levels. Distribution companies have historically planned LV networks to cope with the maximum anticipated demand. Often additional capacity is allocated in order to accommodate long term trends in demand increase. In the case of these technologies however, the assumption of a gradual load increase for all premises is insufficient to capture their true impact in load flow simulations. For example, PVs and Vehicle to Grid (V2G) bring about the possibility of reverse power flow. Additionally, sporadic uptake and variation in charging times may lead to increased load diversity. Within existing research, load flow simulations have been carried out to assess the hosting capacity of LV networks [3]–[6]. Much of this work applies simplifications during load modelling. Loads are typically allocated to individual households based upon a uniform distribution of the upstream transformer load. This results in zero load diversity in the network. When modelling PVs and EVs the penetration level is first chosen. Single units are then randomly scattered throughout the network. This process inherently adds a degree of load diversity on top of the underlying transformer load. Despite this the underlying transformer load typically still represents a significant percentage of the total modelled load, for which load diversity remains unaccounted. Load diversity is likely to be exacerbated by the proliferation of EVs and PVs, and therefore it is important that the consequences of this load modelling simplification are quantified.

There are numerous examples of research publications in which load diversity is accounted for in modelling [7]–[9]. In these examples unique load profiles are assigned to individual installation control points (ICPs) during load flow simulations. Despite this the following are identified as key limitations in existing literature.

- No demonstration of the causal relationship between load diversity and voltage drop
- No quantitative comparison between uniformly distributed and diversified load flow results
- Lack of statistical analysis of sufficient sample size

In this work Smart Meter data is used to model the true load diversity in an LV network. Feeder voltage drop is then compared for the diversified and uniformly distributed cases. Within the remainder of this paper, Section II provides a detailed definition of load diversity with reference to literature. In Section III the voltage drop equations for the uniformly distributed and diversified load models are derived. Scaling factors which relate these voltage drops are also defined. Section IV then presents the Monte Carlo method used to extract these scaling factors from Smart Meter data. Section V presents the results and discusses their significance. Sections VI concludes with the key findings and recommendations for future work.

II. Load Diversity Definition

In the literature load diversity describes the extent to which the peak demands of individual consumers occur at different

times of the day [10] [11] . It is typically measured by the diversity factor seen in Equation 1.

$$F_D = \frac{\sum_{j=1}^{N} D_j^{max}}{D_{system}^{max}} \tag{1}$$

- F_D = Load Diversity Factor
- N = Number of ICPs in Network
- D_j^{max} = Maximum kW Demand of ICP j
- D_{system}^{max} = Coincident Maximum kW Demand for the Group of N ICPs

Alternatively the after diversity maximum demand as seen in Equation 2, may be used.

$$ADMD = max\left\{ \frac{\sum_{j=1}^{N} D_j^i}{N} \right\}_{i=1}^{K} \tag{2}$$

- $ADMD$ = After Diversity Maximum Demand per ICP
- N = Number of ICPs in Network
- D_j^i = kW Demand of ICP *j* During Time Interval *i*
- K = Number of Time Intervals During Period of Interest

Load diversity is used in network planning in order to curb the total capacity requirements of a utility. As the size of a distribution network increases the ADMD decreases [12]. Understanding this relationship allows the sizing of network assets to be optimized. Typically in load flow simulations the upstream transformer load is uniformly distributed throughout the downstream network. The transformer load is obtained from either:

- A known maximum demand indication
- Equation 1 with empirically derived values of F_D

This approach ensures that the aggregated demand on the network accounts for load diversity. Despite this, uniformly distributing the aggregated demand introduces inaccuracies. This approach results in zero load diversity downstream of the transformer, i.e. all ICPs simultaneously consume the same power. This behaviour is rarely reflected in reality. Figure 1 shows the load at 7pm for 10 residential ICPs from a Smart Meter dataset. For each ICP the true load can be compared with the uniformly distributed transformer load, calculated using Equation 3.

$$\bar{D_j} = \frac{\sum_{j=1}^{N} D_j}{N} \tag{3}$$

- $\bar{D_j}$ = Uniformly Distributed kW Demand Per ICP
- N = Number of ICPs
- D_j = True kW Demand of ICP j

Whilst the diversity measures described in Equations 1 and 2 are suitable for the assessment of transformer loading, they may be unsuitable for voltage assessment. Within the context of this work, we define load diversity more broadly as the extent to which the assumption of coincident loading for all premises is invalid. Figure 1 demonstrates considerable load diversity. Understanding and quantifying the impact of this on voltage assessment is the primary focus of this paper. Figure 1 represents only a single snapshot in time. In order to quantify the impact of load diversity more broadly, a wider analysis of Smart Meter data is required. This analysis will be discussed in greater detail within Sections IV and V.

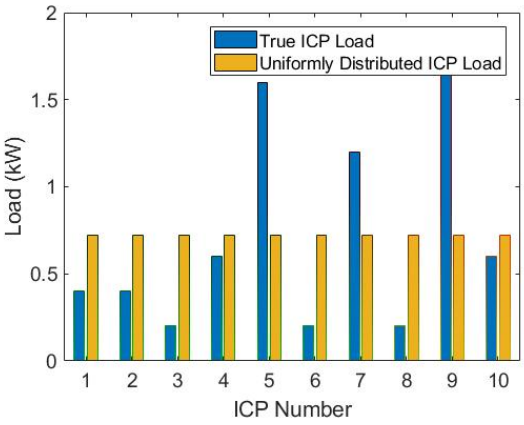

Fig. 1. 7pm Load Diversity for 10 ICPs

III. Voltage Drop in Radial Distribution Networks

In New Zealand LV distribution networks are typically radial in topology, containing one or more feeders branching out from the distribution transformer. These are predominantly three phase, although smaller LV networks may be single phase. Radial feeders typically host multiple ICPs on each network phase. Within the literature an equivalent end of line (EOL) load model has been used to model voltage drop [13]. Rather than model each ICP individually, loads are lumped together as a single load and placed at the end of the feeder. The following subsection discusses the model in detail including the impact of load diversity.

A. Equivalent End of Line Load Model

1) Uniformly Distributed Loads: Figure 2 depicts a single phase radial feeder. The circuit contains *n* uniformly spaced ICPs. The total load current into the feeder is I_{total}.

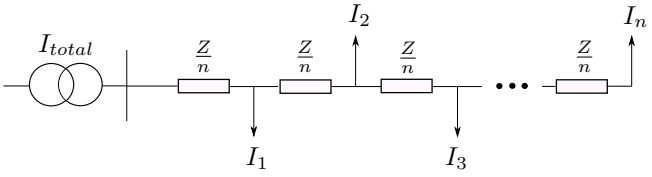

Fig. 2. Single Phase Radial Feeder Circuit

Z is the phase impedance of the entire feeder.

$$Z = R + jX \tag{4}$$

The contributions of each ICP to the total feeder current are equal and can be calculated using Equation 5.

$$I_j = \frac{I_{total}}{n} \tag{5}$$

$$j \in Z : j \in [1, n] \tag{6}$$

The voltage drop between the distribution transformer and the first ICP can be estimated using Equation 7.

$$V_{drop_1} = \mathfrak{Re}\left(\frac{Z}{n} \cdot I_j \cdot n\right) \tag{7}$$

Similarly the voltage drop between the first and second ICPs can be estimated using Equation 8.

$$V_{drop_2} = \mathfrak{Re}\left(\frac{Z}{n} \cdot I_j \cdot (n-1)\right) \tag{8}$$

Summing the incremental voltage drop across each line section impedance $\frac{Z}{n}$ gives the total feeder voltage drop. This can be seen in Equations 9 and 10.

$$V_{drop_{total}} = V_{drop_1} + V_{drop_2} \ldots + V_{drop_n} \tag{9}$$

$$V_{drop_{total}} = \mathfrak{Re}\left(\frac{Z}{n} \cdot I_j \cdot [n + (n-1) \ldots + 1]\right) \tag{10}$$

Recognizing the Taylor expansion in Equation 11 allows Equation 10 to be reduced to Equation 12.

$$1 + 2 + 3 \ldots + n = \frac{n(n+1)}{2} \tag{11}$$

$$V_{drop_{total}} = \mathfrak{Re}\left(Z \cdot I_{total} \cdot \left[\frac{1}{2}\left(1 + \frac{1}{n}\right)\right]\right) \tag{12}$$

The end of line (EOL) load model percentage is defined as seen in Equation 13.

$$EOL_{\%_{uni}} = \left[\frac{1}{2}\left(1 + \frac{1}{n}\right)\right] \tag{13}$$

$$V_{drop_{total}} = \mathfrak{Re}\left(Z \cdot I_{total} \cdot EOL_{\%_{uni}}\right) \tag{14}$$

Figure 3 shows the equivalent EOL load model for the detailed circuit seen in Figure 2.

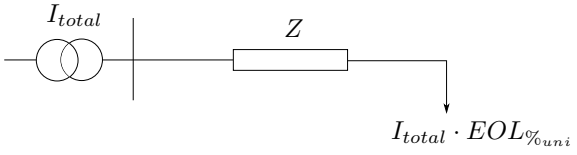

Fig. 3. Equivalent EOL Load Model for a Single Phase Radial Feeder Circuit

The key differences between these are as follows:

- In the equivalent model, each of the *n* uniformly spaced ICPs have been replaced by a single ICP placed at the end of the feeder.
- The load current drawn by the single ICP is equal to the total feeder current I_{total} scaled by $EOL_{\%_{uni}}$.

As seen in Equation 13, $EOL_{\%_{uni}}$ is a function of the number of ICPs. For a given number of ICPs a simple geometric calculation can be used to calculate $EOL_{\%_{uni}}$. This calculation is referred to as the shaded area method. The following example helps to demonstrate the method. Consider a single phase radial feeder with 4 ICPs. Figure 4 shows the shaded area method applied to the detailed circuit model.

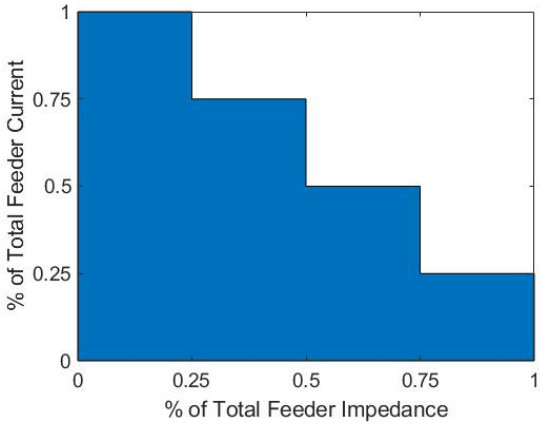

Fig. 4. Shaded Area Method Applied to Detailed Circuit Model with 4 ICPs (Uniformly Distributed loads)

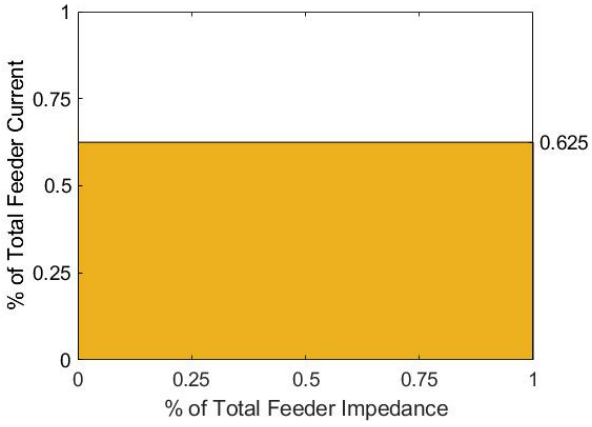

Fig. 5. Shaded Area Method Applied to Equivalent EOL Model with 4 ICPs (Uniformly Distributed loads)

The X axis shows the % of the total phase impedance Z. The Y axis shows the % of the total feeder current I_{total}. We recall that ICPs are uniformly spaced and that load is uniformly distributed. Thus the current flowing though each line section can be seen to monotonically decrease by 25% along the length of the feeder. The dimensionless shaded area seen in Figure 4

is proportional to voltage drop and provides the value for $EOL_{\%_{uni}}$. It can be seen that for a feeder with 4 ICPs per phase $EOL_{\%_{uni}}$ is equal to 0.625. Figure 5 shows the shaded area method applied to the equivalent EOL model. It is noted that the shaded area in both cases is equal, thus demonstrating their equivalence. In general $EOL_{\%_{uni}}$decreases as the number of ICPs increases. As *n* tends to infinity, $EOL_{\%_{uni}}$ tends to 0.5. Figure 6 shows the relationship between $EOL_{\%_{uni}}$ and *n*.

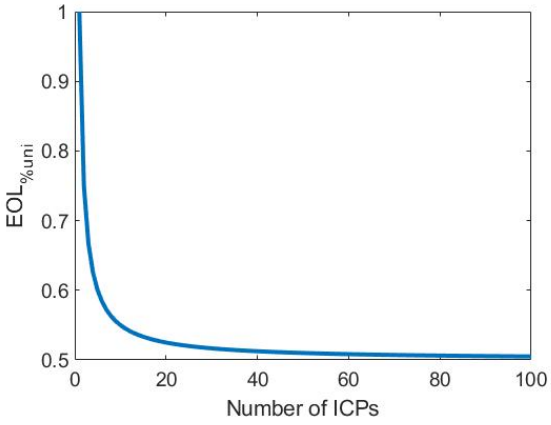

Fig. 6. $EOL_{\%_{uni}}$ as a Function of Number of ICPs

2) Diversified Loads: Within this section uniform distribution of I_{total} is no longer assumed, and instead diversified loads are included during the calculation of $EOL_{\%}$. The assumption that all ICPs in the network are uniformly spaced is upheld. In order to demonstrate the impact of load diversity, again consider the example of a single phase radial feeder with 4 ICPs. When the true load diversity is captured, the four ICPs no longer consume an equal share of I_{total}. For this particular example the percentage contribution of each ICP can be seen in Table I.

TABLE I
DIVERSIFIED LOAD DATA

ICP Number	1	2	3	4
% contribution to I_{total}	5	10	55	30

It is noted that those ICPs consuming the largest shares of I_{total} are located towards the end of the feeder. Consequently a greater proportion of I_{total} is flowing through a greater proportion of Z than in the uniformly distributed case. The impact on voltage drop can be visualized in Figures 7 and 8. It can be seen that the shaded area is now larger when compared to that in Figures 4 and 5. In the diversified case $EOL_{\%}$ is now 0.775 compared to 0.625 with uniform load distribution. In other words the phase voltage drop is 24% higher due to load diversity when compared to that which would have been calculated using uniform load distribution. Whilst in this case the uniform load distribution simplification resulted in an underestimate of the true voltage drop, it is equally possible that it may result in an overestimate of the true voltage drop. This occurs when those ICPs consuming the largest shares of I_{total} are located towards the start of the feeder.

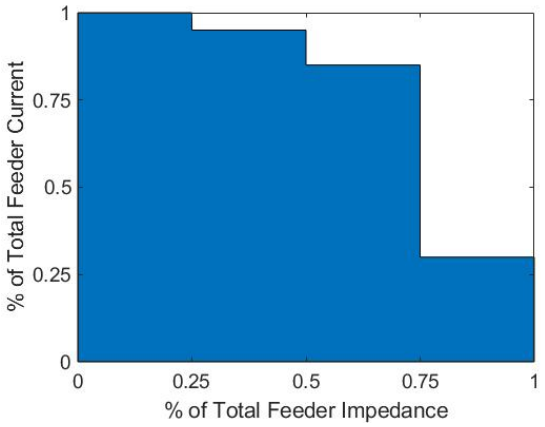

Fig. 7. Shaded Area Method Applied to Detailed Circuit Model with 4 ICPs (Diversified loads)

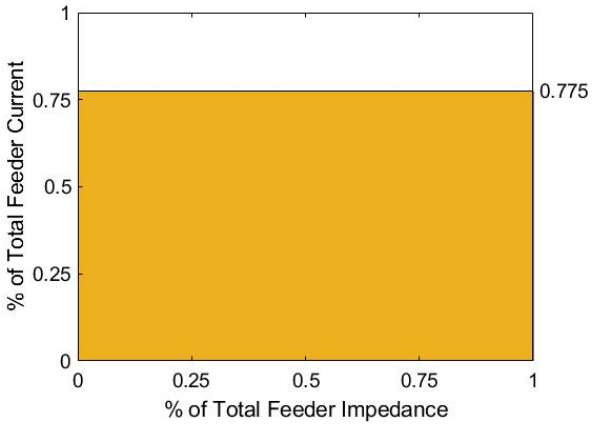

Fig. 8. Shaded Area Method Applied to Equivalent EOL Model with 4 ICPs (Diversified loads)

B. General Case: 3 Phase Radial Feeder Circuit with N ICPs

As mentioned previously LV networks are predominantly 3 phase. Along the length of radial feeders it is assumed that ICPs are assigned to each phase in an alternating manner. Figure 9 depicts the general case 3 phase LV feeder, with ICPs uniformly spaced along its length. The circuit has *n* ICPs per phase, resulting in $N\ (= 3 \times n)$ ICPs in total. Figure 10 depicts the equivalent EOL model representation. In this section the voltage drop equations for the general case feeder are derived. Distinction is made between the uniformly distributed and diversified cases.

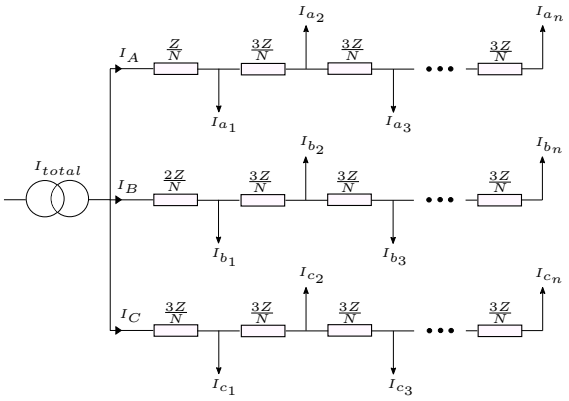

Fig. 9. General Case 3 Phase Feeder

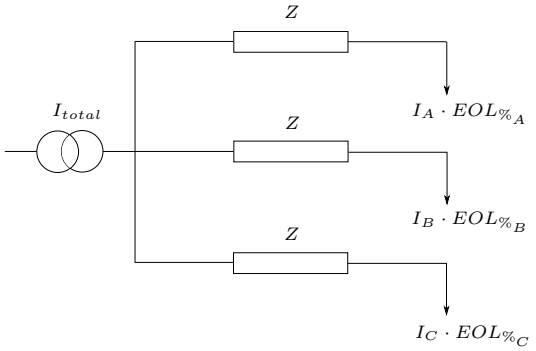

Fig. 10. Equivalent Model for General Case 3 Phase Feeder

1) Uniformly Distributed Loads: As can be seen in Figure 10 there are three parameters which impact voltage drop along each phase. These are:

- Z
- I_ϕ
- $EOL_{\%_\phi}$

where:

$$\phi \in [A, B, C] \tag{15}$$

The consequences of uniformly distributed loads are as follows: firstly, load is uniformly distributed along the length of each phase.

$$EOL^{uni}_{\%_A} = EOL^{uni}_{\%_B} = EOL^{uni}_{\%_C} = EOL^{uni}_{\%} \tag{16}$$

These conditions will be referred to as exhibiting zero longitudinal load diversity. Secondly load is uniformly distributed across the three network phases.

$$I^{uni}_A = I^{uni}_B = I^{uni}_C = \frac{I_{total}}{3} = I^{uni} \tag{17}$$

These conditions will be referred to as exhibiting zero across-phase load diversity. The phase voltage drop equations are thus defined as in Equation 18.

$$\left[V^{uni}_{drop}\right] = \begin{bmatrix} V^{uni}_{drop_A} \\ V^{uni}_{drop_B} \\ V^{uni}_{drop_C} \end{bmatrix} = \begin{bmatrix} \mathfrak{Re}\left(Z \cdot I^{uni} \cdot EOL^{uni}_{\%}\right) \\ \mathfrak{Re}\left(Z \cdot I^{uni} \cdot EOL^{uni}_{\%}\right) \\ \mathfrak{Re}\left(Z \cdot I^{uni} \cdot EOL^{uni}_{\%}\right) \end{bmatrix} \tag{18}$$

Note that each phase experiences an equal voltage drop.

$$V^{uni}_{drop_A} = V^{uni}_{drop_B} = V^{uni}_{drop_C} \tag{19}$$

As seen in Figure 9, ICPs are allocated to the phases in an alternating manner along the length of a feeder. Consequently whichever phase receives the first allocation will in reality have a slightly lower voltage drop than that which receives the second allocation. Whichever phase receives the second allocation will have a slightly lower voltage drop than that which receives the third allocation. However for feeders with numerous ICPs per phase, this difference becomes insignificant and consequently Equation 19 is approximately correct.

2) Diversified Loads: The consequences of load diversity are as follows: firstly, load is no longer uniformly distributed along the length of each phase. Secondly, each phase will experience its own unique diversity and thus EOL load model percentage.

$$EOL^{div}_{\%_A} \neq EOL^{div}_{\%_B} \neq EOL^{div}_{\%_C} \neq EOL^{uni}_{\%} \tag{20}$$

These conditions will be referred to as exhibiting longitudinal load diversity. Thirdly, load is no longer uniformly distributed across the three network phases.

$$I^{div}_A \neq I^{div}_B \neq I^{div}_C \neq \frac{I_{total}}{3} = I^{uni} \tag{21}$$

These conditions will be referred to as exhibiting across phase load diversity. The phase voltage drop equations are defined in Equation 22.

$$\left[V^{div}_{drop}\right] = \begin{bmatrix} V^{div}_{drop_A} \\ V^{div}_{drop_B} \\ V^{div}_{drop_C} \end{bmatrix} = \begin{bmatrix} \mathfrak{Re}\left(Z \cdot I^{div}_A \cdot EOL^{div}_{\%_A}\right) \\ \mathfrak{Re}\left(Z \cdot I^{div}_B \cdot EOL^{div}_{\%_B}\right) \\ \mathfrak{Re}\left(Z \cdot I^{div}_C \cdot EOL^{div}_{\%_C}\right) \end{bmatrix} \tag{22}$$

It is noted that each phase now experiences a unique voltage drop.

$$V^{uni}_{drop_A} \neq V^{uni}_{drop_B} \neq V^{uni}_{drop_C} \tag{23}$$

C. Diversity Scaling Factors

In this section scaling factors are derived which relate the voltage drop equations for the uniformly distributed and diversified cases.

1) Longitudinal Diversity Scaling Factor: A longitudinal diversity factor is first defined as in Equation 24

$$\left[K_{\tilde{\phi}}\right] = \begin{bmatrix} K_{\tilde{\phi}_A} \\ K_{\tilde{\phi}_B} \\ K_{\tilde{\phi}_C} \end{bmatrix} = \begin{bmatrix} EOL^{div}_{\%_A}/EOL^{uni}_{\%} \\ EOL^{div}_{\%_B}/EOL^{uni}_{\%} \\ EOL^{div}_{\%_C}/EOL^{uni}_{\%} \end{bmatrix} \tag{24}$$

2) Across Phase Diversity Scaling Factor: Similarly an across phase diversity factor is defined as seen in Equation 25.

$$\left[K_\phi\right] = \begin{bmatrix} K_{\phi_A} \\ K_{\phi_B} \\ K_{\phi_C} \end{bmatrix} = \begin{bmatrix} I^{div}_A/I^{uni} \\ I^{div}_B/I^{uni} \\ I^{div}_C/I^{uni} \end{bmatrix} \tag{25}$$

3) Combined Diversity Scaling Factor: The longitudinal and across-phase diversity factors can then be used to relate the diversified voltage drops seen in Equation 22, to the uniformly distributed voltage drops seen in Equation 18. This relationship can be seen in Equations 26 and 27.

$$\left[V_{drop}^{div}\right] = \begin{bmatrix} V_{drop_A}^{div} \\ V_{drop_B}^{div} \\ V_{drop_C}^{div} \end{bmatrix} = \begin{bmatrix} \mathfrak{Re}\left(Z \cdot K_{\phi_A} \cdot I^{uni} \cdot K_{\tilde{\phi}_A} \times EOL_{\%}^{uni}\right) \\ \mathfrak{Re}\left(Z \cdot K_{\phi_B} \cdot I^{uni} \cdot K_{\tilde{\phi}_B} \times EOL_{\%}^{uni}\right) \\ \mathfrak{Re}\left(Z \cdot K_{\phi_C} \cdot I^{uni} \cdot K_{\tilde{\phi}_C} \times EOL_{\%}^{uni}\right) \end{bmatrix} \tag{26}$$

$$\left[V_{drop}^{div}\right] = \begin{bmatrix} V_{drop_A}^{div} \\ V_{drop_B}^{div} \\ V_{drop_C}^{div} \end{bmatrix} = \begin{bmatrix} K_{\phi_A} \times K_{\tilde{\phi}_A} \cdot V_{drop_A}^{uni} \\ K_{\phi_B} \times K_{\tilde{\phi}_B} \cdot V_{drop_B}^{uni} \\ K_{\phi_C} \times K_{\tilde{\phi}_C} \cdot V_{drop_C}^{uni} \end{bmatrix} \tag{27}$$

Both the longitudinal and across-phase diversity factors can be combined to produce a single diversity scaling factor as seen in Equation 28.

$$\left[K\right] = \begin{bmatrix} K_A \\ K_B \\ K_C \end{bmatrix} = \begin{bmatrix} K_{\phi_A} \cdot K_{\tilde{\phi}_A} \\ K_{\phi_B} \cdot K_{\tilde{\phi}_B} \\ K_{\phi_C} \cdot K_{\tilde{\phi}_C} \end{bmatrix} \tag{28}$$

$$\left[V_{drop}^{div}\right] = \begin{bmatrix} V_{drop_A}^{div} \\ V_{drop_B}^{div} \\ V_{drop_C}^{div} \end{bmatrix} = \begin{bmatrix} K_A \cdot V_{drop_A}^{uni} \\ K_B \cdot V_{drop_B}^{uni} \\ K_C \cdot V_{drop_C}^{uni} \end{bmatrix} \tag{29}$$

K_{max} and K_{min} are the maximum and minimum combined diversity scaling factors respectively seen across the three network phases.

$$K_{max} = max\{K_A, K_B, K_C\} \tag{30}$$

$$K_{min} = min\{K_A, K_B, K_C\} \tag{31}$$

IV. Calculating Diversity Scaling Factors

Equation 27 describes how the longitudinal and across phase diversity factors relate the phase voltage drops for the uniformly distributed and diversified cases. These diversity factors vary as a function of time due to instantaneous changes in the loading of individual ICPs. Since the value of these is subject to change, a statistical approach is required in order to derive credible planning levels from Smart Meter data. Figure 11 depicts the Monte Carlo method which was implemented in order to empirically derive the necessary statistics. Section IV-A discusses the Smart Meter data which served as input to the method. Section IV-B provides a more detailed description of each stage within Figure 11.

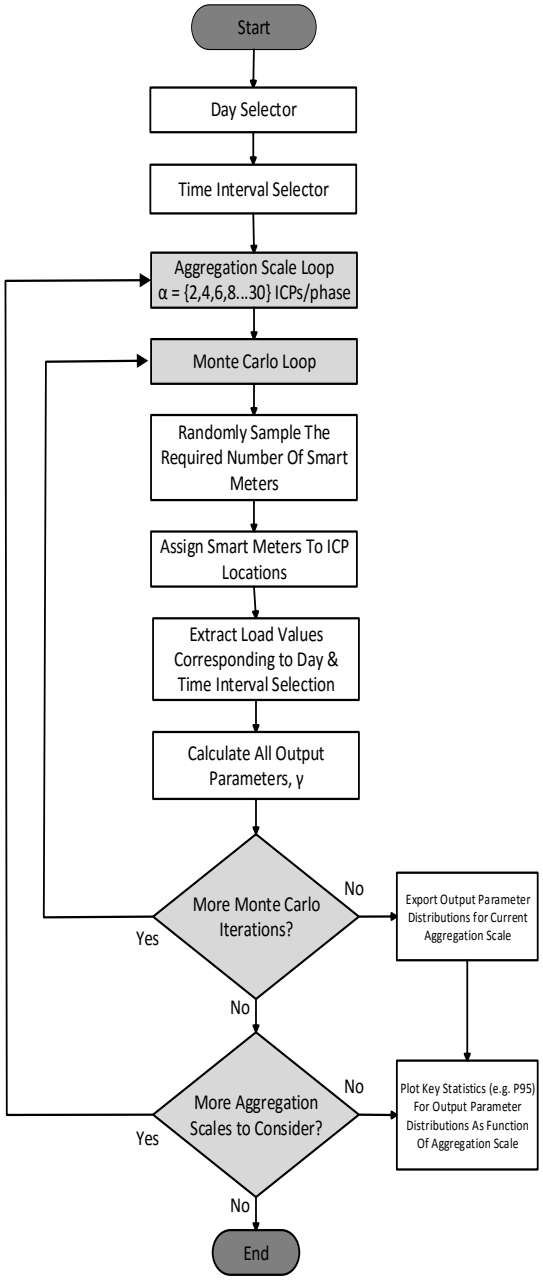

Fig. 11. Monte Carlo Method for Calculating Diversity Scaling Factors

A. Smart Meter Data Sample

In recent years the proliferation of Smart Metering has made ICP-level load data widely available. By 2016 over 70% of New Zealand households had been fitted with Smart Meters [14]. These provide a powerful means for modelling load diversity in LV network analysis. A Smart Meter dataset consisting of over two thousand premises was available for use within this work. For each premise a year's worth of data was available. The entire dataset belongs to a single New Zealand distribution company thus providing evidence of the relative locality of the Smart Meters. Despite this it is not clear which Smart Meters in the dataset belong to which particular LV networks. Consequently, the following approach was implemented in order to identify a subsample of the dataset to use as input to the Monte Carlo Method. The distribution of the dataset, in terms of annual energy consumption was first identified. This can be seen in the histogram in Figure 12.

From this distribution the 200 most similar Smart Meters around the 50th percentile were extracted, in order to form the subsample. The reason for this is that LV networks typically contain premises of the same 'type'-i.e. City, Urban, Rural, Industrial etc. [15]. By selecting the most similar properties around the 50th percentile, only median sized residential properties were included in the subsample. It was noted that this approach will likely provide a conservative insight into the impacts of diversity. This is because LV networks will still contain some variation in property size, socio-economic status, function etc. Future work will compare these results against a data set for which the true network locations are known in order to assess the significance of this.

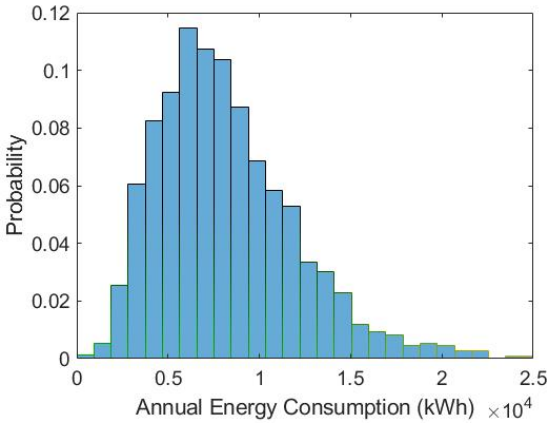

Fig. 12. Distribution of Annual Energy Consumption in Smart Meter Dataset

B. Monte Carlo Method Description

The first stage in the Monte Carlo method selects the day within the year to be considered in the analysis. This could be configured as follows:

- Specific Day e.g. 7^{th} June
- Maximum Peak Demand Day (re-evaluated for each Monte Carlo iteration)
- Minimum Low Demand Day (re-evaluated for each Monte Carlo iteration)

The second stage in the Monte Carlo method selects the half hour time interval within the day to be considered in the analysis. This could be configured as follows:

- Specific Time Interval e.g. 17:00-17:30
- Peak Demand Time Interval (re-evaluated for each Monte Carlo iteration)
- Low Demand Time Interval (re-evaluated for each Monte Carlo iteration)

The outermost loop within the Monte Carlo method dictates the aggregation scale (network size). Within this analysis the aggregation scale was varied between 2 and 30 ICPs/phase. For the current aggregation scale the Monte Carlo loop then commences. The required number of Smart Meters are randomly sampled and assigned to ICP locations. The load values for each ICP are then extracted according the day and time interval selector configurations. The values for $[K_{\tilde{\phi}}]$, $[K_{\phi}]$, $[K]$, K_{max}, and K_{min} are then calculated. The results are placed into an appropriate distribution according to the following:

- Aggregation Scale: $\alpha = \{2, 4, 6, 8..., 30\}$ ICPs/phase
- Output Parameter: $\gamma = \{[K_{\tilde{\phi}}], [K_{\phi}], [K]\ , K_{max}, K_{min}\}$

For the current aggregation scale, the Monte Carlo loop iterates until the statistical properties of the output parameter distributions have converged. This convergence is discussed in greater detail within Section V.

V. Results

A. Statistical Analysis of Scaling Factors

Recalling Equation 29, it is observed that the combined diversity scaling factor $[K]$ relates the phase voltage drops for the uniformly distributed and diversified cases. As discussed previously, load flow simulations typically assume uniform load distribution. $[K]$ thus allows these simplified load flow results to be converted to equivalent results in which load diversity is properly accounted for. For any single load flow solution, the following statement applies to the uniform load distribution simplification:

$$[K] \begin{cases} > 1, & \text{Underestimates True Voltage Drop} \\ < 1, & \text{Overestimates True Voltage Drop} \\ = 1, & \text{Correctly Estimates True Voltage Drop} \end{cases} \quad (32)$$

The distributions of $[K]$ produced by the Monte Carlo Method can be seen in Figures 13-15. Each phase is presented separately. These particular distributions correspond to:

- Aggregation Scale: α = 30 ICPs/phase.
- Day Selector: 7^{th} June (mid-winter)
- Time Interval Selector: 16:00-16:30

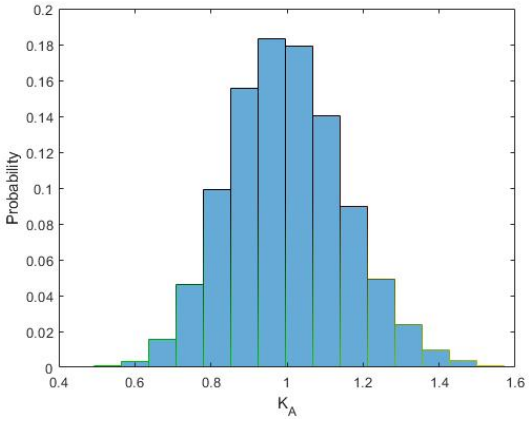

Fig. 13. Histogram of K_A

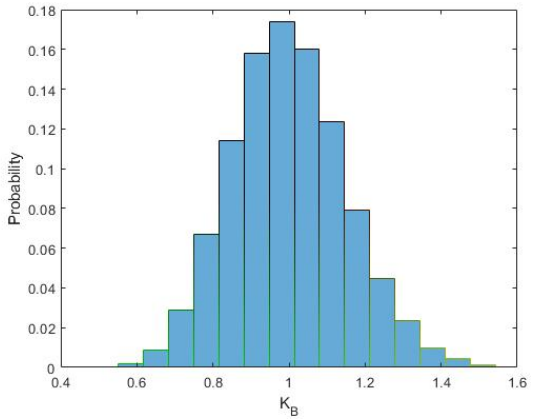

Fig. 14. Histogram of K_B

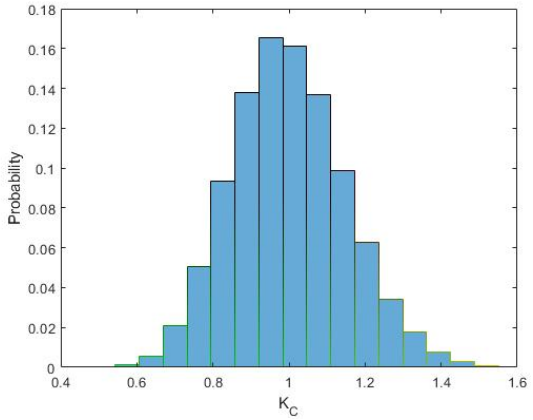

Fig. 15. Histogram of K_C

The distributions are approximately normal and centered on 1. With reference to Equation 32, it can be seen that a value of 1 corresponds to instances where the uniformly distributed voltage drop is equal to the diversified case. These results thus demonstrate that on average the uniformly distributed model is the best approximation of the true voltage drop when diversity is captured. Despite this, there are considerable periods of time when the uniformly distributed load model significantly overestimates or underestimates the true voltage drop. It is proposed that these periods should be considered during planning.

Statutory limits for steady-state voltage are typically quoted with an upper and lower bound. For example 230V$\pm$6% in the case of the New Zealand distribution system [16]. Underestimates of the true voltage drop can potentially obscure under-voltage violations. Overestimations of the true voltage drop can potentially obscure over-voltage violations. In order to be in breach of these limits it is not necessary that all 3 phase voltages are simultaneously over or under voltage. For this reason the distributions of K_{max} and K_{min} are considered within these results. Recalling Equations 30 and 31, these represent the maximum and minimum values of $[K]$ across the 3 phases. Figures 16 and 17 show the distributions of K_{max} and K_{min} respectively. Looking at the distribution of K_{max} it can be seen that there is a significant probability that the uniformly distributed model will underestimate the voltage drop on one particular phase. Conversely, looking at the distribution of K_{min} it can be seen that there is a significant probability that the uniformly distributed model will overestimate the voltage drop on one particular phase. The significance of these misestimations depends on the relative magnitude of the network loading during the particular time period of interest. Underestimates of voltage drop are important during high load periods. This is because it is during these periods when networks typically operate around the lower statutory limit for steady state voltage. Similarly overestimates of drop are important during low load periods. Both overestimates and underestimates of voltage drop during intervals with moderate loading may be insignificant. In order to assess these periods of interest, the test scenarios in Table II were evaluated using the Monte Carlo Method.

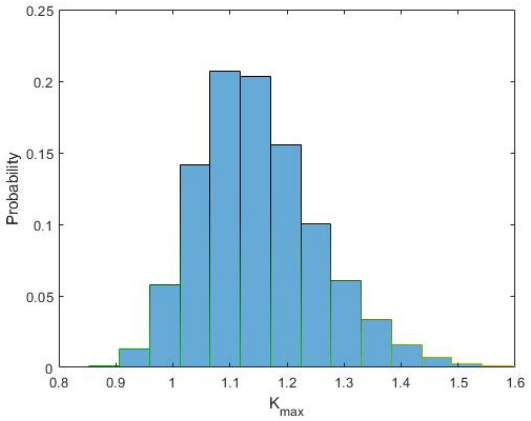

Fig. 16. Histogram of K_{max}

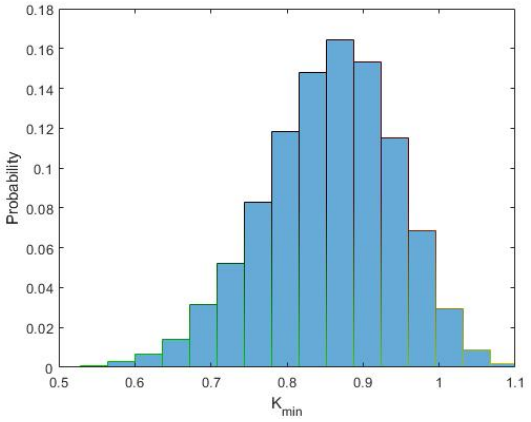

Fig. 17. Histogram of K_{min}

Taking the 95^{th} percentile of the K_{max} distribution from test

TABLE II
MONTE CARLO METHOD TEST SCENARIOS

Test Scenario	$\alpha(ICPs/phase)$	Day Selector	Time Interval Selector	Output Parameter
1	2-30	Maximum Peak Demand Day	Peak Demand Time Interval	K_{max}
2	2-30	Minimum Low Demand Day	Low Demand Time Interval	K_{min}

1 provides the 5% worst underestimates of voltage drop due to the uniform load distribution simplification. Taking the 5^{th} percentile of the K_{min} distribution from test 2 provides the 5% worst overestimates of voltage drop due to the uniform load distribution simplification. These statistics can be seen in Figures 18 and 19 respectively. In both cases the statistics are plotted as a function of aggregation scale. It can be observed that the significance of load diversity on voltage drop decreases with increasing aggregation scale.

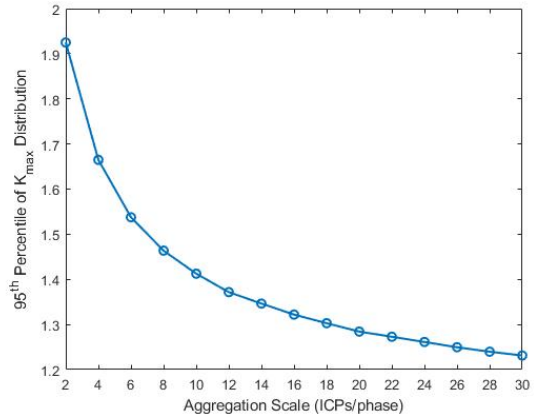

Fig. 18. 95^{th} Percentile of K_{max} During Peak Load Periods

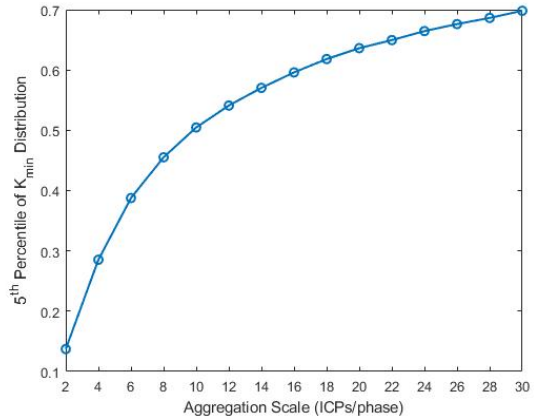

Fig. 19. 5^{th} Percentile of K_{min} During Low Load Periods

At the maximum aggregation scale the 95th percentile of K_{max} is 1.25. This statistic can be interpreted as follows: for a radial feeder with 30 ICPs/phase, there is a 5% chance that the end of line voltage drop during the annual peak load interval will be at least 1.25 times than that resulting from a uniform load flow simulation. At the minimum aggregation scale the 95th percentile of K_{max} is 1.92. At the maximum aggregation scale the 5th percentile of K_{min} is 0.7. This statistic can be interpreted as follows: for a radial feeder with 30 ICPs/phase, there is a 5% chance that the end of line voltage drop during the annual low load interval will be less than or equal to 0.7 times that resulting from a uniform load flow simulation. At the minimum aggregation scale the 5th percentile of K_{min} is 0.13. Even at the maximum aggregation scale these potential misestimates in voltage drop are non-trivial. During planning of LV distribution networks, the extreme operating conditions - maximum and minimum loading - are typically considered. These results demonstrate that during these extreme conditions, uniform load distribution can potentially underestimate extreme voltages. The extent of this underestimate has been captured in a statistical sense, and characterized as a function of aggregation scale. The potential utility of these statistics is discussed within Section VI.

B. Required Number of Monte Carlo Iterations

As described in Figure 11, during each iteration of the Monte Carlo method random sampling is applied to the following parameters.

- The specific *N* Smart Meters chosen
- Placement of the sampled Smart Meters in the feeder

Addressing the placement of the sampled Smart Meters alone, the number of unique placements for N Smart Meters within the general case feeder can be calculated using Equation 33.

$$number\ of\ unique\ placements = N! \tag{33}$$

This number becomes very high even for moderately sized networks. As an example, for a feeder with *N=60* ICPs the number is 8.32×10^{81}. Factoring in the sampling of specific Smart Meters, the number of possible combinations becomes computationally exhaustive even for this moderately sized dataset of only 200 Smart meters. For this reason the number of required Monte Carlo iterations was investigated. Within literature the number of required iterations is identified by observing the convergence of a particular statistic of interest [17] [18]. The statistics of interest here are those presented in Figures 18 and 19. Figure 20 demonstrates the convergence of the former. The impact of aggregation scale on convergence can also be observed.

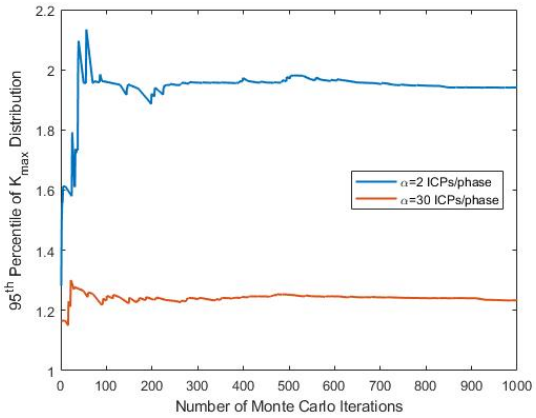

Fig. 20. Convergence of 95^{th} Percentile of K_{max} During Peak Load Periods

It is observed that the statistics are highly volatile over the first one hundred Monte Carlo iterations. For $\alpha = 30$ convergence is reached at around 500 iterations. For $\alpha = 2$ convergence requires a greater number of iterations, being reached at around 800 iterations. Similar observations were made for the statistic seen in Figure 19. Convergence demonstrates that no number of subsequent Monte Carlo iterations would result in the statistics diverging from the values presented in this paper.

C. Assessment of Load Dependence on Voltage

Equation 14 presents the fundamental equation used to estimate the end of line voltage drop. Both I_{total} and $EOL_{\%}$ depend on the ICP-level currents I_j. The Smart Meter Data used within this work provided only real power data. Within the Monte Carlo Method, I_j are estimated based on P_j and the nominal network voltage. In reality I_j is dependent on the ICP voltage. Therefore voltage drop along the length of feeders will result in a mismatch between the estimated I_j, and those observed in reality. The extent of this mismatch is dependent on the voltage drop magnitude. To quantify the impact of this mismatch on the statistics presented in section V-A, full load flow simulations were run in OpenDSS. During these simulations the constant power load model was implemented. The combined diversity scaling factor for the load flow results was calculated using Equation 34.

$$\left[K^{lf}\right] = \begin{bmatrix} K_A^{lf} \\ K_B^{lf} \\ K_C^{lf} \end{bmatrix} = \begin{bmatrix} \Delta V_A^{div} / \Delta V_A^{uni} \\ \Delta V_B^{div} / \Delta V_B^{uni} \\ \Delta V_C^{div} / \Delta V_C^{uni} \end{bmatrix} \tag{34}$$

- ΔV = end of line voltage drop

K_{max}^{lf} and K_{min}^{lf} were similarly calculated as in Equations 30 and 31 respectively. The estimated diversity scaling factors $[K]$ as described in Section III-B were then compared with those resulting from the full load flow simulations $[K^{lf}]$. Each load flow was repeated for 3 distinct values of network strength (impedance) in order to quantify the impact of voltage drop magnitude on the accuracy of the estimated diversity scaling factors $[K]$. Figure 21 depicts the Monte Carlo method which was implemented.

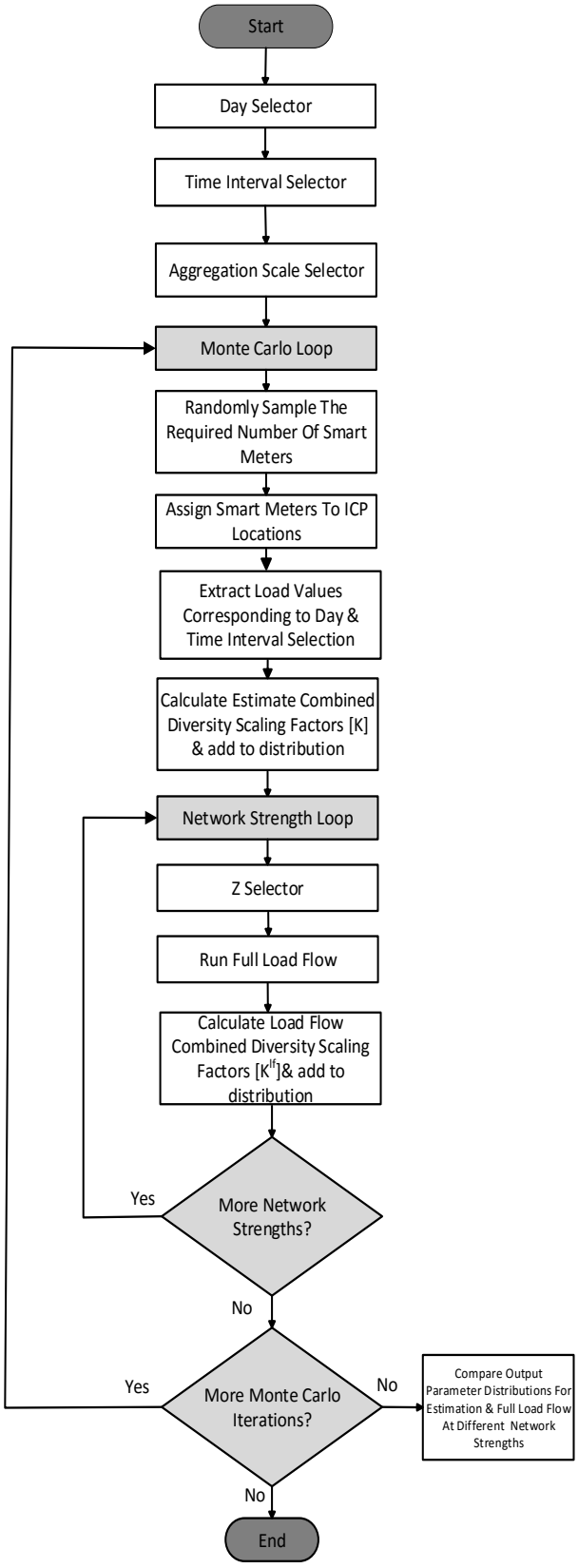

Fig. 21. Monte Carlo Method for Calculating Estimation Error

The results presented here apply to the following:

- Day Selector: Maximum Peak Demand Day
- Time Interval Selector: Peak Demand Time Interval
- Aggregation Scale Selector: α = 30 ICPs/phase
- Network Strength: Z = {0.005,0.015,0.025} Ω

Figure 22 shows the 95^{th} percentile of the K_{max} distributions for the estimation as well as the full load flow simulations at each network strength. The error at each network strength can be seen more clearly in Figure 23. After each iteration of the Monte Carlo Method, ΔV was also added to a corresponding distribution for each network strength. Figure 24 shows a boxplot of the ΔV distributions for each network strength.

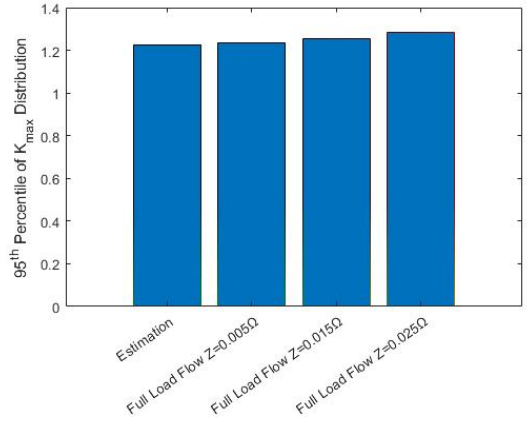

Fig. 22. 95^{th} Percentile of K_{max} for Estimation and Full Load Flow Simulations

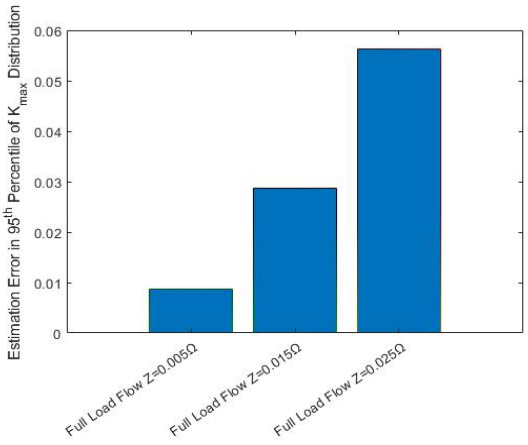

Fig. 23. Error in Estimated 95^{th} Percentile of K_{max} Compared With Full Load Flow Simulations

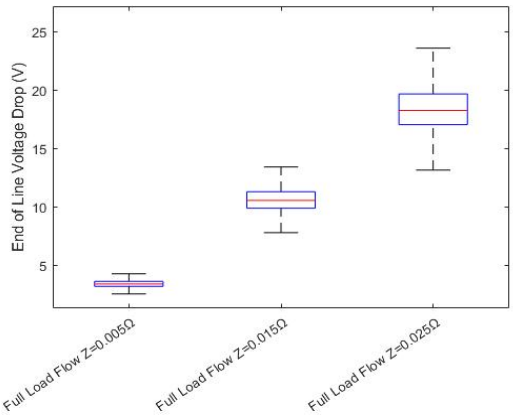

Fig. 24. Boxplot of ΔV Distributions at Each Value of Network Strength

As expected the average end of line voltage drop increases with network impedance. Comparing Figures 23 and 24, it can be seen that as the average end of line voltage drop increases as does the error in the 95^{th} percentile of the K_{max} distribution. This is because the estimate of I_j based on P_j and the nominal network voltage becomes increasingly less accurate as votlage drop increases. The estimation method presented in Section III-B provides a value for the diversity scaling factors which is independent of network strength. As seen in Figure 22, the impact of severe voltage depression tends to increase the significance of load diversity on voltage. Therefore the results presented in Figure 18 can be considered conservative, further strengthening the position that load diversity should be explicitly modelled in LV network analysis.

VI. Conclusion

This paper has demonstrated how load diversity impacts voltage drop in radial distribution circuits. Novel contributions include the development of scaling factors which relate voltage drop for the uniformly distributed and diversified cases. Smart Meter data was analyzed in order to provide a statistical measure of these scaling factors. The results presented here have demonstrated that failing to account for load diversity within LV network simulations can result in inaccurate voltage assessments. It is proposed that these results may be conservative. Firstly due to selecting the most similar Smart Meters from the dataset as discussed in Section IV-A, and secondly due to the load dependence on voltage as discussed in Section V-C. Despite this the results are not trivial. Increased electric vehicle penetration will increase network loading during peak load periods. Increased photovoltaic and vehicle to grid penetration may decrease network loading during low load periods. Sporadic uptake in these emerging technologies, variation in charging time, system sizing, charging technology etc. may also increase load diversity. Impact studies for future scenarios which do not explicitly model the load diversity seen in the underlying load may mask steady state voltage violations. It is thus recommended that load diversity should be considered during load flow simulations for LV distribution networks.

The scaling factors allow results from simplified load flow simulations to be converted to more realistic solutions which account for load diversity. The most appropriate conversion can be made based on the aggregation scale of interest. Whilst in this paper only the 95% confidence level was presented, distribution companies and researchers will be able to make this conversion according to their required level of confidence. The results within this paper are specific to the Smart Meter sample which served as input. Consequently these statistics may not be representative of other regions in New Zealand, or other countries. Despite this, the work presented here has set out a statistical framework to extract these scaling factors from generic Smart Meter data, allowing this work to be repeated with alternative datasets. Future work will look to build on the foundations presented in this paper. The impact on neutral voltage rise will be added to the general case feeder. Additionally more complex network topologies which include tee-off sections may be considered. The potential impacts of emerging technologies on load diversity will also be assessed. This may allow for optimized schemes to be developed such that these technologies can be adopted with minimal network reinforcement.

REFERENCES

[1] Miller A, McNab S, Wood A and Lemon, S, *The Economics and Potential Uptake of PV Solar Power by Region and PV System Cost*, EEA Conference, 22 - 24 June 2016, Wellington, 2016.

[2] Transpower, "Te Mauri Hiko, Energy Futures: Transpower White Paper", New Zealand, 2018.

[3] J. D. Watson, N. R. Watson, D. Santos-Martin, A. R. Wood, S. Lemon and A. J. V. Miller, "Impact of solar photovoltaics on the low-voltage distribution network in New Zealand," in IET Generation, Transmission & Distribution, vol. 10, no. 1, pp. 1-9, 7 1 2016.

[4] Watson N. R., Watson J. D., Watson R. M. K. Sharma and Miller, A, *Impact of Electric Vehicle Chargers on a Low Voltage Distribution System*, EEA Conference, 24-26 June 2015, Wellington.

[5] Chin Ho Tie and Chin Kim Gan, "Impact of grid-connected residential PV systems on the malaysia low voltage distribution network," 2013 IEEE 7th International Power Engineering and Optimization Conference (PEOCO), Langkawi, 2013, pp. 670-675.

[6] A. Bosovic, M. Music and S. Sadovic, "Analysis of the impacts of plug-in electric vehicle charging on the part of a real low voltage distribution network," 2015 IEEE Eindhoven PowerTech, Eindhoven, 2015, pp. 1-5.

[7] M. Thomson and D. G. Infield, "Impact of widespread photovoltaics generation on distribution systems," in IET Renewable Power Generation, vol. 1, no. 1, pp. 33-40, March 2007.

[8] I. A. Essackjee and R. T. F. Ah King, "The impact of increasing Penetration Level of Small Scale Distributed Generations on voltage in a secondary distribution network," 2016 IEEE International Conference on Emerging Technologies and Innovative Business Practices for the Transformation of Societies (EmergiTech), Balaclava, 2016, pp. 245-250.

[9] P. Huppertz, L. Kopczynski, R. Zeise and M. Kizilcay, "Approaching the diversity of unbalanced residential load in low-voltage grids by probabilistic load-flow simulation of cross-sectional data," 2015 IEEE Eindhoven PowerTech, Eindhoven, 2015, pp. 1-6.

[10] UK Power Networks, *Use of Smart Meter information for planning and operation*, Report C1, September 2014.

[11] C. Barteczko-Hibbert, *After Diversity Maximum Demand (ADMD) Report*, University of Durham, February 2015.

[12] A. I. Elombo, T. Morstyn, D. Apostolopoulou and M. D. McCulloch, "Residential load variability and diversity at different sampling time and aggregation scales," 2017 IEEE AFRICON, Cape Town, 2017, pp. 1331-1336. doi: 10.1109/AFRCON.2017.8095675

[13] W. H. Kersting, Distribution System Modeling and Analysis. 2002;2006;2001;.

[14] Electricity Retailers of New Zealand, *Smart meters – everything you needed to know and more*, Smart Meters Summary, July 2017.

[15] J. D. Watson, N. R. Watson, D. Santos-Martin, S. Lemon, A. R. Wood, and A. J. V. Miller *Low Voltage Network Modelling*, EEA Conference, June 2014, Auckland, 2014.

[16] N. Watson, Miller A, *Power Quality Indices*, EEA Conference, June 2015, Wellington, 2015.

[17] S. Raychaudhuri, "Introduction to Monte Carlo simulation," 2008 Winter Simulation Conference, Miami, FL, USA, 2008, pp. 91-100.

[18] M. R. Driels, Y. S. Shin, "Determining the number of iterations for Monte Carlos Simulations of weapon effectiveness", Monterey California, 2004.

The Significance of Load Diversity on Voltage Assessment in Low Voltage Distribution Networks With Multiple Earthed Neutrals

Euan McGill
Electric Power Engineering Centre (EPECentre)
University of Canterbury
Christchurch 8041
Email: euan.mcgill@pg.canterbury.ac.nz

***Abstract*— Low voltage (LV) distribution networks in New Zealand are experiencing an increasing penetration of disruptive technologies such as electric vehicles (EVs). Diversity in the start time and duration of EV charging reduces the impact on transformer peak loading. Load diversity describes variation in the coincident loading of individual consumers. Both conventional load and that due to electric vehicles exhibit load diversity. Whilst load diversity is accounted for in the assessment of transformer peak loading, it is often neglected during voltage assessment. A common simplifying approximation is to assume uniform load distribution throughout the network. Whilst frequently applied, this simplification is rarely reflected in reality. Load diversity results in greater current imbalance between the phases, and consequently neutral voltage displacement. Since the customer supply is between phase and neutral, neutral displacement can worsen steady state voltage drop. Within this work Smart Meter data is used to assess the impact of load diversity on steady state voltage for a residential distribution network. Different neutral grounding approximations are also assessed. The results show that neglecting load diversity underestimates voltage drop, and that neutral voltage rise contributes significantly. In New Zealand distribution networks the neutral conductor is earthed at the LV transformer and at each ICP (installation control point). The assumption of a perfectly grounded neutral conductor underestimates the neutral voltage rise. It is concluded that in order to avoid masking statutory limit voltage violations in future impact studies, load diversity and finite earthing impedances should be considered.**

I. Introduction

Electric vehicles (EVs) are an example of an emerging technology which will impact low voltage (LV) distribution networks. Whilst modest at present, their penetration is forecast to significantly increase in the near future [1], [2]. Diversity in the start time and duration of EV charging reduces the impact on peak loading [3]. Load diversity describes variation in the coincident loading of individual consumers. Both conventional load and that due to electric vehicles exhibit load diversity. Whilst load diversity is accounted for in the assessment of transformer peak loading, it is often neglected during voltage assessment. Within modelling, load is typically allocated to individual households based upon a uniform distribution of the transformer load [4]–[6]. This results in zero load diversity in the network. When modelling EVs the penetration level is first chosen. Single units are then randomly scattered throughout the network [7]. This process inherently adds a degree of load diversity. Previous research compared the phase to ground voltage drops for uniform and diversified loads [8]. It was shown that uniform load distribution underestimates extreme voltages due to averaging load along the length of feeders and across the phases. The significance of modelling load diversity decreases with increasing aggregation scale. Previously only the phase to ground voltage drop was considered. Load diversity causes current imbalance between the phases. This results in greater neutral currents and consequently neutral voltage displacement. Since the customer supply is between phase and neutral, neutral displacement can worsen steady state voltage deviation.

In this work half hour Smart Meter data is used to model the load diversity in a residential distribution network. A quasi steady-state (QSS) load flow simulation is implemented which captures an entire year's worth of load data. Voltages are compared for the diversified and uniformly distributed cases. The contribution of the neutral voltage is observed in isolation. The New Zealand LV distribution system is a multiple earthed neutral (MEN) system. In this system, the neutral conductor is earthed at the LV transformer and at each ICP throughout the distribution network. Different approximations regarding neutral grounding are often made. The extreme ends of these approximations are the isolated and perfectly grounded neutral. In reality, the earthing impedances at the LV transformer and ICPs are finite, placing the true connectivity somewhere between these extremes [9]. The impact of different neutral grounding approximations are also assessed.

In the remainder of this paper, Section II provides review of relevant literature. Section III provides a detailed definition of load diversity. Section IV describes the different neutral grounding approximations. Section V presents the residential LV distribution network which is modelled. Section VI describes the load data used, and distinguishes between the uniform and diversified load models. The simulation method is then described in Section VII. Section VIII presents the results and discusses their significance. Section IX concludes with the key findings and recommendations for future work.

II. Literature Review

Urquhart et al. [9] provides a qualitative assessment of common approximations used in LV network analysis. Both load diversity and neutral to ground connectivity are considered important. The work stops short of any quantitative assessment. In Frame et al. [10] individual household load profiles are generated from normal distributions. There is a unique distribution for each half hour interval in the day. The distribution variance is altered to simulate the effect of varying load diversity. A year long load flow is carried out to assess the impact of varying load diversity on the number of voltage violations. The neutral to ground connectivity was not detailed. In McQueen et al. [11] load profiles are generated from a gamma distribution. A shorter period of two weeks was simulated. The work concludes that the use of after diversity demand may result in inaccurate voltage assessment. In this case neutral earthing connections were neglected. Reese et al. [12] and Huppertz et al. [13] generate synthetic load profiles based on appliance ownership, household type, and seasonal effects. In Huppertz et al. load flow results are compared with practical measurements in order to validate the model. In Reese et al. results are compared with a simplified load flow which uses uniform loads. The uniform load flow underestimates the number of voltage violations by a significant margin. Again the neutral to ground connectivity is not detailed. In Csatár et al. [14] and Sunderland et al. [15] households are assigned unique loads from measurement records. In both cases only a single snapshot is analyzed. The neutral earthing resistances are varied over a range of values and the impact on voltage assessed. No justification is provided for the proposed range of resistances. In Ahmadi et al. [16] rather the number of earth connections is varied. Again only a single snapshot is analyzed. The aforementioned publications have different strengths and weaknesses. Those which consider a significant sample of load data do not asses the significance of neutral grounding approximations. Those which do asses the significance of neutral grounding approximations consider only a snapshot in time. Of all the papers above only Reese et al. compares the results from uniform and diversified load flows. The value of this work is in overcoming the individual limitations in the literature. The key contributions are summarized below.

- Quantitative comparison between uniformly distributed and diversified load flow results
- Sensitivity of results across a range of neutral grounding approximations
- Large sample of real life load data

III. Load Diversity Definition

In the literature load diversity describes the extent to which the peak demands of individual consumers occur at different times of the day [17] [18] . It is typically measured by the diversity factor seen in Equation 1.

$$F_D = \frac{\sum_{j=1}^{N} D_j^{max}}{D_{system}^{max}} \tag{1}$$

- F_D = Load Diversity Factor
- N = Number of ICPs in Network
- D_j^{max} = Maximum kW Demand of ICP j
- D_{system}^{max} = Coincident Maximum kW Demand for the Group of N ICPs

Alternatively the after diversity maximum demand as seen in Equation 2, may be used.

$$ADMD = max\left\{ \frac{\sum_{j=1}^{N} D_j^i}{N} \right\}_{i=1}^{K} \tag{2}$$

- $ADMD$ = After Diversity Maximum Demand per ICP
- N = Number of ICPs in Network
- D_j^i = kW Demand of ICP *j* During Time Interval *i*
- *K* = Number of Time Intervals During Period of Interest

Load diversity is used in network planning in order to curb the total capacity requirements of a utility. As the size of a distribution network increases the ADMD decreases [19]. Understanding this relationship allows the sizing of network assets to be optimized. Typically in load flow simulations the upstream transformer load is uniformly distributed throughout the downstream network. The transformer load is obtained from either:

- A known maximum demand indication
- Equation 1 with empirically derived values of F_D

This approach ensures that the aggregated demand on the network accounts for load diversity. Despite this, uniformly distributing the aggregated demand introduces inaccuracies. This approach results in zero load diversity downstream of the transformer, i.e. all ICPs simultaneously consume the same power. This behaviour is rarely reflected in reality. Figure 1 shows the load at 7pm for 10 residential ICPs from a Smart Meter dataset. For each ICP the true load can be compared with the equivalent uniformly distributed load, calculated using Equation 3.

$$\bar{D_j} = \frac{\sum_{j=1}^{N} D_j}{N} \tag{3}$$

- $\bar{D_j}$ = Uniformly Distributed kW Demand Per ICP
- N = Number of ICPs
- D_j = True kW Demand of ICP j

Whilst ADMD as seen in Equation 2 may be suitable for the assessment of transformer loading, it may be unsuitable for voltage assessment. Within this work we define load diversity more broadly as the extent to which the assumption of coincident loading for all premises is invalid. Figure 1 demonstrates an example of considerable load diversity.

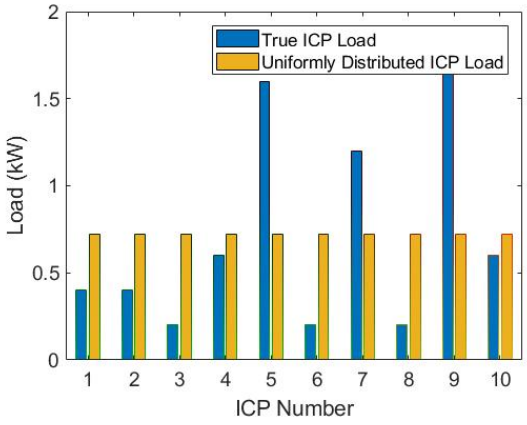

Fig. 1. 7pm Load Diversity for 10 ICPs

IV. Neutral Grounding Approximations

In New Zealand, LV distribution networks are multiple earthed neutral (MEN) systems. When modelling LV networks, approximations are often made regarding connections between the neutral conductor and ground. These approximations are not always explicitly stated. Despite this they can significantly impact the results of load flow simulations. Load diversity leads to increased loading imbalance across the phases. Depending on the connectivity, this imbalance will return to the LV transformer star point through either the neutral conductor and/or earth. Since the voltage supplied to customers is between phase and neutral, this can significantly impact voltage drop throughout the network.
The following subsections describe the three neutral grounding approximations which are considered in this analysis. The first is the most detailed approximation of the New Zealand MEN system. The second and third are two common simplifications. The first of these simplifications is the isolated neutral conductor. This provides an indication of the worst case voltage drop. The second is the perfectly grounded neutral conductor. This may underestimate the true voltage drop.

A. Detailed Multiple Earthed Neutral (MEN) Approximation

In MEN systems, the neutral conductor is earthed at the LV transformer and at each ICP throughout the network. Generally the earthing system at the transformer provides a better connection to ground than those at each ICP. Transformer earthing is typically provided by an earth grid or mat. An earth stake provides the earthing at each ICP. In some cases earth stakes are also used at the transformer, however these are larger and provide a lower earthing resistance. At the transformer the earthing system is required to have a maximum resistance to earth based upon its rating. The values seen in Table I are taken from the design standard used by a New Zealand distribution company.

TABLE I
Transformer Earthing System Maximum Resistances

Transformer Rating (kVA)	Maximum Earthing Resistance (Ω)
Tx $\leq$ 50	30
50 $<$ Tx $\leq$ 500	15
Tx $>$ 500	10

The requirements for earthing connections at ICPs are specified in NZS/AS 3000 [20]. The standard does not explicitly state a maximum earthing resistance. Instead the required depth and stake diameter are specified. With reference to Figure 2, the minimum requirements are:

- L=1.8m
- d=20mm
- Soil not excessively dry

The resistance to earth can be calculated using Equation 4 which provides a value of 52Ω.

$$R = \frac{\rho}{2\pi L} \ln\left(\frac{4L}{d}\right) \tag{4}$$

- ρ = earth resistivity = 100Ωm [21]

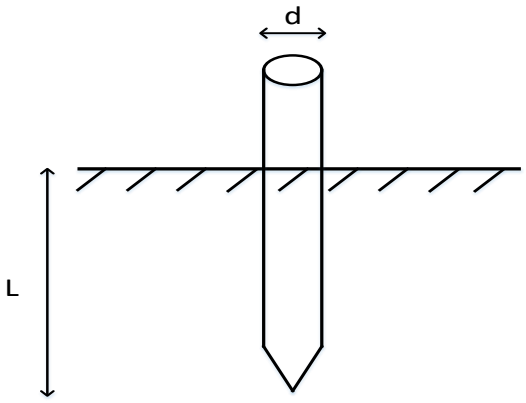

Fig. 2. Earth Stake Dimensions

Earthing resistance is variable depending on the local soil and weather conditions. The calculated value provides only an approximation. Figure 3 shows how the distribution network is modelled for the most detailed approximation of the MEN system. Earthing resistances can be considered in parallel since ICPs will be spaced by greater than $\frac{L}{4}$, and thus current flows do not interfere.

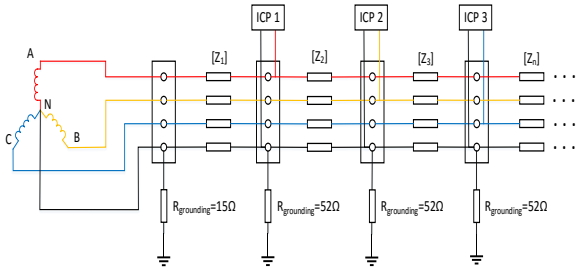

Fig. 3. Detailed MEN Approximation Model

B. Isolated Neutral Approximation

Distribution companies do not maintain records of ICP earthing resistances. These installations are the responsibility of an electrician, and are thus outside the network operators jurisdiction. The following modelling approximations are often made to aid simplicity.

- All neutral earthing downstream of the transformer is neglected
- Transformer neutral point is perfectly grounded

This connectivity describes the isolated neutral approximation. Figure 4 shows how the distribution network is modelled in this case.

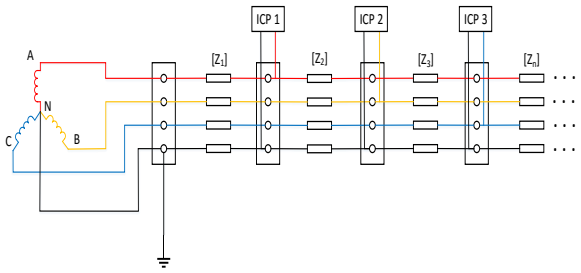

Fig. 4. Isolated Neutral Approximation Model

C. Perfectly Grounded Neutral Approximation

The final neutral grounding approximation is the perfectly grounded neutral. In many applications the 4×4 primitive impedance matrix used to model a 4 wire line segment is reduced to a 3×3 phase frame impedance matrix using the Kron reduction [22]. This reduction requires that the neutral conductor is perfectly grounded at both ends of the line, allowing the neutral and ground to be treated as a single conductor. Figure 5 shows how the distribution network is modelled in this case.

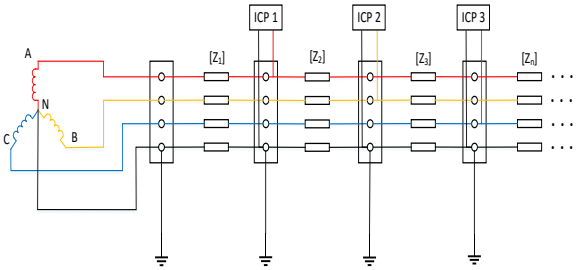

Fig. 5. Perfectly Grounded Neutral Approximation Model

V. Residential LV Distribution Network

LV distribution networks in New Zealand can be broadly classified as either city, urban, rural or industrial. Cluster analysis allowed each LV feeder from within a group of 10,558 to be classified [23]. The cluster parameters used within this process were as follows.

- Number of residential ICPs
- Number of non-residential ICPs
- Average distance between ICPs
- Average kW per ICP

The network in Figure 6 is closest to the centre of the urban cluster. It provides a typical urban network on which to asses the impacts of load diversity. The network contains a mixture of overhead line and underground cable. These sections are depicted by solid and dashed lines respectively. There are 71 ICPs in total, 68 of which are residential properties. Loads are assigned to each of the phases in an alternating manner along the length of both feeders. Three versions of the network were modelled in OpenDSS, corresponding to the neutral grounding approximations seen in Figures 3-5.

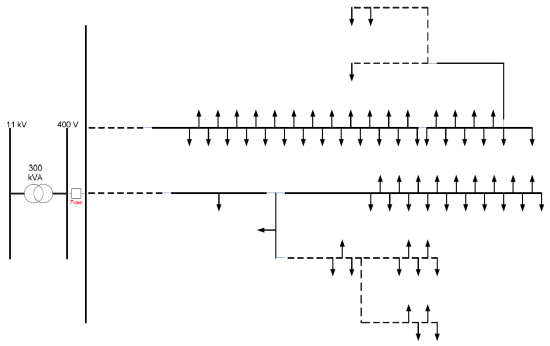

Fig. 6. Typical Urban LV Distribution Network

VI. Load Modelling

This section discusses the Smart Meter data which serves as input to the load flow simulation. It also provides further distinction between the uniformly distributed and diversified load models. In recent years the proliferation of Smart Metering

has made ICP-level load data widely available. By 2016 over 70% of New Zealand households had been fitted with Smart Meters [24]. These provide a powerful means for modelling load diversity. A Smart Meter dataset consisting of over two thousand premises was available for use within this work. For each premise a year's worth of half hour data was available. However, anonymity requirements mean that the ICP locations were not known. Consequently the following approach was implemented in order to identify a subsample of the dataset to use. The distribution of the dataset in terms of annual energy consumption was first identified. This can be seen in the histogram in Figure 7. From this distribution the 71 most similar Smart Meters around the 50th percentile were extracted. The reason for this is that LV networks typically contain premises of similar size. By selecting the most similar properties around the 50th percentile, only median sized residential properties were included in the subsample. It was noted that this approach will provide a conservative insight into the impacts of diversity. This is because the actual network contains 3 non-residential properties, and also property size will vary.

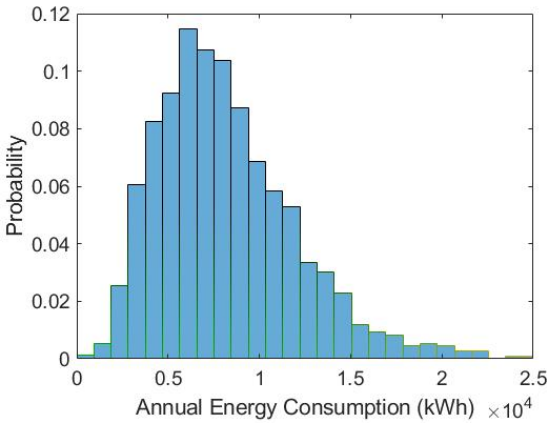

Fig. 7. Distribution of Annual Energy Consumption in Smart Meter Dataset

Each ICP within the network is randomly assigned a unique load profile from the smart meter subsample. Each load profile provides a years worth of half hourly averaged load data.

- P_j^i = kW Demand of ICP *j* During Time Interval *i*
- $j = 1, ..., 71$
- $i = 1, ..., 17520$

At each time step the uniformly distributed load per ICP $\bar{P}^i$ is calculated as the mean of P_j^i over all ICPs.

VII. Simulation Method

The impact of load diversity on voltage assessment varies as a function of time due to changes in loads. A years worth of continuous load data provided a large enough sample to capture the impact statistically. Figure 8 depicts the simulation method which was implemented.

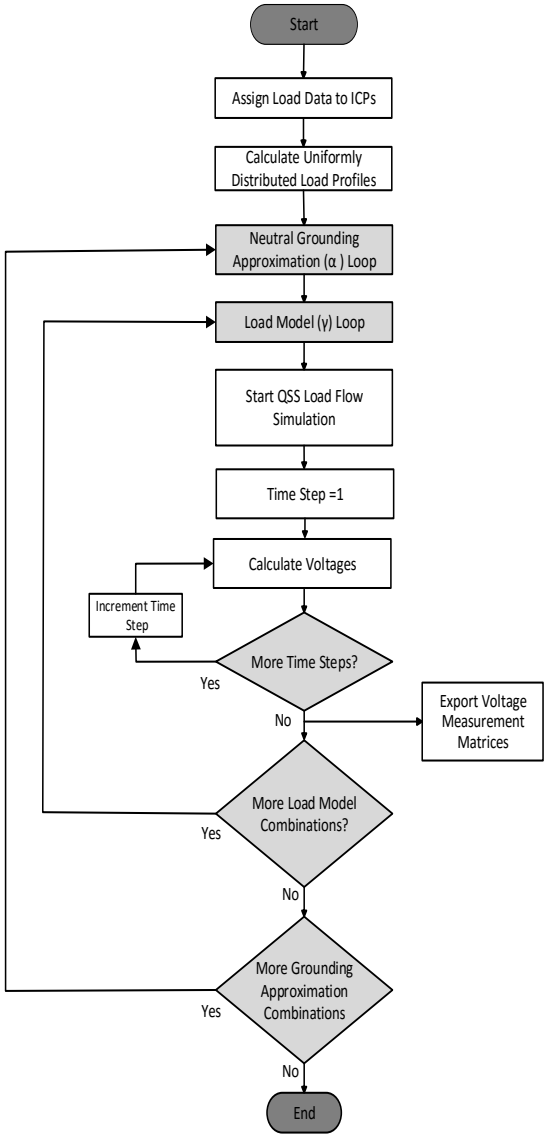

Fig. 8. Simulation Method Flow Chart Diagram

First the 71 Smart Meters from the subsample are randomly assigned to ICP locations within the network. The uniformly distributed load profiles per ICP are then calculated. The outer loop selects the neutral grounding approximation, whilst the inner loop selects the load model.

- α = {Perfectly grounded, Detailed MEN, Isolated}
- γ = {Uniform, Diversified}

For each combination of α and γ, a year long QSS load flow is executed. At each time step the phase to neutral, phase to ground, and neutral to ground voltages are recorded at each ICP location.

- ${V_{pn}}_j^i$ = Phase to neutral voltage at ICP *j* During Time Interval *i*

- ${V_{pg}}_j^i$ = Phase to ground voltage at ICP j During Time Interval i
- ${V_{ng}}_j^i$ = Neutral to ground voltage at ICP j During Time Interval i

The phase to neutral voltages are then placed within a structure as seen in Equation 5.

$$V_{pn}^i = \begin{bmatrix} {V_{pn}}_1^i \\ {V_{pn}}_2^i \\ \vdots \\ {V_{pn}}_{71}^i \end{bmatrix} \tag{5}$$

The minimum phase to neutral voltage within the network is calculated for each time step using Equation 6.

$${V_{pn}}_{min}^i = min\{V_{pn}^i\} \tag{6}$$

- k = Index of the ICP with the minimum phase to neutral voltage

The corresponding phase to ground and neutral to ground voltages are then extracted as seen in Equations 7 and 8.

$${V_{pg}}_{min}^i = {V_{pg}}_k^i \tag{7}$$

$${V_{ng}}_{min}^i = {V_{ng}}_k^i \tag{8}$$

Once the final time step is complete, Equations 9-11 are formed by concatenating the voltage measurements in Equations 6-8 across all time steps.

$$V_{pn_{min}} = \left[{V_{pn}}_{min}^1, \quad {V_{pn}}_{min}^2, \quad \ldots, \quad {V_{pn}}_{min}^{17520}\right] \tag{9}$$

$$V_{pg_{min}} = \left[{V_{pg}}_{min}^1, \quad {V_{pg}}_{min}^2, \quad \ldots, \quad {V_{pg}}_{min}^{17520}\right] \tag{10}$$

$$V_{ng_{min}} = \left[{V_{ng}}_{min}^1, \quad {V_{ng}}_{min}^2, \quad \ldots, \quad {V_{ng}}_{min}^{17520}\right] \tag{11}$$

$V_{pn_{min}}$, $V_{pg_{min}}$ and $V_{ng_{min}}$ are exported, saved and refreshed before the next combination of α and γ.

VIII. Results

Statutory limits for steady-state voltage are typically quoted with an upper and lower bound. For example the New Zealand Electricity (Safety) Regulations 2010 define the allowable voltage variation at the point of supply as 230V $\pm 6\%$ [25]. Voltage drop is the sole concern here since no distributed generation was modelled. The minimum allowable supply voltage is 216.2V.

Figure 9 shows a box plot of $V_{pn_{min}}$ for the uniform load model, and each of the neutral grounding approximations. Figure 10 shows a box plot of $V_{pn_{min}}$ for the diversified load model, and each of the neutral grounding approximations. On each box the central mark indicates the median, while the bottom and top edges indicate the 25th and 75th percentiles respectively. The whiskers extend to the most extreme data points not considered outliers. The outliers are plotted individually using the '+' symbol. The dashed horizontal line depicts the threshold for violation of the statutory limits.

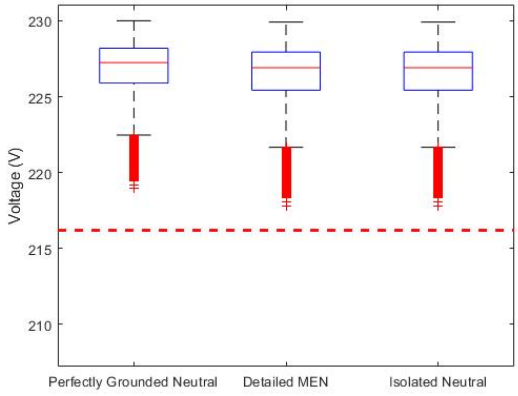

Fig. 9. Box Plot of $V_{pn_{min}}$ for γ = Uniform

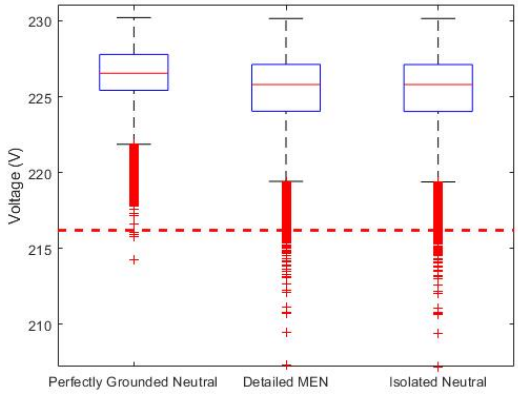

Fig. 10. Box Plot of $V_{pn_{min}}$ for γ = Diversified

It can be seen that when the uniform load model is implemented, there are no voltage violations recorded over the entire year. This is irrespective of the neutral grounding approximation. When the diversified load model is implemented, voltage violations are observed. The total number of violations varies depending on the neutral grounding approximation. This can be seen more clearly in Table II. Looking at the diversified cases, the perfectly grounded neutral approximation significantly underestimates the number of voltage violations. The isolated neutral approximation overestimates the number of voltage violations, though only slightly. With reference to Figure 10, all of the violations are considered statistical outliers. This is because all half hour intervals within the day are considered in this analysis. Whilst peak loading only occurs for short periods of the day, networks must be designed to cope with these peaks. Although considered outliers within the entire years worth of data, these intervals still present considerable periods of time for which the network operates outside of the statutory limits.

TABLE II
ANNUAL VOLTAGE VIOLATION COUNT

	Perfectly Grounded Neutral	Detailed MEN	Isolated Neutral
Uniform	0	0	0
Diversified	4	82	84

The customer supply voltage is between phase and neutral V_{pn}. This can be decomposed into phase to ground V_{pg} and neutral to ground V_{ng} components. The supply voltage is affected by both their magnitudes, and phase relationship. Figures 11, 12 and 13 show box plots of $V_{pn_{min}}$, $V_{pg_{min}}$ and $V_{ng_{min}}$ respectively. Both the uniform and diversified load models can be seen. All cases use the detailed MEN approximation.

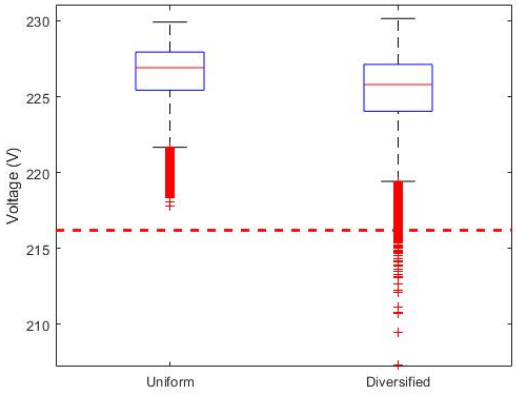

Fig. 11. Box Plot of $V_{pn_{min}}$ for α = Detailed MEN

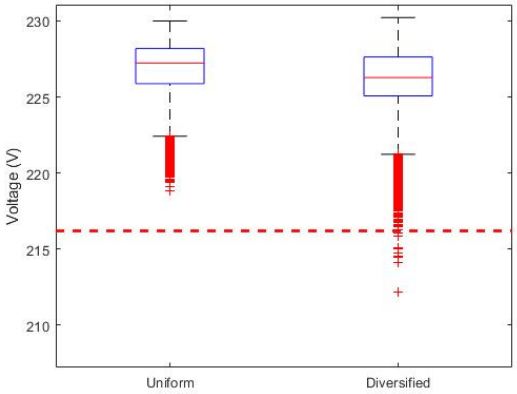

Fig. 12. Box Plot of $V_{pg_{min}}$ for α = Detailed MEN

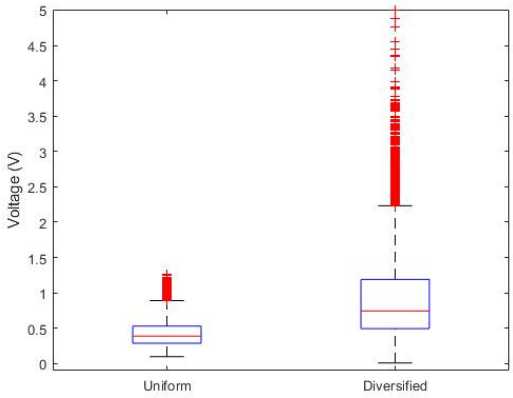

Fig. 13. Box Plot of $V_{ng_{min}}$ for α = Detailed MEN

It can be seen in Figures 12 and 13 that load diversity impacts both the phase to ground and neutral to ground voltages. The lowest phase to ground voltages are in the diversified case. This is due to longitudinal and across phase diversity [8]. The former describes conditions when the total network load is disproportionately skewed towards the end of feeders. The latter describes conditions when the total network load is disproportionately skewed on a particular phase. It can also be seen that the worst neutral to ground voltages are higher in the diversified case. This is because load diversity results in greater current imbalance across the phases. Current imbalance returns to the transformer star point through a combination of the earth and neutral conductor. Therefore greater current imbalance results in greater voltage rise along the length of the neutral conductor. The contribution of the neutral voltage is not trivial. Comparing Figures 11 and 12, there are only 9 voltage violations recorded over the year when considering $V_{pg_{min}}$, compared to 82 when considering $V_{pn_{min}}$.

As previously stated V_{pn} is affected by both the magnitudes, and phase relationship of V_{pg} and V_{ng}. The following example aims to demonstrate how V_{ng} can increase the number of voltage violations observed for V_{pn}. Figure 14 shows how V_{pn} varies throughout the network, and over the course of a given day. It can be seen that there are certain ICPs more prone to voltage depression. These are those located towards the remote ends of the primary feeders seen in Figure 6. Additionally there are certain times of day more prone to significant voltage depression, around 08:00 and between 18:00 and 22:00. Table III shows the supply voltage decomposition for ICP 38 (remote end of the first primary feeder) at 18:30. The neutral to ground voltage V_{ng} is significantly displaced. Additionally it is in the same phase quadrant as the phase to ground voltage V_{pg}. Consequently V_{pn} is below the lower statutory limit, whilst V_{pg} remains within bounds.

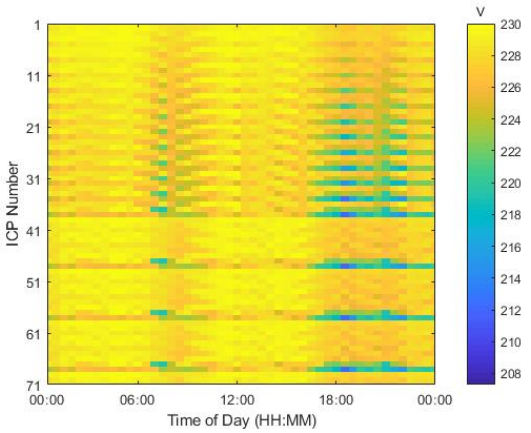

Fig. 14. Network Daily Voltage Drop Heat Map

TABLE III
ICP 38 SUPPLY VOLTAGE DECOMPOSITION: 6:30PM

	Voltage Magnitude (V)	Voltage Angle (deg)
V_{pn}	212.24	-122.83
V_{pg}	216.46	-122.24
V_{ng}	4.76	-94.91

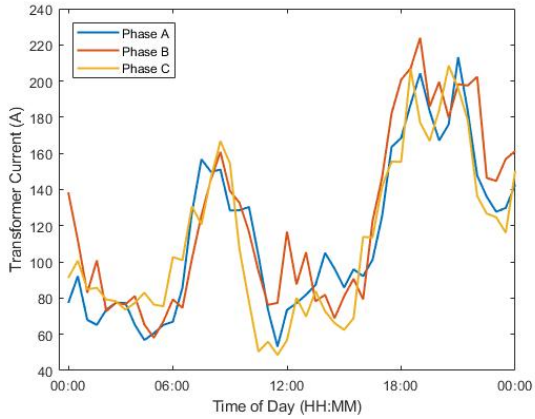

Fig. 15. Daily Transformer Current Profile

These results demonstrate that regulation of neutral voltage could be a powerful means to reduce voltage variation throughout the network. Since neutral voltage rise is related to current imbalance, one may assume that this problem could be fixed by reassigning ICP phase allocations such as to balance the transformer phase currents. This is not necessarily the case for the following reasons. Firstly, transformer phase imbalance varies with time. As can be seen in Figure 15, the rank order of the phases changes multiple times over the course of a day. Therefore a reassignment which benefits the network for one particular snapshot in time, may exacerbate the problem during another. Secondly, balancing the phase currents at the transformer does not necessarily balance the system further downstream and significant current may still flow in the neutral wire.

For the example in Table III, displacement of V_{ng} worsened the voltage depression seen for V_{pn}. This is not always the case. Figure 16 shows the distribution of V_{ng} over the entire year. Again these results are for ICP 38.

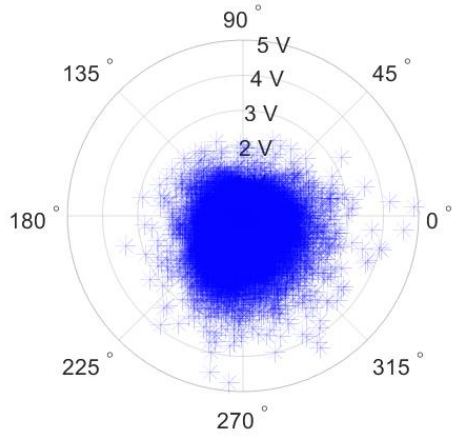

Fig. 16. Annual Neutral Voltage Scatter plot

It can be seen that V_{ng} experiences displacement in all 4 quadrants. In those cases were V_{ng} is out of phase with V_{pg}, neutral voltage rise boosts V_{pn}. An example of this can be seen in Table IV. Whilst this seems like a positive impact for this particular example, it can become problematic when over-voltage is a possible concern due to photovoltaics.

TABLE IV
ICP 38 SUPPLY VOLTAGE DECOMPOSITION: 12:30PM

	Voltage Magnitude (V)	Voltage Angle (deg)
V_{pn}	227.96	-121.01
V_{pg}	225.70	-121.05
V_{ng}	2.26	62.06

IX. CONCLUSION

ADMD per customer is a useful tool in sizing transformers to cope with peak demand. However, using this average value in load flow simulations is insufficient to make accurate voltage assessments. When load diversity in the downstream network is modelled, greater voltage variation is observed. This can be attributed to both the phase and neutral conductors. When modelling MEN systems care should be taken regarding approximations of the neutral to ground connectivity. The perfectly grounded neutral approximation can considerably underestimate voltage variation and mask voltage violations. Though conservative the isolated neutral approximation is a better estimate of the New Zealand MEN system. Neutral voltage displacement can have the effect of increasing or decreasing the supply voltage, depending on its relative phase angle. Decreasing the supply voltage during heavily loaded periods can cause under-voltage violations. When PV is present,

increasing the supply voltage during lightly loaded periods can cause over-voltage violations. Reassignment of ICP phasing would be ineffective in reducing neutral voltage displacement. This is because instantaneous changes in ICP-level loading cause phase imbalance to vary over the course of the day. It is possible that regulation of the neutral voltage though some other means could provide effective voltage control in LV distribution networks. This however is outside the scope of this work. It should be recalled that these results are based on half hourly temporal resolution. The impacts of load diversity on voltage assessment will be worse at higher temporal resolution. In order to reduce the impact of EVs on peak loading, diversity in the start time and duration of EV charging is required. Additionally variation in charging technologies e.g. standard domestic socket or dedicated fast charger, will impact load diversity. It is concluded that in order to avoid masking statutory limit voltage violations in future impact studies, load diversity and finite earthing impedances should be considered in the analysis.

REFERENCES

[1] Concept Consulting, *"Driving Change" - issues and options to maximise the opportunities from large-scale electric vehicle uptake in New Zealand*, 7 March 2018.

[2] Transpower, "Te Mauri Hiko, Energy Futures: Transpower White Paper", New Zealand, 2018.

[3] Jake Roos & Concept Consulting, *Report on Electric Vehicle Charging trial*, July 2018.

[4] J. D. Watson, N. R. Watson, D. Santos-Martin, A. R. Wood, S. Lemon and A. J. V. Miller, "Impact of solar photovoltaics on the low-voltage distribution network in New Zealand," in IET Generation, Transmission & Distribution, vol. 10, no. 1, pp. 1-9, 7 1 2016.

[5] Chin Ho Tie and Chin Kim Gan, "Impact of grid-connected residential PV systems on the malaysia low voltage distribution network," 2013 IEEE 7th International Power Engineering and Optimization Conference (PEOCO), Langkawi, 2013, pp. 670-675.

[6] A. Bosovic, M. Music and S. Sadovic, "Analysis of the impacts of plug-in electric vehicle charging on the part of a real low voltage distribution network," 2015 IEEE Eindhoven PowerTech, Eindhoven, 2015, pp. 1-5.

[7] Watson N. R., Watson J. D., Watson R. M. K. Sharma and Miller, A, *Impact of Electric Vehicle Chargers on a Low Voltage Distribution System*, EEA Conference, 24-26 June 2015, Wellington.

[8] McGill E, *The Significance of Load Diversity on Voltage Assessment in Low Voltage Distribution Networks*, EEA Conference, 22 - 24 June 2016, Wellington, 2016.

[9] Urquhart, A.J. & Thomson, M., 2013. Assumptions and approximations typically applied in modelling LV networks with high penetrations of low carbon technologies. Solar Integration Workshop 2013, London, October 21st-22nd 2013, 6pp.

[10] D.F. Frame, G.W. Ault & S. Huang, "The uncertainties of probabilistic LV network analysis," 2012 IEEE Power and Energy Society General Meeting, San Diego, CA, USA, 22-26 July 2012, doi: 10.1109/PESGM.2012.6344587

[11] D. H. O. McQueen, P. R. Hyland & S. J. Watson, "Application of a Monte Carlo simulation method for predicting voltage regulation on low-voltage networks," in IEEE Transactions on Power Systems, vol. 20, no. 1, pp. 279-285, Feb. 2005. doi: 10.1109/TPWRS.2004.841214

[12] Constantin Reese & Lutz Hofmann, "Analysis and reduction of effects of single-phase loads and generators on low voltage distribution grids," 21st International Conference on Electricity Distribution Frankfurt, 6-9 June 2011

[13] P. Huppertz, L. Kopczynski, R. Zeise & M. Kizilcay, "Approaching the diversity of unbalanced residential load in low-voltage grids by probabilistic load-flow simulation of cross-sectional data," 2015 IEEE Eindhoven PowerTech, Eindhoven, 2015, pp. 1-6. doi: 10.1109/PTC.2015.7232624

[14] Csatár, J & Dan, A. (2017). Neutral Voltage Comparison of Different Grounding Configurations and Calculation Methods in Multi-Grounded Low Voltage Network. Periodica Polytechnica Electrical Engineering and Computer Science. 61. 77-81. 10.3311/PPee.10379.

[15] Sunderland, Keith & F. Conlon, Michael. (2012). 4-Wire load flow analysis of a representative urban network incoprating SSEG. 1-6. 10.1109/UPEC.2012.6398569.

[16] Ahmadi, G & Shahrtash, S. Mohammad. (2009). Neutral to earth voltage reduction methods in three-phase four wire distribution systems. I-134.

[17] UK Power Networks, *Use of Smart Meter information for planning and operation*, Report C1, September 2014.

[18] C. Barteczko-Hibbert, *After Diversity Maximum Demand (ADMD) Report*, University of Durham, February 2015.

[19] A. I. Elombo, T. Morstyn, D. Apostolopoulou and M. D. McCulloch, "Residential load variability and diversity at different sampling time and aggregation scales," 2017 IEEE AFRICON, Cape Town, 2017, pp. 1331-1336. doi: 10.1109/AFRCON.2017.8095675

[20] Australian/New Zealand Standards, *AS/NZS 3000:2007 Electrical Installations*, 12 November 2007.

[21] IEEE-SA Standards Board, *IEEE Std 80-2000: IEEE Guide for Safety in AC Substation Grounding*, 30 January 2000.

[22] W. H. Kersting, Distribution System Modeling and Analysis. 2002;2006;2001;.

[23] J. D. Watson, N. R. Watson, D. Santos-Martin, S. Lemon, A. R. Wood, and A. J. V. Miller *Low Voltage Network Modelling*, EEA Conference, June 2014, Auckland, 2014.

[24] Electricity Retailers of New Zealand, *Smart meters – everything you needed to know and more*, Smart Meters Summary, July 2017.

[25] N. Watson, Miller A, *Power Quality Indices*, EEA Conference, June 2015, Wellington, 2015.

REFERENCES

Andren, F., Brundlinger, R. and Strasser, T. (2014), 'IEC 61850/61499 Control of Distributed Energy Resources: Concept, Guidelines, and Implementation', *IEEE Transactions on Energy Conversion*, Vol. 29, No. 4, pp. 1008–1017.

Archer, D., Eby, M., Brovkin, V., Ridgwell, A., Cao, L., Mikolajewicz, U., Caldeira, K., Matsumoto, K., Munhoven, G., Montenegro, A. and Tokos, K. (2009), 'Atmospheric Lifetime of Fossil Fuel Carbon Dioxide', *Annual Review of Earth and Planetary Sciences*, Vol. 37, No. 1, pp. 117–134.

AS/NZS 3000 (2018), 'Electrical Installations - Known as the Australian/New Zealand Wiring Rules', .

Bizzozero, F., Giambattista, G. and Nicol'o, V. (2016), 'A Time-of-use-based Residential Electricity Demand Model for Smart Grid Application', In *2016 IEEE 16th International Conference on Environment and Electrical Engineering (EEEIC)*, .

Caramia, P., Carpinelli, G., Pagano, M. and Varilone, P. (2007), 'Probabilistic three-phase load flow for unbalanced electrical distribution systems with wind farms', *IET Renewable Power Generation*, Vol. 1, No. 2, p. 115.

Ciric, R., Feltrin, A. and Ochoa, L. (2003), 'Power flow in four-wire distribution networks-general approach', *IEEE Transactions on Power Systems*, Vol. 18, No. 4, pp. 1283–1290.

Concept Consulting (2018), 'Driving change: Issues and options to maximise the opportunities from large-scale electric vehicle uptake in New Zealand', .

Conti, S. and Raiti, S. (2007), 'Probabilistic load flow using Monte Carlo techniques for distribution networks with photovoltaic generators', *Solar Energy*, Vol. 81, No. 12, pp. 1473–1481.

Cundeva, S., Mateska, A.K. and Bollen, M.H. (2018), 'Hosting capacity of LV residential grid for uncoordinated ev charging', In *2018 18th International Conference on Harmonics and Quality of Power (ICHQP)*, IEEE, Ljubljana, pp. 1–5.

Degefa, M., Millar, R., Koivisto, M., Humayun, M. and Lehtonen, M. (2013), 'Load Flow Analysis Framework for Active Distribution Networks Based on Smart Meter Reading System', *Engineering*, Vol. 5, pp. 1–8.

Electric Vehicles Initiative (2019), 'Electric Vehicles Initiative: EV30@30 Campaign', .

Electricity Authority (2014), 'Reliability risk framework in the electricity industry', Tech. rep.

EN IEC 61851-1 (2019), 'Electric Vehicle Conductive Charging System - Part 1: General requirements', .

Energy Efficiency and Conservation Authority (2019), 'Electric Vehicle Charging Technology: New Zealand Residential Charging Perspective', .

Farkas, C., Szabó, K. and Prikler, L. (2011), 'Impact assessment of electric vehicle charging on a LV distribution system', In *Proceedings of the 2011 3rd International Youth Conference on Energetics (IYCE)*, .

Fernandez, E. and Patrick, J. (2019), 'Emergency and Cyclic Ratings of HV Cables', Tech. rep., Electrotechnik Pty Ltd.

Hatziargyriou, N., Karakatsanis, T. and Papadopoulos, M. (1993), 'Probabilistic load flow in distribution systems containing dispersed wind power generation', *IEEE Transactions on Power Systems*, Vol. 8, No. 1, pp. 159–165.

Hes, S., Kula, J. and Svec, J. (2019), 'Analysis of Smart Technical Measures Impacts on DER and EV Hosting Capacity Increase in LV and MV Grids in the Czech Republic in Terms of European Project InterFlex', In *2019 International Conference on Smart Energy Systems and Technologies (SEST)*, IEEE, Porto, Portugal, pp. 1–6.

Idaho National Laboratory (2012), 'Steady State Vehicle Charging Fact Sheet: 2012 Nissan Leaf', .

IEEE Std 80 (2013), 'IEEE Guide for Safety in AC Substation Grounding', Tech. rep., IEEE.

Intergovernmental Panel on Climate Change (2014), 'Climate Change 2014 Impacts, Adaptation, and Vulnerability Part B: Regional Aspects', .

International Energy Agency (2020), 'IEA Data Browser: New Zealand', https://www.iea.org/countries/new-zealand.

Iwabuchi, K., Kaneko, T. and Shimoo, T. (2014), 'Estimation Method for Distribution Network Voltage Utilizing Smart Meter Measurements', In *2014 IEEE Innovative Smart Grid Technologies - Asia (ISGT Asia 2014)*, IEEE, Piscataway, NJ.

Jake Roos Consulting (2018), 'Wellington Electricity: Report on Electric Vehicle Charging Trial', .

Jambagi, A., Kramer, M. and Cheng, V. (2015), 'Residential Electricity Demand Modelling Activity Based Modelling for a model with high time and spatial resolution', In *Proceedings of 2015 IEEE International Renewable and Sustainable Energy Conference (IRSEC'15)*, .

Johnson, B., Starke, M., Abdelaziz, O., Jackson, R. and Tolbert, L. (2014), 'A MATLAB Based Occupant Driven Dynamic Model for Predicting Residential Power Demand', In *2014 IEEE PES Transmission and Distribution Conference and Exposition (T&D 2014)*, IEEE, Piscataway, NJ.

Kelly, L., Rowe, A. and Wild, P. (2009), 'Analyzing the Impacts of Plug-in Electric Vehicles on Distribution Networks in British Columbia', In *2009 IEEE Electrical Power & Energy Conference, October 22-23, 2009, Montreal, Canada*, IEEE, New Jersey.

Kersting, W.H. (2002), *Distribution System Modeling and Analysis*, The Electric Power Engineering Series, CRC Press, Boca Raton.

Leou, R.C., Su, C.L. and Lu, C.N. (2013), 'Impact analysis of electric vehicles on distribution systems considering uncertainties', In *IECON 2013 - 39th Annual Conference of the IEEE Industrial Electronics Society*, IEEE, Vienna, Austria, pp. 2063–2068.

Li, Y. and Crossley, P. (2014), 'Monte Carlo study on impact of electric vehicles and heat pumps on LV feeder voltages', In *12th IET International Conference on Developments in Power System Protection (DPSP 2014)*, Institution of Engineering and Technology, Copenhagen, Denmark, pp. 12.13–12.13.

Lillebo, M., Zaferanlouei, S., Zecchino, A. and Farahmand, H. (2019), 'Impact of large-scale EV integration and fast chargers in a Norwegian LV grid', *The Journal of Engineering*, Vol. 2019, No. 18, pp. 5104–5108.

Maduranga, R., Maddumage, M., Kaushalya, P., Samith, D. and Jayatunga, U. (2019), 'Investigation of Grid Connected Solar PV Hosting Capacity in LV Distribution Networks', In *2019 14th Conference on Industrial and Information Systems (ICIIS)*, IEEE, Kandy, Sri Lanka, pp. 390–394.

Masetti, C. (2010), 'Revision of European Standard EN 50160 on power quality: Reasons and solutions', In *Proceedings of 14th International Conference on Harmonics and Quality of Power - ICHQP 2010*, IEEE, Bergamo, Italy, pp. 1–7.

Ministry of Business, Innovation & Employment (2019), 'Energy In New Zealand 2019', .

Ministry of Transport (2017), 'New Zealand Household Travel Survey 2015-2017', .

Ministry of Transport (2020), 'Monthly Electric and Hybrid Light Vehicle Registrations', https://www.transport.govt.nz/mot-resources/vehicle-fleet-statistics.

NASA (2020), 'Global Climate Change: Vital Signs of The Planet', https://climate.nasa.gov/evidence/.

New Zealand Transport Agency (2020), 'Enabling a nationwide network of public charging infrastructure', https://www.nzta.govt.nz/planning-and-investment/planning/transport-planning/planning-for-electric-vehicles/national-guidance-for-public-electric-vehicle-charging-infrastructure/enabling-a-nationwide-network-of-public-charging-infrastructure/.

Orion (2017), 'How To Use Ripple Signals On Orion's Network', .

Ovalle, A., Hably, A. and Bacha, S. (2018), *Grid Optimal Integration of Electric Vehicles: Examples with Matlab Implementation*, Vol. 137 of *Studies in Systems, Decision and Control*, Springer International Publishing, Cham.

Papadopoulos, P., Skarvelis-Kazakos, S., Grau, I., Cipcigan, L. and Jenkins, N. (2012), 'Electric vehicles' impact on British distribution networks', *IET Electrical Systems in Transportation*, Vol. 2, No. 3, p. 91.

Putrus, A., Suwanapingkarl, P., Johnston, D., Bentley, C. and Narayana, M. (2009), 'Impact of Electric Vehicles on Power Distribution Networks', In *2009 IEEE Vehicle Power and Propulsion Conference*, IEEE, Piscataway, NJ.

Quirós-Tortós, J., Ochoa, L. and Lees, B. (2015), 'A Statistical Analysis of EV Charging Behavior in the UK', In *IEEE PES Conference on Innovative Smart Grid Technologies Latin America*, .

Rahman, A. and Arnob, S. (2016), 'Developing Load Profile for Domestic Customers of Dhaka City through Statistical Prediction', In *2016 3rd International Conference on Electrical Engineering and Information & Communication Technology (iCEEiCT) Dates: 22 to 24 September 2016, Venue: Military Institute of Science and Technology (MIST)*, .

Richardson, P., Flynn, D. and Keane, A. (2010), 'Impact Assessment of Varying Penetrations of Electric Vehicles on Low Voltage Distribution Systems', In *2010 IEEE Power and Energy Society General Meeting: [IEEE PES-GM 2010]*, IEEE, Piscataway, NJ.

Roger C. Dugan (2020), 'The Open Distribution System Simulator (OpenDSS): Reference Guide:', .

Roy, J. and Mather, B. (2019), 'Study of Voltage-Dependent Harmonic Characteristics of Residential Appliances', In *2019 IEEE Texas Power and Energy Conference (TPEC)*, IEEE, College Station, TX, USA, pp. 1–6.

Schneider, K., Gerkensmeyer, C., Kintner-Meyer, M. and Fletcher, R. (2008), 'Impact assessment of plug-in hybrid vehicles on pacific northwest distribution systems', In *2008 IEEE Power and Energy Society General Meeting - Conversion and Delivery of Electrical Energy in the 21st Century*, IEEE, Pittsburgh, PA, USA, pp. 1–6.

Shariff, N., Al Essa, M. and Cipcigan, L. (2016), 'Probabilistic Analysis of Electric Vehicles Charging Load Impact on Residential Distributions Networks', In *2016 IEEE International Energy Conference (ENERGYCON).*, IEEE, Piscataway.

SP Energy Networks (2015), 'Enhanced Transformer Ratings Tool : A Design and Planning Application Guide', .

SR 2010/36 (2010), 'Electricity Safety Regulations', .

Stephenson, J., Ford, R., Nair, N.K., Watson, N., Wood, A. and Miller, A. (2018), 'Smart grid research in New Zealand – A review from the GREEN Grid research programme', *Renewable and Sustainable Energy Reviews*, Vol. 82, pp. 1636–1645.

The Ministry for the Environment (2018), 'New Zealand's Greenhouse Gas Inventory 1990–2016', .

Tijani, S. and Butler-Purry, K. (2019), 'Investigation of Approaches for Incorporating Smart Meter Data in Load and PV Models in Medium Voltage Power System Studies', In *2019 IEEE Texas Power and Energy Conference (TPEC)*, 2019 IEEE Texas Power and Energy Conference (TPEC).

Tran-Quoc, T., Le Pivert, X., Saheli, M. and Beaude, O. (2012), 'Stochastic Approach to Assess Impacts of Electric Vehicles on the Distribution Network', In *2012 3rd IEEE PES Innovative Smart Grid Technologies Europe (ISGT Europe 2012)*, IEEE, Piscataway, NJ.

United Nations (2015), 'Paris Agreement', .

Urquhart, A. and Thomson, M. (2013), 'Assumptions and approximations typically applied in modelling LV networks with high penetrations of low carbon technologies.', In *Solar Integration Workshop*, London,.

Watson, J.D., Watson, N.R., Santos-Martin, D., Wood, A.R., Lemon, S. and Miller, A.J. (2016), 'Impact of solar photovoltaics on the low-voltage distribution network in New Zealand', *IET Generation, Transmission & Distribution*, Vol. 10, No. 1, pp. 1–9.

Watson, N., Watson, J. and Watson, R. (2015), 'Impact of Electric Vehicle Chargers on a Low Voltage Distribution System', In *EEA Conference & Exhibition 2015, June 2015, Wellington*, .

Watson, N.R. (2016), 'Power-Quality Management in New Zealand', *IEEE Transactions on Power Delivery*, Vol. 31, No. 5, pp. 1963–1970.

WorkSafe NZ (2017), 'WorkSafe New Zealand: Electricity industry structure', https://worksafe.govt.nz/topic-and-industry/energy-safety/electrical-industry-structure/.

WorkSafe NZ (2019), 'WorkSafe New Zealand: Electric Vehicle Charging Safety Guidelines', .

World Resources Institute (2020), 'World Resources Institute: CAIT Climate Data Explorer', http://cait.wri.org/.

Zdraveski, V., Krstevski, P., Vuletic, J. and Angelov, J. (2019), 'Analyzing the Impact of Battery Electric Vehicles on Distribution Networks Using Nondeterministic Model', In *IEEE EUROCON 2019: 18th International Conference on Smart Technologies : 1st - 4th July 2019, Novi Sad, Serbia*, .